Mitochondrial behavior, morphology, and animal performance

by

Kyle Benton Heine

A dissertation submitted to the Graduate Faculty of
Auburn University
in partial fulfillment of the
requirements for the degree of
Doctor of Philosophy

Auburn, Alabama
December 11, 2021

Keywords: copepod, life history, oxidative stress,
respiration, *Tigriopus californicus*, transmission electron microscopy

Approved by

Wendy R. Hood, Chair, Associate Professor of Biological Sciences
Geoffrey E. Hill, Professor of Biological Sciences
Daniel A. Warner, Associate Professor of Biological Sciences
Alan E. Wilson, Professor of Fisheries, Aquaculture, and Aquatic Sciences

Abstract

We have a limited understanding of the proximate mechanisms that are responsible for the development of variation in animal performance and life-history strategies. Many components of an organism's successful life history–for example, mate competition, gestation, lactation, etc.–require a substantial increase in daily energy expenditure. Mitochondrial behavior (positioning within the cell and communication between mitochondria) and morphology affect variation in energy production at the molecular, cellular, and organismal levels. Chapter 1 reviews the adaptations in mitochondrial behavior and morphology that favor efficient energy production and increased animal performance. Previous work has linked greater proportions of inter-mitochondrial junctions and density of the inner mitochondrial membrane, among other traits, with increased energetic demand. Both endogenous and exogenous factors contribute to organism survival and reproduction. One ecologically relevant factor that influences the life history of aquatic organisms is ultraviolet (UV) radiation. Chapter 2 evaluates the impact of UV-A/B irradiation on life history characteristics in *Tigriopus californicus* copepods. After exposing copepods to UV-A/B irradiation (control, 1-, and 3-hr UV treatments at 0.5 W/m^2), I measured the impact of exposure on fecundity, reproductive effort, and longevity. UV irradiation increased size of the first clutch among all reproducing females in both the 1- and 3-hr experimental groups and decreased longevity among all females that mated in the 1-hr treatment. UV irradiation had no effect on the number of clutches females produced. These findings indicate a potential benefit of UV irradiation on reproductive performance early in life, although the same exposure came at a cost to longevity. Chapter 3 tests the hypothesis that mitochondria change their behavior and morphology to meet energetic demands of responding to changes in oxidative stress. Using transmission electron microscopy, I found that both three and six hours of UV-A/B irradiation (0.5 W/m^2) increased the proportion of inter-mitochondrial junctions (with increasing mitochondrial aspect ratio) and density of the inner mitochondrial membrane in myocytes of *T. californicus* copepods. Mitochondrial density increased following both irradiation treatments, but mitochondrial size decreased under the six-hour treatment. Metabolic rate was maintained under three hours of

irradiation but decreased following six hours of exposure. These observations demonstrate that the density of inner mitochondrial membrane and proportion of inter-mitochondrial junctions can play formative roles in maintaining whole-animal metabolic rate, and ultimately organismal performance, under exposure to an oxidative stressor. Chapter 4 investigates the effect that increasing temperatures impose on copepod respiration. This study used 32 studies spanning 78 years of research and 50 copepod species (three orders) to quantify percent change in respiration rates per one-unit change in temperature. Copepod respiration rates increased by approximately 7% per °C increase in water temperature across the orders Calanoida, Cyclopoida, and Harpacticoida. Neither food availability nor scaling respiration to copepod dry weight affected the rate of change of respiration rates. Chapter 5 reviews how density and morphology of the inner mitochondrial membrane influence performance of the electron transport system. This review outlines the evidence that inner mitochondrial membrane density, association between ATP synthases, and cristae morphology, impact the efficiency of energy production by mitochondria. Further, we consider possible constraints on the capacity of mitochondria to improve efficiency by increasing inner mitochondrial membrane density. The aforementioned studies accomplish two goals: 1) understanding how exogenous, environmental stressors influence whole-animal performance, including metabolic rate and life history variation, and 2) understanding how mitochondrial behavior and morphology can act as mediators in these relationships by being influenced by environmental stressors and influencing animal performance.

Acknowledgments

This body of work is dedicated to my son, Benton Reed Heine. Benton was born midway through my PhD studies on February 18, 2019. He has inspired me to work harder than I thought possible, and he will always be my greatest source of inspiration.

Table of Contents

List of Tables

List of Figures

Chapter 1: **Mitochondrial behavior, morphology, and animal performance**

Published with Wendy R. Hood (2020) in *Biological Reviews* **95**(3), 730-737

INTRODUCTION

The efficiency with which dietary and endogenous nutrient stores can be converted to adenosine triphosphate (ATP) plays an important role in determining individual and species-specific patterns of whole-animal performance (Drent & Daan, 1980; Gittleman & Thompson, 1988; Kenagy *et al.,* 1990; Scantlebury *et al.*, 2001; McBride *et al.*, 2015; Salin *et al.*, 2015). Herein, animal performance is defined as an animal's ability to produce enough ATP to support growth, self-maintenance, reproduction, and other energetically demanding activities that promote survival and future reproductive efforts. Investigators have taken a number of approaches to understanding energy expenditure among individuals and species including, but not limited to, measuring whole-animal and basal metabolic rates, relating energy intake to performance, measuring oxidative stress in relation to mitochondrial performance, and most recently, measuring oxygen use and ATP production of mitochondria (e.g., Gittleman & Thompson, 1988; Reinhold, 1999; Biro & Stamps, 2010; Burton *et al.*, 2011; Speakman *et al.*, 2015; Mowry *et al.*, 2017; Hill *et al*., 2019). For example, Salin et al. (2019) recently showed that individual differences in the growth rate of brown trout (*Salmo trutta*) are correlated with the efficiency of ATP production by the liver. While recent studies have made great strides in understanding the relationship between energy production and whole-animal performance, there is still considerable, unexplained variation in performance among individuals and species. The capacity to support the production of offspring is, arguably, the most important measure of an animal's performance. The behaviors and physiological processes that support each reproductive event, such as territory acquisition and maintenance, intraspecific competition for mates, gestation, and offspring nourishment, typically require a large increase in nutrient intake or mobilization of endogenous fuel stores to support energy production. Thus, the efficient production of ATP within mitochondria is an important determinant of animal performance.

The mechanisms underlying variation in energy production, and how that variation influences whole-organism performance, are poorly understood. Investigators are beginning to understand better what drives variation in mitochondrial physiology, but the link between cellular and whole-organism performance is an area of inquiry in need of further research. This lack of a clear relationship between energy production and whole-organism performance has led researchers to evaluate mitochondrial respiratory performance and, in particular, how oxidative stress modifies mitochondrial performance. Variation in mitochondrial behavior and morphology have been largely ignored in studies of functional ecology. An increasing number of studies have shown that the behavior and morphology of mitochondria are highly dynamic, influencing energy production and the capacity of mitochondria to respond to both endogenous and exogenous stressors (Youle & Van Der Bliek, 2012; Rafelski, 2013). By studying these aspects of mitochondria, we may gain insight into how organization and performance at the cellular level influence whole-organism performance.

Here, we propose that the development of energetically demanding behaviors and life-history strategies are enhanced by changes in the behavior (positioning and communication) and morphology of mitochondria within tissues that directly influence animal performance. These changes include structural modifications such as the small-scale coordination of cristae within individual mitochondria (Zick *et al.*, 2009) that can alter ATP production and influence the large-scale function of tissues within and between organ systems (**Figure 1.1**; see Strohm & Daniels, 2003). This idea builds on our understanding of protein functions that control mitochondrial behavior and morphology (e.g., Schrepfer & Scorrano, 2016) by aiming to understand how small-scale changes in organelle structure can influence large-scale changes in tissue and organ function. Although studies of mitochondrial behavior and morphology are becoming more common, most studies examine how these two facets of mitochondria change in response to extreme conditions (e.g., disease, parasitism, starvation; Mannella, 2006*a*). By investigating mitochondrial behavior and morphology, we can understand the proximate mechanisms that are causally responsible for variation in animal performance, as opposed simply to characterizing further the variation itself.

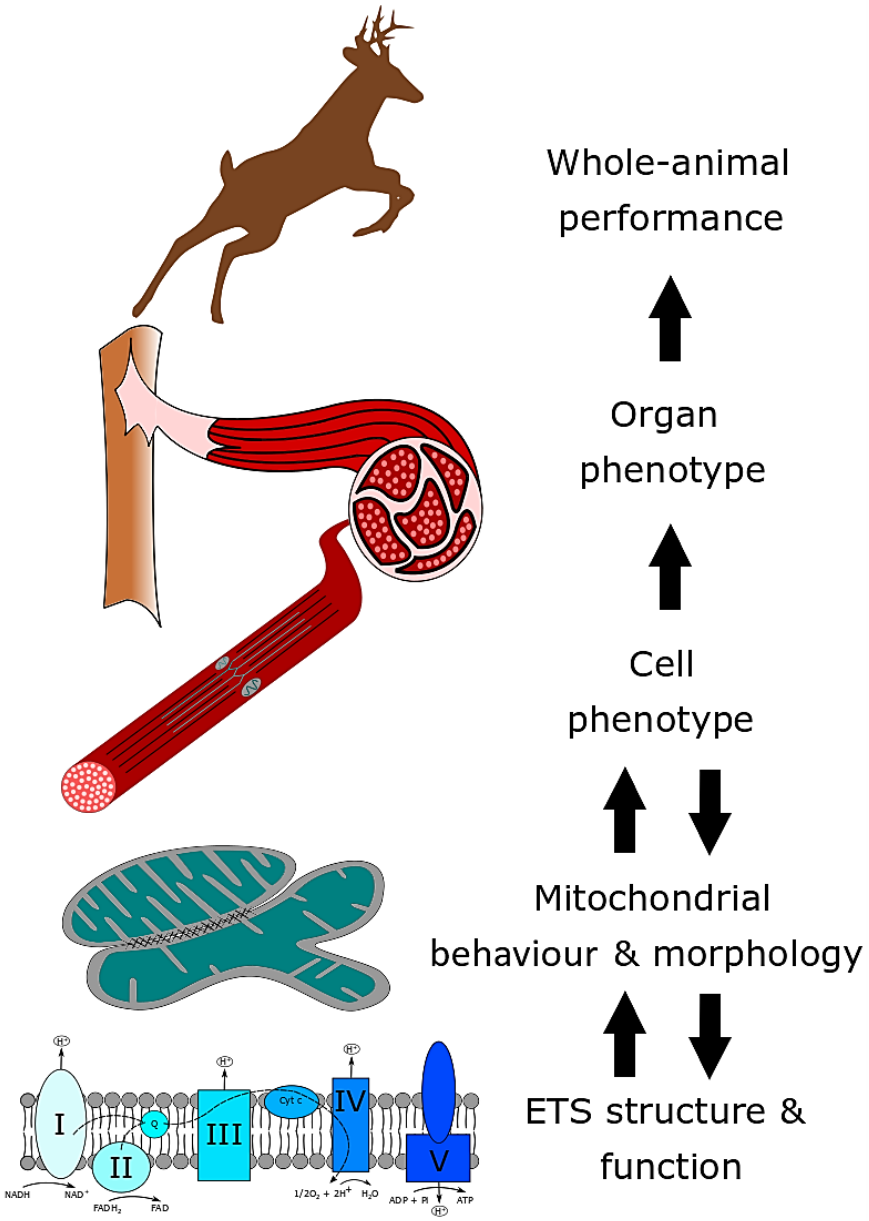

Figure 1.1. Illustration of how variation in morphology and organization within and between mitochondria translates to variation in whole-animal performance. From the bottom of the figure, the structure and function of the electron transport system (ETS) influences the behavior and morphology of mitochondria, which influence cell phenotype. In turn, cell phenotype influences organ phenotype, leading to variation in whole-animal performance. Cell phenotype may also influence mitochondrial behavior and morphology, leading to changes in structure and function of the ETS. Cyt c, cytochrome c; FAD, oxidized flavin adenine dinucleotide; $FADH_2$, reduced flavin adenine dinucleotide; NAD^+, oxidized nicotinamide adenine dinucleotide; NADH, reduced nicotinamide adenine dinucleotide; Q, ubiquinone; I, NADH dehydrogenase; II, succinate dehydrogenase; III, cytochrome c reductase; IV, cytochrome c oxidase; V, ATP synthase.

This review outlines how mitochondrial behavior and morphology are inherently linked to animal performance by first discussing how mitochondrial behavior and morphology directly influence mitochondrial performance. In addition, we outline how mitochondrial morphology and performance are both influenced by, and directly alter, oxidative stress. We briefly summarize how measures of mitochondrial behavior and morphology are predicted to offer insight into our understanding of individual and species-specific variation in reproductive performance and reproductive strategies, respectively. Lastly, we provide an overview of how future research may better clarify the link between mitochondrial morphology and variation in animal performance, both among individuals within populations and among closely related taxa that have developed variants of certain life-history strategies.

MITOCHONDRIAL BEHAVIOR, MORPHOLOGY, AND PERFORMANCE

To understand how mitochondria are linked to organism performance, we must first understand how mitochondrial behavior and morphology influence mitochondrial performance. Mitochondria are highly dynamic organelles that continuously change their function, position, and structure to meet the energetic demands of any given cell (Zick *et al.*, 2009; Rafelski, 2013). To do so, individual mitochondria not only undergo fission and fusion, but readily change their size and relative proportions of inner membrane, inter-membrane space, matrix, and outer membrane, density (Mannella, 2006*b*), and structural connections with one another (**Figure 1.2**). These changes form the foundation from which mitochondria can respond to changes in energetic demand (Paumard *et al.*, 2002).

Variation in organism performance has been attributed to variation in mitochondrial physiology (e.g., Salin *et al.*, 2012, 2015; Zhang & Hood, 2016; Mowry *et al.*, 2017; Hill *et al.*, 2019). Genetic and environmental factors can have direct impacts on animal performance such as lifespan and reproductive output (Navarro *et al.*, 2005; Liau *et al.*, 2007), but they also affect mitochondrial morphology (Sogo & Yaffe, 1994; Visser *et al.*, 1995; Zick *et al.*, 2009; Putti *et al.*, 2016). In particular, energy production can increase significantly from changes in the morphology of the inner mitochondrial

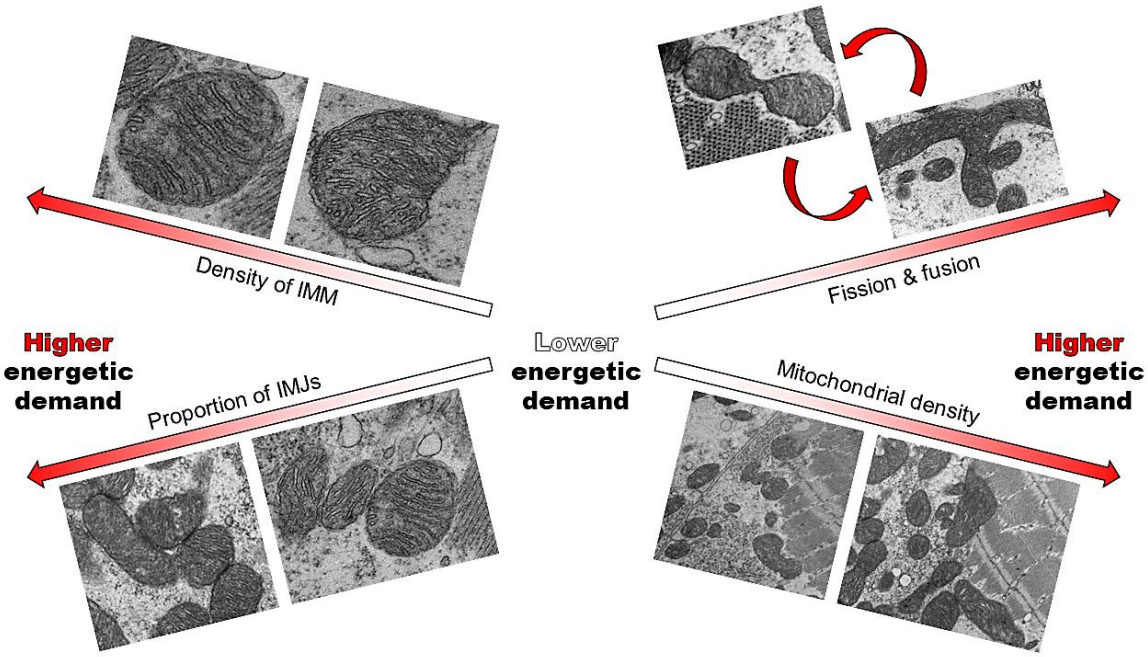

Figure 1.2. Proposed changes in mitochondrial behavior and morphology under increased energetic demand. Includes: density of inner mitochondrial membrane (IMM), proportion of inter-mitochondrial junctions (IMJs), mitochondrial density, and mitochondrial fission and fusion. The first three traits are predicted to increase (to an extent) under increased energetic demand, whereas the rates of fission and fusion will depend on the need to discard damaged regions of mitochondria and rescue organelle disfunction. The proportions of these traits relative to one another influence the function of each individual mitochondrion and cellular function as a whole. All micrographs are of myocytes of the copepod *Tigriopus californicus*.

membrane (IMM; Mannella *et al.*, 2013; Nielsen *et al.*, 2017; Afzal *et al.*, 2019). Previous work using cryo-electron tomography in rat liver and cattle heart has shown that cristae structure modulates bioenergetic capacity through the positioning of ATP synthase dimers and the folding of cristae (Strauss *et al.*, 2008; Cogliati *et al.*, 2016). Additionally, inter-mitochondrial junctions (IMJs) are present in greater proportions in more active types of tissue (e.g., heart and diaphragm; Picard *et al.*, 2015) and also increase in density following a rise in metabolic demand from events such as running (Picard *et al.*, 2013*a*). IMJs are electron-dense regions connecting two or more adjacent mitochondria (**Figure 1.3**; Duvert *et al.*, 1985), where the cristae of adjacent mitochondria align in a parallel fashion. This form of 'kissing communication' between mitochondria has been linked to cardiac function in rats (Cao & Zheng, 2019) and exercise in mice (Picard *et al.*, 2013*a*;

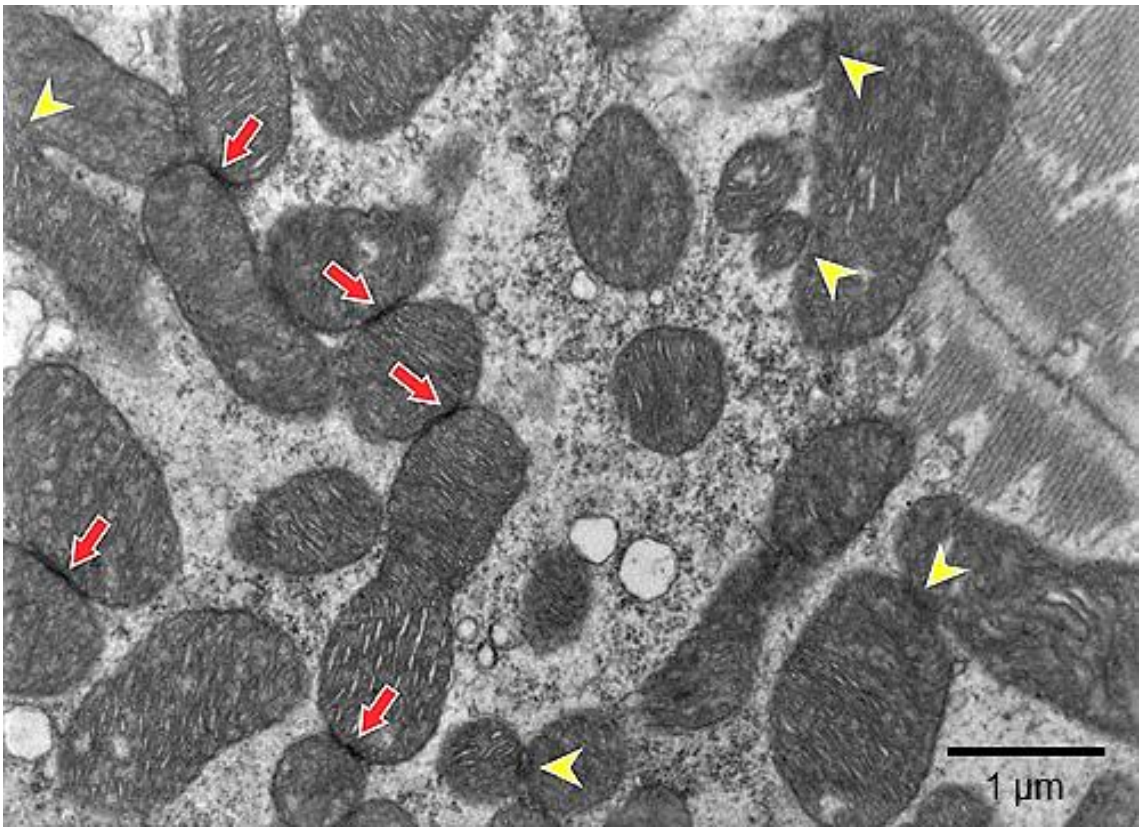

Figure 1.3. Transmission electron micrograph of a myocyte from the copepod *Tigriopus californicus*. Electron-dense (darker regions) inter-mitochondrial junctions are shown by red arrows. Contact sites showing no increase in electron density (lighter regions) between mitochondria are shown by yellow arrowheads.

see also Daghistani *et al.*, 2018). Thus, the density of IMM and proportion of IMJs may be crucial morphological components of mitochondrial performance.

The relative area covered by the IMM has a direct impact on ATP production. Protein complexes I, III, and IV of the electron transport system (ETS) are embedded within the inner membrane and are responsible for pumping protons across the IMM into the inter-membrane space, as Complex II delivers electrons to the quinone pool where they also enter the ETS through Complex I (**Figure 1.1**). This proton gradient ultimately leads to the production of ATP as protons flow down an electrochemical gradient and through Complex V, as Complex IV reduces oxygen to water (Hatefi, 1985). The presence of complexes I–V, and their proportion relative to the amount of inter-membrane space, mitochondrial matrix, and mitochondrial size, directly influences the amount of ATP any given mitochondrion can produce (**Figures 1.1** and **1.2**; Afzal *et al.*,

2019). A greater amount of IMM can be populated with more ETS complexes, but this change may come with costs of increased oxidative stress (see Section III). For example, Strohm & Daniels (2003) correlated an increase in density of IMM within the flight muscle mitochondria of beewolf wasps (*Philanthus triangulum*) with the wasps' ability to provision honeybees to their offspring. In this example, wasps with a greater energetic capacity of their flight muscles were able to collect and carry more bees back to their broods within a given amount of time. Such work has demonstrated that a greater density of the IMM may be linked to greater reproductive success. However, area of the IMM is not the only morphological feature that impacts functional capacity.

Not only do protein complexes embedded in the IMM contribute to its morphology (Paumard *et al.*, 2002), but fission and fusion of the IMM directly influence the formation of cristae (Mannella, 2006*b*) and efficiency of the ETS [see Zick *et al.* (2009) for a review of how protein function is related to cristae morphology; Chen *et al.*, 2011; Cogliati *et al.*, 2016]. Such changes resulting from fission and fusion processes can regulate different mitochondrial conformations (condensed, orthodox, etc.) that result from changes in energetic demand and/or nutrient availability (Hackenbrock, 1966). As is the case in bacteria (Lane, 2006), the size of mitochondria is directly linked to efficiency of the ETS within any given cell, limiting the amount of IMM that can exist within a single mitochondrion. However, density of IMM cannot increase indefinitely with mitochondrial size, as respiratory efficiency may decrease when mitochondrial volume and density of IMM greatly exceed the surface area of the mitochondrion (Navratil *et al.*, 2008); this may be one of many reasons why there are thousands rather than a few mitochondria within a given cell. Additionally, mitochondrial function can be upregulated by increasing mitochondrial density irrespective of the density of IMM. Therefore, mitochondrial function can be altered beyond changes in morphology through changes in mitochondrial behavior.

Herein, mitochondrial behavior refers to the movement and position of mitochondria within cells, including their position relative to other mitochondria that may possibly mediate communication between mitochondrial tubules. These mitochondrial movements stem, in part, from changes in mitochondrial morphology. One of the most recent strides in understanding mitochondrial morphology, and therefore behavior, is the

study of IMJs (Bakeeva *et al.*, 1983; Picard *et al.*, 2015). Two aspects of these structures infer why they likely influence mitochondrial function: (*i*) the alignment of cristae at a right angle to the IMJ and (*ii*) the increased proportion of IMJs in tissues with greater energetic demands (Picard *et al.*, 2015).

The alignment of cristae at IMJs has been suggested to regulate the communication of information between mitochondria, including gene expression (Ng & Bassler, 2009) and/or the transfer of electrochemical gradients (Ichas *et al.*, 1997; Pacher & Hajnoczky, 2001; Santo-Domingo *et al*., 2013); this would ultimately mediate differential function of mitochondrial populations, however, this relationship must be confirmed through empirical research. For example, in myocytes of *Mus musculus*, populations of inter-myofibrillar and subsarcolemmal mitochondria differ significantly in their morphology (Picard *et al.*, 2012) and, therefore, likely their function. Similar examples have been found in bar-headed geese (*Anser indicus*), where subsarcolemmal mitochondria are redistributed near the cell membrane to facilitate greater diffusion of oxygen in flight muscles at high altitudes (Storz *et al.*, 2010). A greater proportion of IMJs was also found in both inter-myofibrillar and subsarcolemmal mitochondria immediately following a single bout of exercise in mice, indicative of increased metabolic function (Picard *et al.*, 2013*a*). If IMJs are tightly coupled to mitochondrial function, then the presence of these structures may influence adaptations of life-history strategies that rely heavily on increased mitochondrial performance. For example, in outbred laboratory mice, food intake gradually increases to match energy demands until peak lactation when nutrient intake is five times greater than that of non-reproductive animals (Speakman & Król, 2005). Just as exercise increases the density of IMJs in skeletal muscle, the same may be true for mitochondria in the liver which provide energy needed for the mammary glands and milk synthesis.

Aside from changes in mitochondrial ultrastructure, metabolic function can also be influenced by non-morphological changes, for example, through increases in the amount of free intra-mitochondrial Ca^{2+} (McCormack *et al.*, 1990) or permeability of the IMM (Brand *et al.*, 1991). However, changes in metabolic function without changes in mitochondrial structure can only occur within certain limits. For instance, to increase the rate of conversion of ADP to ATP, a mitochondrion may increase the amount of substrate

available within the mitochondrial matrix through several intra- and extracellular pathways such as those involving the supply of fatty acids (Brown, 1992). Such events may then lead to a greater proton gradient within the inter-membrane space as more electrons are passed across the IMM. However, without any significant change in mitochondrial size or the number of complexes embedded in a more densely packed IMM, there is likely a hard limit on the quantity of protons that can be pumped at a given rate into an inter-membrane space of a given size without a change in morphology (Willis *et al*., 2016).

Significant increases in density of the IMM within mitochondria (Mannella, 2006*b*; Nielsen *et al.*, 2017) and the proportion of IMJs within a cell (Picard *et al.*, 2015) could influence tissue function and, therefore, whole-organism performance (e.g., Strohm & Daniels, 2003). However, the proximate function of IMJs warrants further research, and it remains to be established whether these relationships are causal or correlative. If changes in these two traits favour increased ATP production, then organisms that develop favourable changes in these traits may be able to develop more energetically demanding and successful means of reproduction (e.g., greater mate guarding durations, increased clutch size, greater provisioning of resources to young). Provided that certain aspects of mitochondrial behavior and morphology vary among individuals and are heritable, such changes may be inherited by offspring of reproductively successful individuals and account for individual, if not species-specific, variation in animal performance. Not only is mitochondrial ultrastructure, along with fission and fusion dynamics, heritable in yeast (Sogo & Yaffe, 1994), but differences in the distribution of subsarcolemmal mitochondria have evolved in bar-headed geese in comparison to other species, irrespective of phylogenetic relatedness (Scott *et al.*, 2009).

Changes in mitochondrial morphology between individuals within populations is predicted to be exacerbated across populations of organisms and closely related taxa as selective pressures change over evolutionary time. Future research should aim to understand how the behavior and morphology of mitochondria change in response to adverse and detrimental conditions that affect whole-animal performance, such as aging and the collapse of biological systems (Gottschling & Nystrom, 2017). As we have outlined above, the function of mitochondria is often linked to mitochondrial behavior

and morphology. However, such molecular studies should be interpreted with care, and the limitations of using experimental as opposed to natural systems should be made explicit and discussed at length (Picard *et al*., 2013*b*). Additionally, mitochondrial behavior and morphology likely play formative roles in the regulation of, and damage due to, oxidative stress, which ultimately influences mitochondrial function.

OXIDATIVE STRESS AND MITOCHONDRIAL MORPHOLOGY

Mitochondrial behavior and morphology directly impact mitochondrial performance, however, the production of ATP is only a single variable among a suite of traits that impact both cellular and organismal performance (Eisner *et al.*, 2018). Therefore, we must take into account other traits that change in relation to mitochondrial function. One such trait that has a major impact on ETS function is the production of reactive oxygen species (ROS). ROS are produced by a number of endogenous (e.g., oxidative phosphorylation) and exogenous (e.g., radiation) factors and inevitably impact the stability and performance of mitochondria (Zhang *et al*., 2017) and, therefore, whole-animal performance (Zhang *et al.*, 2018; Heine *et al*., 2019).

ROS are highly reactive molecules that contain oxygen (e.g., hydrogen peroxide, hydroxyl radicals, superoxide) and are formed, in part, as byproducts of the ETS. Due to the reactive nature of ROS, these molecules can readily damage DNA, lipids, and proteins within the cell (Finkel & Holbrook, 2000) and have the potential to decrease mitochondrial function and/or act as signaling molecules (Zhang *et al*., 2017; Hood *et al.*, 2018, 2019). To mediate ROS-induced damage and improve performance, mitochondria can alter their behavior and morphology to reduce and/or repair oxidative damage. This can be accomplished through fission and fusion dynamics that either eliminate damaged regions of mitochondria or rescue organelle disfunction, respectively (Westermann, 2010). These dynamics likely result from significant changes in membrane morphology (Cogliati *et al.*, 2016; Cao & Zheng, 2019) and may stem from (or produce) IMJs, although IMJs are present following the knockout of proteins responsible for inter-mitochondrial tethering (mitofusins 1 and 2). Further evidence suggests that IMJs are closely related to increased mitochondrial function (Picard *et al.*, 2015). Additionally, the density of IMM may directly influence the regulation of ROS.

Oxidative damage is known to induce mitochondrial fragmentation *via* lipid peroxidation (Fan *et al.*, 2010) and, therefore, significantly remodel mitochondrial structure. This can occur either directly *via* oxidative damage to IMM or indirectly through mitochondrial fission and repair mechanisms, changing the density of IMM within a mitochondrion of a given size. In both cases, the amount of ATP produced is likely to change under elevated ROS production. Although ATP production can be upregulated from a more densely packed IMM (Nielsen *et al.*, 2017), we should consider whether or not this benefit is balanced against the cost of increased ROS production and oxidative damage (see Strohm & Daniels, 2003). Aside from antioxidants that are capable of quenching ROS (Ristow, 2014), ROS can be regulated through changes in morphology as mentioned above. Since IMJs and density of IMM have been linked to increased energetic demand (Mannella, 2006*a*; Picard *et al.*, 2013*a*; Afzal *et al.*, 2019), it is plausible that these traits regulate mitochondrial function concurrently in response to oxidative stress.

ANIMAL PERFORMANCE AND REPRODUCTIVE SUCCESS

The ability to maximize ATP production to support reproductive performance could begin with changes in mitochondrial behavior and morphology that improve bioenergetic efficiency. Within a given population, we predict that individuals that are most efficient at converting available nutrients into ATP will typically have higher reproductive success than those that do so less efficiently. Greater efficiency of ATP production will be achieved, in part, by changes in mitochondrial behavior and morphology.

Reproductive success can be defined as the ability of an organism to produce viable offspring (Clutton-Brock, 1988); this can be viewed as the number of offspring produced either per reproductive bout or over an organism's lifetime and varies greatly among eukaryotic organisms. Different species and taxonomic groups vary in the strategy used to maximize reproductive performance (e.g., gestation, iteroparity, lactation, mate guarding), and individuals vary in their capacity to allocate resources to, and modify, each of these variables. For instance, variation in reproductive success is often linked to body size (Clutton-Brock, 1985; Bosch & Vicens, 2006; Milenkaya *et al.*, 2015),

however, body size alone explains a small portion of variation in reproductive success. To carry out the aforementioned strategies, organisms must have access to sufficient food or stored nutrients to elevate ATP production well above maintenance. When access to ATP is sufficient, an organism should be able to fuel any changes in morphology and organ structure that support gamete production, mating, and offspring nourishment. Further, any individual that is able to allocate relatively more resources to reproduction is likely to achieve enhanced reproductive success *via* the production of more and/or higher quality offspring. This energy is produced almost entirely by mitochondria and regulated, in part, by mitochondrial behavior and morphology. For energy to be allocated efficiently to reproduction, mitochondria must up- or downregulate energy production, as required, across different types of tissue and organs. Although increased energy intake can be important in accomplishing this, how nutrients are utilized within the mitochondrion is influenced by mitochondrial structure. Therefore, energy allocation to reproductive strategies, through changes in mitochondrial behavior and morphology, largely influences variation in reproductive success.

Numerous reproductive strategies exist among eukaryotic organisms. Although vast differences exist between taxa, individuals of the same species in the same environment may differ in the number and quality of the young they produce. Both genetic and environmental factors influence strategies of reproduction. As a consequence, reproductive strategies have evolved over large time scales to maximize reproductive success under typical conditions, but short-term plasticity allows animals to modify their effort to match current conditions and their physiological state (Bernardes, 1996; Gross, 1996). Therefore, intra- or interspecific differences in energy allocation to reproduction likely stem from differences in physiology. Mate guarding is a prime example of a reproductive strategy that can be highly energetically demanding and varies greatly among extant taxa (Grafen & Ridley, 1983; Boxshall, 1990) but also varies at an individual level (Tsuboko-Ishii & Burton, 2017), leading to differential reproductive success. For such energetically demanding behaviors to be sustained, large amounts of energy would need to be produced over short periods of time. In addition to reproductive success, changes in mitochondrial behavior and morphology are also likely to occur

following high energetic demands of other performance correlates, such as rapid development, response to an immune challenge, and migration.

CONCLUSIONS

(1) The behavior and morphology of mitochondria play a vital role in efficient ATP production. Although research to date has successfully characterized variation in animal performance and energy expenditure, we do not fully understand the physiology behind how that variation in energy production develops. We propose that individual differences in the behavior and morphology of mitochondria contribute to variation in energetic capacity among individuals.

(2) Further, we propose that the development of energetically demanding behaviors and life-history strategies are enhanced by the behavior and morphology of mitochondria that increase ATP production in relevant organs. In particular, we argue that an increase in the proportion of IMJs and density of the IMM facilitate an upregulation of ATP production.

(3) The hypothesis presented here provides a mechanism for how energy production can vary among individuals within populations and between closely related taxa, partly leading to some of the variation we see in animal performance. Yet, there are currently few data that support these ideas in an ecological context. We believe that evaluating the relationships between mitochondrial behavior, morphology, and animal performance will be a fruitful avenue of research. We encourage others to consider the importance of variation in mitochondrial behavior and morphology in both intra- and interspecific variation in animal performance and reproductive success.

REFERENCES

Afzal, N., Mannella, C., Lederer, W. J. & Jafri, M. S. (2019). Mitochondrial metabolic function is affected by inner membrane morphology. *Biophysical Journal* **116**, 266a-267a.

Bakeeva, L. E., Chentsov, Y. S. & Skulachev, V. P. (1983). Intermitochondrial contacts in myocardiocytes. *Journal of Molecular & Cellular Cardiology* **15**, 413-420.

Bernardes, A. T. (1996). Strategies for reproduction and ageing. *Annalen der Physik* **508**, 539-549.

Biro, P. A. & Stamps, J. A. (2010). Do consistent individual differences in metabolic rate promote consistent individual differences in behavior? *Trends in Ecology & Evolution* **25**, 653-659.

Bosch, J. & Vicens, N. (2006). Relationship between body size, provisioning rate, longevity and reproductive success in females of the solitary bee *Osmia cornuta*. *Behavioral Ecology & Sociobiology* **60**, 26-33.

Boxshall, G. A. (1990). Precopulatory mate guarding in copepods. *Bijdragen tot de Dierkunde* **60**, 209-213.

Brand, M. D., Couture, P., Else, P. L., Withers, K. W. & Hulbert, A. J. (1991). Evolution of energy metabolism. Proton permeability of the inner membrane of liver mitochondria is greater in a mammal than in a reptile. *Biochemical Journal* **275**, 81-86.

Brown, G. C. (1992). Control of respiration and ATP synthesis in mammalian mitochondria and cells. *Biochemical Journal* **284**, 1-13.

Burton, T., Killen, S. S., Armstrong, J. D. & Metcalfe, N. B. (2011). What causes intraspecific variation in resting metabolic rate and what are its ecological consequences? *Proceedings of the Royal Society B: Biological Sciences* **278**, 3465-3473.

Cao, Y. P. & Zheng, M. (2019). Mitochondrial dynamics and inter-mitochondrial communication in the heart. *Archives of Biochemistry & Biophysics* **663**, 214-219.

Chen, Y., Liu, Y. & Dorn, G. W. (2011). Mitochondrial fusion is essential for organelle function and cardiac homeostasis. *Circulation Research* **109**, 1327-1331.

Clutton-Brock, T. H. (1985). Reproductive success in red deer. *Scientific American* **252**, 86-93.

Clutton-Brock, T. H. (1988). Reproductive success: studies of individual variation in contrasting breeding systems. University of Chicago Press. Chicago, IL.

Cogliati, S., Enriquez, J. A. & Scorrano, L. (2016). Mitochondrial cristae: where beauty meets functionality. *Trends in Biochemical Sciences* **41**, 261-273.

Daghistani, H. M., Rajab, B. S. & Kitmitto, A. (2018). Three-dimensional electron microscopy techniques for unravelling mitochondrial dysfunction in heart failure and identification of new pharmacological targets. *British Journal of Pharmacology* **176**, 4340-4359.

Drent, R. H. & Daan, S. (1980). The prudent parent: energetic adjustments in avian breeding. *Ardea* **68**, 225-252.

Duvert, M., Mazat, J. P. & Barets, A. L. (1985). Intermitochondrial junctions in the heart of the frog, *Rana esculenta*. *Cell & Tissue Research* **241**, 129-137.

Eisner, V., Picard, M. & Hajnóczky, G. (2018). Mitochondrial dynamics in adaptive and maladaptive cellular stress responses. *Nature Cell Biology* **20**, 755-765.

Fan, X., Hussien, R. & Brooks, G. A. (2010). H2O2-induced mitochondrial fragmentation in C2C12 myocytes. *Free Radical Biology & Medicine* **49**, 1646-1654.

Finkel, T. & Holbrook, N. J. (2000). Oxidants, oxidative stress and the biology of ageing. *Nature* **408**, 239-247.

Gittleman, J. L. & Thompson, S. D. (1988). Energy allocation in mammalian reproduction. *American Zoologist* **28**, 863-875.

Gottschling, D. E. & Nyström, T. (2017). The upsides and downsides of organelle interconnectivity. *Cell* **169**, 24-34.

Grafen, A. & Ridley, M. (1983). A model of mate guarding. *Journal of Theoretical Biology* **102**, 549-567.

Gross, M. R. (1996). Alternative reproductive strategies and tactics: diversity within sexes. *Trends in Ecology & Evolution* **11**, 92-98.

Hackenbrock, C. R. (1966). Ultrastructural bases for metabolically linked mechanical activity in mitochondria: I. Reversible ultrastructural changes with change in metabolic steady state in isolated liver mitochondria. *The Journal of Cell Biology* **30**, 269-297.

Hatefi, Y. (1985). The mitochondrial electron transport and oxidative phosphorylation system. *Annual Review of Biochemistry* **54**, 1015-1069.

Heine, K. B., Powers, M. J., Kallenberg, C., Tucker, V. L. & Hood, W. R. (2019). Ultraviolet irradiation increases size of the first clutch but decreases longevity in a marine copepod. *Ecology & Evolution* **9**, 9759-9767.

Hill, G. E., Hood, W. R., Ge, Z., Grinter, R., Greening, C., Johnson, J. D., Park, N. R., Taylor, H. A., Andreasen, V. A., Powers, M. J., Justyn, N. M., Parry, H. A., Kavazis, A. N. & Yufeng, Z. (2019). Plumage redness signals mitochondrial function in the house finch. *Proceedings of the Royal Society B* **286**, 20191354.

Hood, W. R., Zhang, Y., Mowry, A. V., Hyatt, H. W. & Kavazis, A. N. (2018). Life history trade-offs within the context of mitochondrial hormesis. *Integrative & Comparative Biology* **58**, 567-577.

Hood, W. R., Zhang, Y., Taylor, H. A., Park, N. R., Beatty, A. E., Weaver, R. J., Yap, K. N. & Kavazis, A. N. (2019). Prior reproduction alters how mitochondria respond to an oxidative event. *Journal of Experimental Biology* **222**, jeb195545.

Ichas, F., Jouaville, L. S. & Mazat, J. P. (1997). Mitochondria are excitable organelles capable of generating and conveying electrical and calcium signals. *Cell* **89**, 1145-1153.

Kenagy, G. J., Masman, D., Sharbaugh, S. M. & Nagy, K. A. (1990). Energy expenditure during lactation in relation to litter size in free-living golden-mantled ground squirrels. *The Journal of Animal Ecology* **59**, 73-88.

Lane, N. (2006). Power, sex, suicide: mitochondria and the meaning of life. Oxford University Press. Oxford, ENG.

Liau, W. S., Gonzalez-Serricchio, A. S., Deshommes, C., Chin, K. & LaMunyon, C. W. (2007). A persistent mitochondrial deletion reduces fitness and sperm performance in heteroplasmic populations of *C. elegans*. *BMC genetics* **8**, 8.

Mannella, C. A. (2006*a*). The relevance of mitochondrial membrane topology to mitochondrial function. *Biochimica et Biophysica Acta (BBA)-Molecular Basis of Disease* **1762**, 140-147.

Mannella, C. A. (2006*b*). Structure and dynamics of the mitochondrial inner membrane cristae. *Biochimica et Biophysica Acta (BBA)-Molecular Cell Research* **1763**, 542-548.

Mannella, C. A., Lederer, W. J. & Jafri, M. S. (2013). The connection between inner membrane topology and mitochondrial function. *Journal of Molecular & Cellular Cardiology* **62**, 51-57.

McBride, R. S., Somarakis, S., Fitzhugh, G. R., Albert, A., Yaragina, N. A., Wuenschel, M. J., Alonso-Fernández, A. & Basilone, G. (2015). Energy acquisition and allocation to egg production in relation to fish reproductive strategies. *Fish & Fisheries* **16**, 23-57.

McCormack, J. G., Halestrap, A. P. & Denton, R. M. (1990). Role of calcium ions in regulation of mammalian intramitochondrial metabolism. *Physiological Reviews* **70**, 391-425.

Milenkaya, O., Catlin, D. H., Legge, S. & Walters, J. R. (2015). Body condition indices predict reproductive success but not survival in a sedentary, tropical bird. *PLoS ONE* **10**, e0136582.

Mowry, A. V., Donoviel, Z. S., Kavazis, A. N. & Hood, W. R. (2017). Mitochondrial function and bioenergetic trade-offs during lactation in the house mouse (*Mus musculus*). *Ecology & Evolution* **7**, 2994-3005.

Navarro, A., Gómez, C., Sánchez-Pino, M. J., González, H., Bández, M. J., Boveris, A. D. & Boveris, A. (2005). Vitamin E at high doses improves survival, neurological performance, and brain mitochondrial function in aging male mice. *American Journal of Physiology-Regulatory, Integrative & Comparative Physiology* **289**, R1392-R1399.

Navratil, M., Terman, A. & Arriaga, E. A. (2008). Giant mitochondria do not fuse and exchange their contents with normal mitochondria. *Experimental Cell Research* **314**, 164-172.

Ng, W. L. & Bassler, B. L. (2009). Bacterial quorum-sensing network architectures. *Annual Reviews of Genetics* **43**, 197-222.

Nielsen, J., Gejl, K. D., Hey-Mogensen, M., Holmberg, H. C., Suetta, C., Krustrup, P., Elemans, C. P. & Ørtenblad, N. (2017). Plasticity in mitochondrial cristae density allows metabolic capacity modulation in human skeletal muscle. *The Journal of Physiology* **595**, 2839-2847.

Pacher, P. & Hajnoczky, G. (2001). Propagation of the apoptotic signal by mitochondrial waves. *The EMBO Journal* **20**, 4107-4121.

Paumard, P., Vaillier, J., Coulary, B., Schaeffer, J., Soubannier, V., Mueller, D. M., Brèthes, D., di Rago, J. P. & Velours, J. (2002). The ATP synthase is involved in generating mitochondrial cristae morphology. *The EMBO Journal* **21**, 221-230.

Picard, M., Gentil, B. J., McManus, M. J., White, K., Louis, K. S., Gartside, S. E., Wallace, D. C. & Turnbull, D. M. (2013*a*). Acute exercise remodels mitochondrial membrane interactions in mouse skeletal muscle. *Journal of Applied Physiology* **115**, 1562-1571.

Picard M., McManus, M. J., Csordás, G., Várnai, P., Dorn II, G. W., Williams, D., Hajnóczky, G. & Wallace, D. C. (2015). Trans-mitochondrial coordination of cristae at regulated membrane junctions. *Nature Communications* **6**, 6259.

Picard, M., Shirihai, O. S., Gentil, B. J. & Burelle, Y. (2013*b*). Mitochondrial morphology transitions and functions: implications for retrograde signaling? *American Journal of Physiology-Regulatory, Integrative & Comparative Physiology* **304**, R393-R406.

Picard, M., White, K. & Turnbull, D. M. (2012). Mitochondrial morphology, topology and membrane interactions in skeletal muscle: A quantitative three-dimensional

electron microscopy study. *American Journal of Physiology-Heart & Circulatory Physiology* **114**, 161-171.

Putti, R., Migliaccio, V., Sica, R. & Lionetti, L. (2016). Skeletal muscle mitochondrial bioenergetics and morphology in high fat diet induced obesity and insulin resistance: focus on dietary fat source. *Frontiers in Physiology* **6**, 426.

Rafelski, S. M. (2013). Mitochondrial network morphology: building an integrative, geometrical view. *BMC Biology* **11**, 71.

Reinhold, K. (1999). Energetically costly behaviour and the evolution of resting metabolic rate in insects. *Functional Ecology* **13**, 217-224.

Ristow, M. (2014). Unraveling the truth about antioxidants: mitohormesis explains ROS-induced health benefits. *Nature Medicine* **20**, 709-711.

Salin, K., Auer, S. K., Rey, B., Selman, C. & Metcalfe, N. B. (2015). Variation in the link between oxygen consumption and ATP production, and its relevance for animal performance. *Proceedings of the Royal Society B: Biological Sciences* **282**, 20151028.

Salin, K., Luquet, E., Rey, B., Roussel, D. & Voituron, Y. (2012). Alteration of mitochondrial efficiency affects oxidative balance, development and growth in frog (*Rana temporaria*) tadpoles. *Journal of Experimental Biology* **215**, 863-869.

Salin, K., Villasevil, E. M., Anderson, G. J., Lamarre, S. G., Melanson, C. A., McCarthy, I., Selman, C. & Metcalfe, N. B. (2019). Differences in mitochondrial efficiency explain individual variation in growth performance. *Proceedings of the Royal Society B* **286**, 20191466.

Santo-Domingo, J., Giacomello, M., Poburko, D., Scorrano, L. & Demaurex, N. (2013). OPA1 promotes pH flashes that spread between contiguous mitochondria without matrix protein exchange. *The EMBO Journal* **32**, 1927-1940.

Scantlebury, M., Butterwick, R. & Speakman, J. R. (2001). Energetics and litter size variation in domestic dog *Canis familiaris* breeds of two sizes. *Comparative Biochemistry and Physiology Part A: Molecular & Integrative Physiology* **129**, 919-931.

Schrepfer, E. & Scorrano, L. (2016). Mitofusins, from mitochondria to metabolism. *Molecular Cell* **61**, 683-694.

Scott, G. R., Egginton, S., Richards, J. G. & Milsom, W. K. (2009). Evolution of muscle phenotype for extreme high altitude flight in the bar-headed goose. *Proceedings of the Royal Society B: Biological Sciences* **276**, 3645-3653.

Sogo, L. F. & Yaffe, M. P. (1994). Regulation of mitochondrial morphology and inheritance by Mdm10p, a protein of the mitochondrial outer membrane. *The Journal of Cell Biology* **126**, 1361-1373.

Speakman, J. R., Blount, J. D., Bronikowski, A. M., Buffenstein, R., Isaksson, C., Kirkwood, T. B., Monaghan, P., Ozanne, S. E., Beaulieu, M., Briga, M. & Carr, S. K. (2015). Oxidative stress and life histories: unresolved issues and current needs. *Ecology & Evolution* **5**, 5745-5757.

Speakman, J. R. & Król, E. (2005). Limits to sustained energy intake IX: a review of hypotheses. *Journal of Comparative Physiology B* **175**, 375-394.

Storz, J. F., Scott, G. R. & Cheviron, Z. A. (2010). Phenotypic plasticity and genetic adaptation to high-altitude hypoxia in vertebrates. *Journal of Experimental Biology* **213**, 4125-4136.

Strauss, M., Hofhaus, G., Schröder, R. R. & Kühlbrandt, W. (2008). Dimer ribbons of ATP synthase shape the inner mitochondrial membrane. *The EMBO Journal* **27**, 1154-1160.

Strohm, E. & Daniels, W. (2003). Ultrastructure meets reproductive success: performance of a sphecid wasp is correlated with the fine structure of the flight–muscle mitochondria. *Proceedings of the Royal Society London B, Biological Science* **270**, 749-754.

Tsuboko-Ishii, S. & Burton, R. S. (2017). Sex-specific rejection in mate-guarding pair formation in the intertidal copepod, *Tigriopus californicus*. *PLoS One* **12**, e0183758.

Visser, W., van Spronsen, E. A., Nanninga, N., Pronk, J. T., Kuenen, J. G. & van Dijken, J. P. (1995). Effects of growth conditions on mitochondrial morphology in *Saccharomyces cerevisiae*. *Antonie Van Leeuwenhoek* **67**, 243-253.

Westermann, B. (2010). Mitochondrial fusion and fission in cell life and death. *Nature Reviews Molecular Cell Biology* **11**, 872-884.

Willis, W. T., Jackman, M. R., Messer, J. I., Kuzmiak-Glancy, S. & Glancy, B. (2016). A simple hydraulic analog model of oxidative phosphorylation. *Medicine & Science in Sports & Exercise* **48**, 990-1000.

Youle, R. J. & Van Der Bliek, A. M. (2012). Mitochondrial fission, fusion, and stress. *Science* **337**, 1062-1065.

Zhang, Y., Brasher, A. L., Park, N. R., Taylor, H. A., Kavazis, A. N. & Hood, W. R. (2018). High activity before breeding improves reproductive performance by

enhancing mitochondrial function and biogenesis. *Journal of Experimental Biology* **221**, 177469.

Zhang, Y. & Hood, W. R. (2016). Current versus future reproduction and longevity: a re-evaluation of predictions and mechanisms. *Journal of Experimental Biology* **219**, 3177-3189.

Zhang, Y., Humes, F., Almond, G., Kavazis, A. N. & Hood, W. R. (2017). A mitohormetic response to pro-oxidant exposure in the house mouse. *American Journal of Physiology-Regulatory, Integrative & Comparative Physiology* **314**, R122-R134.

Zick, M., Rabl, R. & Reichert, A. S. (2009). Cristae formation—linking ultrastructure and function of mitochondria. *Biochimica Biophysica Acta - Molecular Cell Research* **1793**, 5-19.

Chapter 2: **Ultraviolet irradiation increases size of the first clutch but decreases longevity in a marine copepod**

Published with Matthew J. Powers, Christine Kallenberg, Victoria L. Tucker, and Wendy R. Hood (2019) in *Ecology and Evolution* **9**(17), 9759-9767

INTRODUCTION

The life history of sexually reproducing organisms can vary greatly both within and between populations and is influenced by numerous endogenous and exogenous factors (Fisher, 1930; Stearns, 2000). To understand this variation, it is important to delineate how the environment influences survival and reproductive success. For organisms to survive and achieve reproductive success in the face of changing environments, they must balance the costs and benefits of exogenous stressors with maintaining basic metabolic functions, surviving to reproductive age, and producing viable offspring (Williams, 1966; Speakman, 2008). Many exogenous stressors to which organisms are exposed can have beneficial effects on organism performance at certain levels of exposure but detrimental effects at other levels of exposure. This dichotomy can make it challenging for an investigator to predict the impact of a stressor on animal performance.

A hormetic response improves organismal performance under low levels of exposure to a stressor that is detrimental at higher levels of exposure (Mattson, 2008; Yun & Finkel, 2014; Hood *et al.*, 2018). Hormetic responses are ubiquitous (Constantini, 2014), occurring in varied organisms, including insects (Shephard *et al.*, 2018), humans (Radak *et al.*, 2008), and rodents (Zhang *et al.*, 2017), and they have been shown to occur as a consequence of both endogenous and environmental stressors (Zhang & Hood, 2016). One such factor that is often considered harmful but can also benefit organism performance at low levels of exposure is ultraviolet (UV) radiation (Williamson *et al.*, 2001; Paul & Gwynn-Jones, 2003; Hessen, 2008; Hylander, 2014). In mammals, the interaction between UV-B radiation and intracellular catalase produces reactive oxygen species (ROS; Heck *et al.*, 2003). ROS are highly reactive molecules that can directly damage DNA, lipids, and proteins. High levels of UV irradiation can directly damage

DNA (Setlow & Setlow, 1962; Boyle & Setlow, 1970; Cadet *et al.*, 2005) and can indirectly reduce cellular performance via ROS-induced cellular damage (Finkel & Holbrook, 2000). However, lower levels of ROS have been shown to serve as a cellular signal to increase antioxidants, repair enzymes, and stimulate mitochondrial biogenesis (Zhang *et al.*, 2017). This hormetic response can increase cellular performance. Whether UV radiation can have a hormetic effect on organism performance, and therefore, a beneficial effect on the life history of organisms, remains to be further explored.

Ultraviolet radiation is a prime example of an exogenous factor that is ecologically relevant for small-bodied invertebrates. Copepods found near the water's surface are naturally exposed to UV radiation. While UV radiation has been shown to negatively affect copepod reproduction and survival (Scott, 1995; Kane & Pomory, 2001; Won *et al.*, 2014, 2015; Puthumana *et al.*, 2017), most studies have evaluated the effect of UV radiation at relatively high levels of exposure. Following Han et al. (2016), who demonstrated increased antioxidant production in *Tigriopus* copepods following 3-hr UV irradiation at 0.5 W/m^2, we hypothesized that UV irradiation increases organism performance through enhanced life history characteristics.

We evaluated the impact of UV irradiation on reproductive performance and longevity in the temperate splash zone copepod *Tigriopus californicus* using various performance correlates. Copepods were exposed to 0-, 1-, or 3-hr UV-A/B irradiation at an intensity of 0.5 W/m^2. We quantified the number of offspring (nauplii) produced in the first clutch for each female to estimate fecundity (Barreto & Burton, 2013). Given that clutch size and gestation duration (i.e., incubation) often co-vary (Okkens *et al.*, 2001; Dobbs *et al.*, 2006; Brown & Shine, 2009), we also quantified the gestation duration of the first clutch. We evaluated the impact of UV irradiation on reproductive effort by quantifying the total number of clutches produced per female. Finally, we measured the impact of UV irradiation on longevity. Assuming a beneficial response, we predicted that fecundity, reproductive effort, and longevity would increase under UV irradiation.

MATERIALS AND METHODS

Copepod husbandry

This study took place from September 2017 to August 2018. *T. californicus* copepods were obtained from Reef Nutrition, Campbell, CA in two phases—September 2017 and January 2018. Panmictic cultures of *T. californicus* were maintained in 739 mL containers with artificial sea water (ASW) of salinity S = 32 and fed *Isochrysis* and *Tetraselmis* algae ad libitum. Individuals were kept on a natural, ambient light cycle from lab windows at 20-23ºC. Herein, we refer to these as stock cultures.

Data collection

Male *T. californicus* clasp and guard virgin females until they become reproductively mature (Burton, 1985). Mating clasped pairs were collected from stock cultures and placed into a 24-well plate half-filled with ASW of salinity S = 32. For irradiation, the plate was placed inside a black bin with a UV light (wavelengths $\geq$290 nm; Exo Terra 10.0 UVB Repti Glo Desert Terrarium Lamp) overhead and covered with a black drape to remove effects of ambient light. The majority of photons from the UV light were derived from UV-A radiation between 340 and 370 nm, decreasing in exposure up to 400 nm and down to UV-B radiation at 290 nm. Lamp distance from the plate was predetermined to produce an intensity of 0.5 W/m^2 (Han *et al.*, 2016), measured using a Sper Scientific UV-A/B light meter. Clasped pairs were randomly assigned to short (1-hr) and long-term (3-hr) UV treatments (see Han *et al.*, 2016), or a 1-hr, full-spectrum control treatment (no UV-B produced, placed at a distance so that no UV-A was detected; Exo Terra Full Spectrum Natural Daylight Bulb). All females were irradiated while clasped by males to ensure that females had not previously mated, allowing us to manipulate which females would or would not mate following treatment. After irradiation, clasped pairs were placed into 100 x 15 mm petri dishes with ad libitum algae and exposed to indirect, natural light from lab windows; UV radiation was measured at 0.0 W/m^2 at this location in the lab on a clear, sunny day. Therefore, copepods were only exposed to UV radiation during the aforementioned treatments. All petri dishes were aerated by hand each day. Water salinity was checked weekly, and fresh ASW was added to dishes each week to replace any water loss due to evaporation. Males were removed from petri dishes once females became gravid, and all nauplii were placed back into stock culture once counted. To prevent insemination within a subset of females, virgin females

were separated from males during mate guarding immediately after treatment. This allowed us to determine the effects of UV irradiation on longevity between mating and non-mating (virgin) females.

To examine effects of UV irradiation on fecundity, we recorded the number of nauplii produced from the first clutch and the number of days from the appearance of an egg sac to hatching (i.e., gestation) of the first clutch. We assessed reproductive effort and survival by measuring the number of clutches (egg sacs) produced and longevity. *T. californicus* females mate while undergoing five copepodid molts (Burton, 1985; see Raisuddin *et al.*, 2007). To control for age at the time of irradiation, the number of molted exoskeletons in each petri dish was quantified once females became gravid. Molts remained in petri dishes throughout the experiments and were checked again once females were deceased. That value was subtracted from five and included as a covariate in longevity models.

Analytical design

All analyses were performed using R version 3.5.0 (R Core Team, 2018). We used the "MASS" library (Venables & Ripley, 2002) for modeling and the "ggplot2" package (Wickham, 2009) for graphical development.

The number of clutches per female was modeled as a dependent variable relative to treatment (control, short, long UV irradiation) as an independent variable using zero-inflated negative binomial regression due to over-dispersed, discrete count data containing excess zeros—likely due to UV-induced sterility and/or unsuccessful mating. The number of nauplii produced in the first clutch was modeled as a dependent variable relative to treatment using a Poisson generalized linear model (GLM) due to skewed count data containing zeros (Hu *et al.*, 2011). The fully saturated model included an interaction between treatment and gestation duration as independent variables and was reduced using the "step" function. The final model was compared to both the null model and the fully saturated model using χ^2 analysis.

Nonzero counts of gestation duration and longevity were log and square-root transformed, respectively, to achieve residual normality. Gestation duration and longevity were modeled as dependent variables using general linear models (LMs) with treatment

as an independent variable. To evaluate the effect of UV irradiation on the trade-off between reproduction and longevity, we modeled the interactive effect of UV irradiation and reproduction on longevity by comparing female copepods that reproduced, those that did not reproduce, and virgins that did not mate—longevity was not transformed in this model.

We also modeled longevity as a dependent variable with the interaction between the number of clutches and treatment while controlling for age—in this model, longevity was square-root transformed and included all females that mated. Because this interaction was not retained in the final model, the resulting model represents differences in longevity between treatment groups while controlling for the additional effect of the number of clutches on longevity. Females that were not aged were not included in longevity models. Saturated models were reduced using the "step" function; model comparisons were conducted using χ^2 analysis. Final LMs were validated by extracting model residuals using the "resid" function and testing them for normality using the Shapiro-Wilk test.

RESULTS

Effects on fecundity

Descriptive statistics are presented in **Table 2.1**. Of females that mated and produced a first clutch, the number of nauplii produced was significantly greater for 1- and 3-hr UV treatments relative to the control while controlling for gestation duration (**Table 2.2A**; **Figure 2.1A**). Clutch size did not differ between 1- and 3-hr UV exposure (Est. = -0.04; *SE* = 0.07; $p = 0.58$). Clutch size significantly decreased with increasing gestation duration (**Table 2.2A**; **Figure 2.2A**). Lastly, there was a trend suggesting that 1-hr UV exposure could reduce gestation duration, but this was not statistically significant (**Table 2.2B**; **Figure 2.1B**). Gestation duration under 3-hr UV exposure did not differ from the 1-hr treatment (Est. = 0.03; *SE* = 0.09; $p = 0.69$).

Effects on reproductive effort and longevity

To determine the effects of UV irradiation on reproductive effort, we quantified the number of clutches produced by all females that mated. We also quantified the

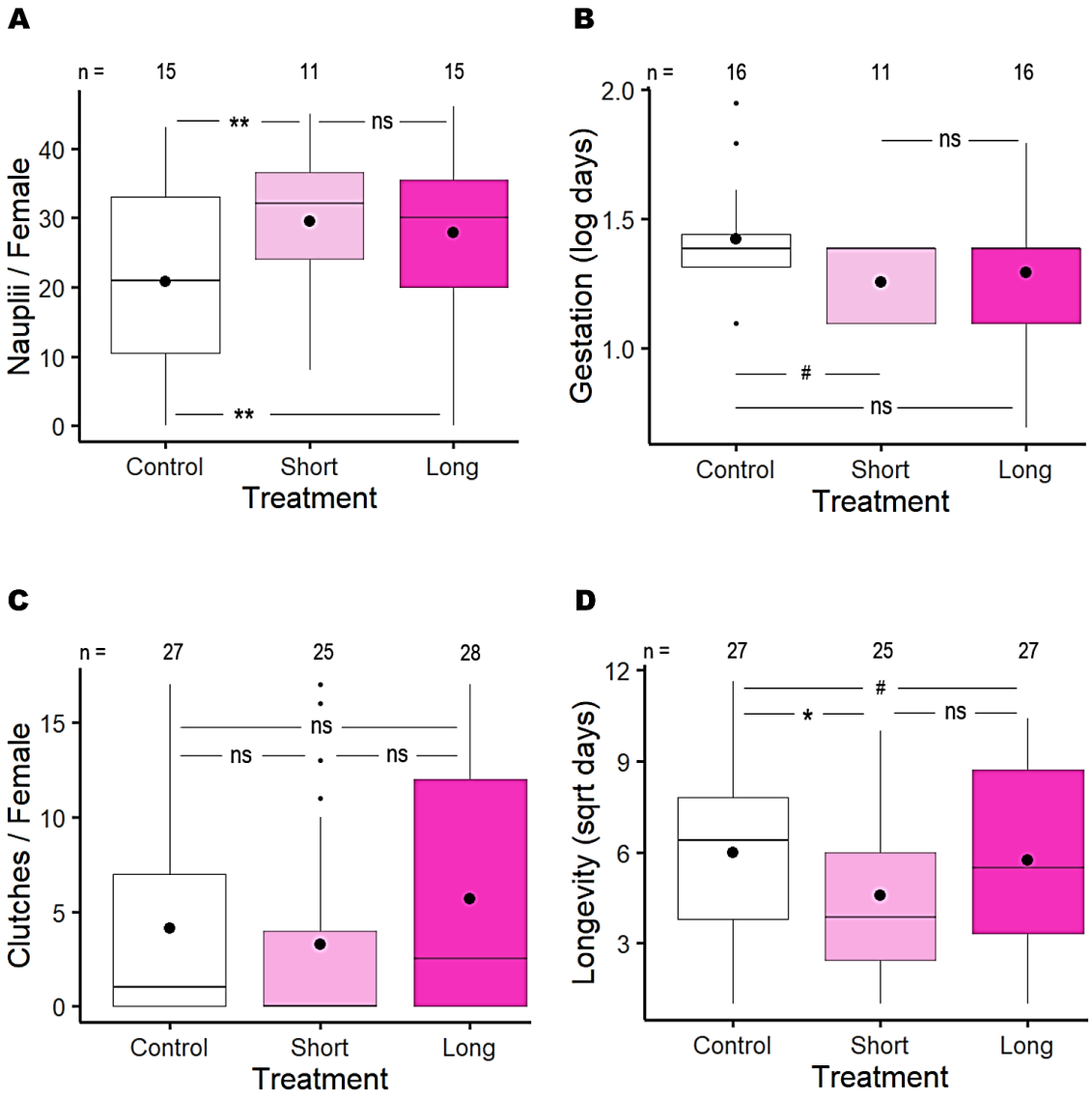

Figure 2.1. Boxplots showing effects of UV irradiation treatments on fecundity and longevity in female copepods. A) the number of nauplii produced in the first clutch with gestation duration as a covariate and B) first-clutch gestation duration. The effects of UV irradiation on reproductive effort are indicated by C) the number of clutches (eggs sacs) produced per female, and additionally, the impact of treatment on D) longevity with the number of clutches and age as covariates. Large dots represent mean estimates, and n is sample size. Significance codes: ns – not significant, #0.1, *0.05, **0.01, and ***0.001.

longevity of both mated and virgin females. Of females that mated, UV exposure had no effect on the number of clutches produced (**Table 2.2-C1**; **Figure 2.1C**), nor on the odds of not producing clutches (**Table 2.2-C2**).

To avoid collinearity, we modeled longevity using two different methods: first, with reproductive status (virgin, failed mating, or produced clutches) as an independent

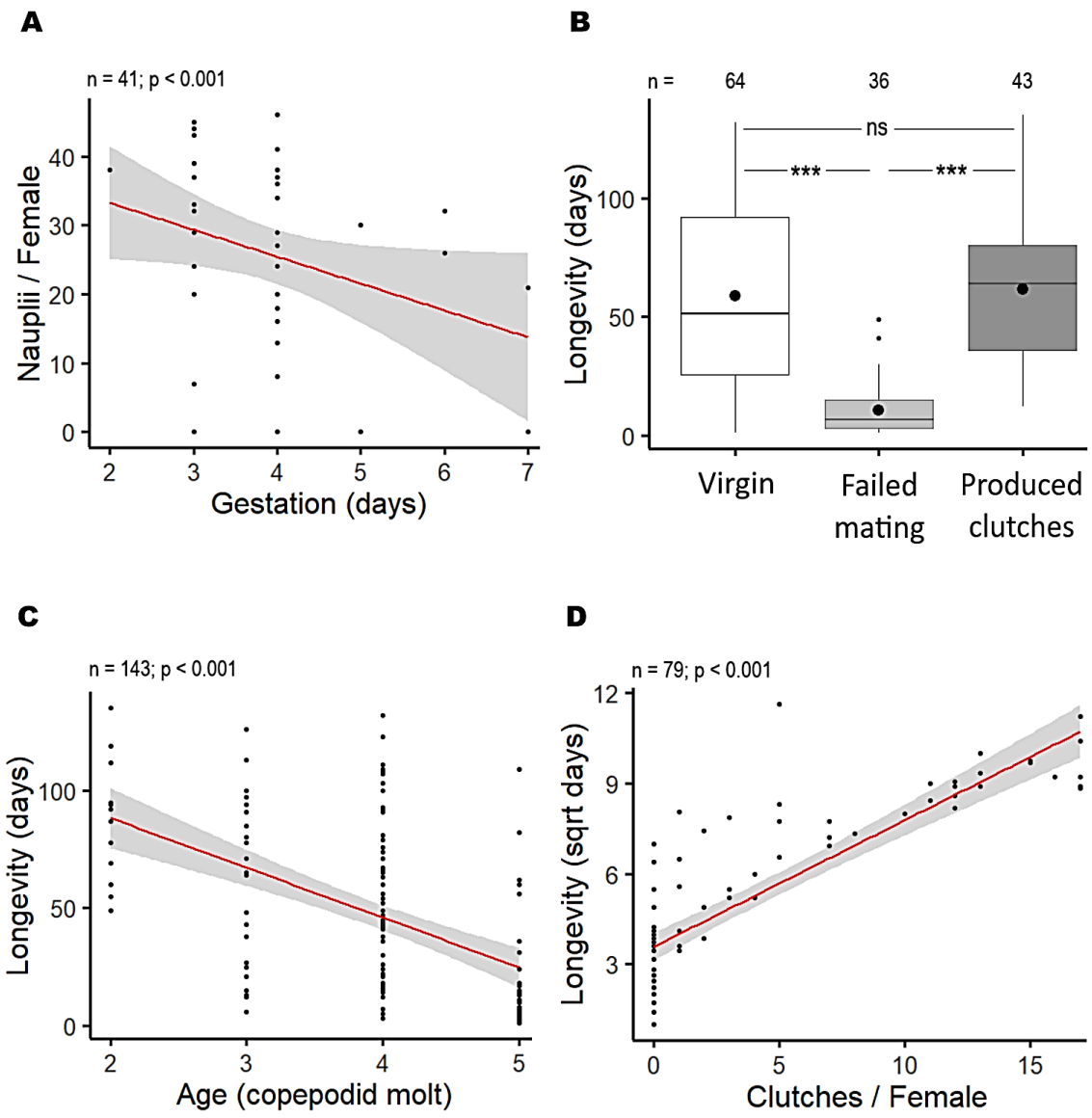

Figure 2.2. Scatterplots and boxplot showing variation between life history traits. A) the relationship between the number of nauplii produced in the first clutch and gestation duration with UV irradiation as a covariate, B) the relationship between longevity and reproduction of virgin female copepods and females that mated and did or did not (failed mating) produce clutches with age as a covariate, C) the relationship between longevity and age with reproduction as a covariate, and D) the relationship between longevity and the number of clutches with age and UV irradiation as covariates. Large dots represent mean estimates, and n is sample size. Gray shading in scatterplots denotes 95% confidence intervals. Significance codes: ns – not significant, #0.1, *0.05, **0.01, and ***0.001.

variable, and second, with the number of clutches produced by mated females as an independent variable. Females that mated but failed to produce clutches had significantly

reduced longevity relative to both virgin females and females that did produce clutches (**Table 2.2D**; **Figure 2.2B**). The longevity of virgin females did not differ from the longevity of females that produced clutches (Est. = 0.03; *SE* = 5.70; *p* = 0.99). UV treatment was not retained in this model. While controlling for the number of clutches, longevity was lower following 1-hr UV irradiation (**Table 2.2E**; **Figure 2.1D**). Longevity under 3-hr UV exposure did not differ from the 1-hr treatment (Est. = 0.22; *SE* = 0.41; *p* = 0.59). Age at the time of irradiation and longevity were inversely related in both longevity models (**Table 2.2D**, **2.2E**; **Figure 2.2C**). The number of clutches produced increased significantly with longevity (**Table 2.2E**; **Figure 2.2D**).

DISCUSSION

An important focus of life history research is understanding how natural variation in organism performance arises within and between populations. The ability of organisms to survive to reproductive age and produce viable offspring is affected by numerous endogenous and exogenous factors (Fisher, 1930; Stearns, 2000; Devreker *et al.*, 2009). UV radiation is an exogenous, environmental factor that is known to play a significant role in the survival and reproduction of small-bodied invertebrates such as copepods (Damkaer *et al.*, 1980; Bidigare, 1989; Caramujo *et al.*, 2012). Accordingly, the aim of this study was to determine if UV irradiation can benefit organism performance in *T. californicus* copepods. We hypothesized that UV irradiation increases organism performance through enhanced fecundity, longevity, and reproductive effort. Our findings indicate that UV irradiation increased the number of nauplii produced from the first clutch of *T. californicus* females but also decreased the longevity among females that mated (**Figure 2.1A**, **2.1D**). Our results may be explained by any single or combination of the following mechanisms: hormesis, antagonistic pleiotropy, or a reduction in pathogen load.

Under hormetic theory, low levels of exposure to a stressor improve organismal function, where higher levels of exposure decrease organism performance (Mattson, 2008; Handy & Loscalzo, 2012; Ristow, 2014; Yun & Finkel, 2014; Zhang *et al.*, 2017; Hood *et al.*, 2018). We speculate that the increase in copepod fecundity in both 1- and 3-hr treatment groups suggests that the proximate, cellular benefits associated with modest

UV irradiation (increased antioxidant production, signaled by increased oxidative stress) may have manifested in improved organism performance (Ristow, 2014; Zhang & Hood, 2016). The intensity of UV irradiation used in our study is similar to that of Han et al. (2016). In their study, Han et al. showed that other *Tigriopus* copepods exposed to three and six hours of UV irradiation at this intensity showed a rapid stress response at 96 hours post treatment. Not only did ROS production increase significantly in ovigerous females in their study, but the production of antioxidant enzymes increased for both 3- and 6-hr treatments, but not a 1-hr treatment. Given that ROS was not upregulated at one hour in Han's study, but we found both an increase in nauplii production and decrease in longevity at this time point, other mechanisms could be at play. Souza et al. (2012) has also shown that freshwater copepods exposed to 38.9-233 kJ/m^2 of UV-A irradiation can elicit a short-term stress response by upregulating the production of enzymes that counteract peroxidation, cell death, and enable neurotransmissions. While the 1-hr UV treatment in our study was associated with increased fecundity, it was also associated with reduced survival. As such, the benefits of ROS exposure to fecundity may not have been enough to overturn oxidative damage that may be responsible for reduced longevity, although other mechanisms are possible. We also observed a decrease in longevity among females that mated but did not produce clutches. This may be due to poor condition of select females entering the study—irrespective of UV irradiation—ultimately leading to poor reproductive performance.

Alternate forms of radiation and stress have also been shown to elicit hormetic effects in other organisms (Zhang *et al.*, 2017; Shephard *et al.*, 2018). Shephard et al. (2018) recently characterized the effect of ɣ-radiation on reproductive performance in the cricket *Acheta domesticus*. Similarly, they found that modest irradiation was associated with an increase in fecundity. While longevity was not reported, they also found an increase in average egg size. This result, along with the reduced gestation duration found in our study, suggests that radiation exposure may allow females to increase the quality of young, in addition to the quantity produced. In addition to exogenous, environmental stressors, endogenous stressors have also been found to benefit organismal performance. Work by Zhang et al. (2018) indicated that female mice that ran on a wheel before breeding produced more pups that were heavier at weaning than females that did not have

a wheel. Consistent with hormetic theory (Mattson, 2008; Yun & Finkel, 2014; Hood *et al.*, 2018), low exposure to a stressor in their study was shown to increase mitochondrial density in several organs and may be associated with increased organism performance. While modest levels of a stressor may be immediately beneficial, it is feasible that damage from oxidative stress may accumulate and have delayed impacts on performance and offspring quality (Rodríguez-Graña *et al.*, 2010).

Our study indicates that UV irradiation may increase reproduction early in life but also increase the rate of senescence later in life. In this respect, UV radiation may hold an adaptive significance and partly explain the short life cycles of copepods if individuals are able to increase their reproductive output at an early age (see Fernández *et al.*, 2018 for an example in cladocerans; Hylander *et al.*, 2014). Trade-offs between reproduction and longevity are predicted under antagonistic pleiotropy and the disposable soma theory of aging. Under antagonistic pleiotropy, selection is predicted to favor genes responsible for shorter lifespan when they are linked to increased reproductive success early in life (Williams, 1957; He & Zhang, 2006). Therefore, it is feasible that a gene, or suite of genes, is responsible for improved fecundity under UV irradiation. The disposable soma theory of aging states that allocating more resources to reproduction can reduce the allocation of resources to processes that support self-maintenance and longevity (Kirkwood, 1977; Gavrilov & Gavrilova, 2002; Nussey *et al.*, 2006). Thus, it is feasible that the hormetic response to UV irradiation pulls resources away from maintenance, reducing longevity. Each of these mechanisms are speculative and warrant further investigation.

Finally, there are several other mechanisms that may be responsible for the observed effects. Pathogen infection of zooplankton—including copepods—is a widespread phenomenon in both freshwater and marine environments (Seki & Fulton, 1969; Overholt *et al.*, 2012). Although UV radiation is often deemed detrimental to the life history of organisms, its effects may benefit host survival and/or reproductive performance by decreasing the survivability and prevalence of pathogens (Williamson *et al.*, 2017). Evidence for a reduction of pathogen prevalence following UV irradiation has been supported in a fungal parasite of water fleas (Overholt *et al.*, 2012), the bacterial load of rotifers (Munro *et al.*, 1999), a nematode parasite of moths (Gaugler & Boush,

1978), and reduction of human parasites by UV-B irradiation in vitro (Connelly *et al.*, 2007), among other examples. Pathogen infection of copepods can decrease fecundity, egg production, respiration rates, and increase mortality (Kimmerer & McKinnon, 1990; Albaina & Irigoien, 2006; Fields *et al.*, 2014). Aside from reducing the prevalence of pathogens, UV radiation can also influence reproduction in accordance with diet. Work by Hylander et al. (2014) has shown that female reproductive performance can increase following sublethal exposure to UV irradiation when females are fed a diet rich in mycosporine-like amino acids that aid in screening UV radiation. Although diet may have had an influence on the ability of female copepods to defend against harmful UV irradiation in our study, it is unlikely that the observed effects herein are due to diet, provided that all females were supplied ad libitum access to the same algae throughout the study (see Lee *et al.*, 2018 for how caloric restriction may influence the life history of aquatic organisms). Furthermore, UV radiation is necessary for endogenous vitamin D production; an induced increase in vitamin D via UV irradiation in *Daphnia* has been shown to increase fecundity (Connelly *et al.*, 2015). However, previous work has demonstrated that vitamin D is likely not present in copepods (Karlsen *et al.*, 2015).

We show that UV irradiation had an immediate, positive impact on fecundity, increasing the number of nauplii that females produced in their first clutch. This finding indicates that females exposed to UV radiation prior to reproducing may have an increased capacity to produce more offspring, at least early in their reproductive lifetime. Additionally, females with larger clutches also displayed relatively shorter gestation periods than females with smaller clutches. Reduced gestation could be associated with more rapid development or constraints on egg sac capacity. Further work is needed to determine if the total number of nauplii produced over a female's lifetime also increases significantly under UV irradiation. Additionally, our study has tested the effects of UV irradiation in a marine species of copepod (*T. californicus*) that exists above the intertidal zone along the west coast of North America. These copepods exist in shallow splash pools and are likely exposed to greater amounts of UV radiation in natural environments than in this study or other species of lake and ocean-dwelling taxa of zooplankton. Alonso et al. (2004) and Overholt et al. (2016) demonstrate how copepods may exhibit UV radiation avoidance behavior, which may ultimately expose individuals to low-

intensity, UV radiation. As indicated by Williamson et al. (2019), the effects of ROS may only be relevant in species that exist within the top few centimeters of aquatic environments. Therefore, further research is needed to determine the likelihood that cellular signaling or ROS plays any role in the responses observed herein. If possible, future studies may also benefit from using natural sunlight to determine the effects of UV radiation on reproductive performance and life history characteristics (Williamson *et al.*, 2019). Provided our aim was to demonstrate that UV irradiation can benefit organism performance, future work should aim to identify the proximate mechanisms that underly both the organismal benefit (increased fecundity) and detriment (decreased longevity) of UV irradiation.

REFERENCES

Albaina, A. & Irigoien, X. (2006). Fecundity limitation of *Calanus helgolandicus*, by the parasite Ellobiopsis sp. *Journal of Plankton Research* **28**, 413-418.

Alonso, C., Rocco, V., Barriga, J. P., Battini, M. A. & Zagarese, H. (2004). Surface avoidance by freshwater zooplankton: Field evidence on the role of ultraviolet radiation. *Limnology & Oceanography* **49**, 225-232.

Barreto, F. S. & Burton, R. S. (2013). Elevated oxidative damage is correlated with reduced fitness in interpopulation hybrids of a marine copepod. *Proceedings of the Royal Society B: Biological Sciences* **280**, 20131521.

Bidigare, R. R. (1989). Potential effects of UV-B radiation on marine organisms of the southern ocean: distributions of phytoplankton and krill during austral spring. *Photochemistry & Photobiology* **50**, 469-477.

Boyle, J. M. & Setlow, R. B. (1970). Correlations between host-cell reactivation, ultraviolet reactivation and pyrimidine dimer excision in the DNA of bacteriophage λ. *Journal of Molecular Biology* **51**, 131-144.

Brown, G. P. & Shine, R. (2009). Beyond size–number trade-offs: clutch size as a maternal effect. *Philosophical Transactions of the Royal Society B: Biological Sciences* **364**, 1097-1106.

Burton, R. S. (1985). Mating system of the intertidal copepod *Tigriopus californicus*. *Marine Biology* **86**, 247-252.

Cadet, J., Sage, E. & Douki, T. (2005). Ultraviolet radiation-mediated damage to cellular DNA. *Mutation Research/Fundamental & Molecular Mechanisms of Mutagenesis* **571**, 3-17.

Caramujo, M. J., de Carvalho, C. C., Silva, S. J. & Carman, K. R. (2012). Dietary carotenoids regulate astaxanthin content of copepods and modulate their susceptibility to UV light and copper toxicity. *Marine Drugs* **10**, 998-1018.

Connelly, S. J., Walling, K., Wilbert, S. A., Catlin, D. M., Monaghan, C. E., Hlynchuk, S., Meehl, P. G., Resch, L. N., Carrera, J. V., Bowles, S. M. & Clark, M. D. (2015). UV-stressed *Daphnia pulex* increase fitness through uptake of Vitamin D3. *PLoS ONE* **10**, e0131847.

Connelly, S. J., Wolyniak, E. A., Williamson, C. E. & Jellison, K. L. (2007). Artificial UV-B and solar radiation reduce in vitro infectivity of the human pathogen *Cryptosporidium parvum*. *Environmental Science & Technology* **41**, 7101-7106.

Constantini, D. (2014). Oxidative stress and hormesis in evolutionary ecology and physiology. Springer, Berlin and Heidelberg, 1-38.

Damkaer, D. M., Dey, D. B., Heron, G. A. & Prentice, E. F. (1980). Effects of UV-B radiation on near-surface zooplankton of Puget Sound. *Oecologia* **44**, 149-158.

Devreker, D., Souissi, S., Winkler, G., Forget-Leray, J. & Leboulenger, F. (2009). Effects of salinity and temperature on the reproduction of *Eurytemora affinis* (Copepoda; Calanoida) from the Seine estuary: a laboratory study. *Journal of Experimental Marine Biology & Ecology* **368**, 113-123.

Dobbs, R. C., Styrsky, J. D. & Thompson, C. F. (2006). Clutch size and the costs of incubation in the house wren. *Behavioral Ecology* **17**, 849-856.

Fernández, C. E., Campero, M., Uvo, C. & Hansson, L. A. (2018). Disentangling population strategies of two cladocerans adapted to different ultraviolet regimes. *Ecology & Evolution* **8**, 1995-2005.

Fields, D. M., Runge, J. A., Thompson, C., Shema, S. D., Bjelland, R. M., Durif, C. M. F., Skiftesvik, A. B. & Browman, H. I. (2014). Infection of the planktonic copepod *Calanus finmarchicus* by the parasitic dinoflagellate, Blastodinium spp: effects on grazing, respiration, fecundity and fecal pellet production. *Journal of Plankton Research* **37**, 211-220.

Finkel, T. & Holbrook, N. J. (2000). Oxidants, oxidative stress and the biology of ageing. *Nature* **408**, 239-247.

Fisher, R. A. (1930). The genetical theory of natural selection. Oxford, England: Clarendon Press.

Gaugler, R. & Boush, G. M. (1978). Effects of ultraviolet radiation and sunlight on the entomogenous nematode, *Neoaplectana carpocapsae*. *Journal of Invertebrate Pathology* **32**, 291-296.

Gavrilov, L. A. & Gavrilova, N. S. (2002). Evolutionary theories of aging and longevity. *The Scientific World Journal* **2**, 339-356.

Han, J., Puthumana, J., Lee, M. C., Kim, S. & Lee, J. S. (2016). Different susceptibilities of the Antarctic and temperate copepods *Tigriopus kingsejongensis* and *T. japonicus* to ultraviolet (UV) radiation. *Marine Ecology Progress Series* **561**, 99-107.

Handy, D. E. & Loscalzo, J. (2012). Redox regulation of mitochondrial function. *Antioxidants & Redox Signaling* **16**, 1323-1367.

He, X. & Zhang, J. (2006). Toward a molecular understanding of pleiotropy. *Genetics* **173**, 1885-1891.

Heck, D. E., Vetrano, A. M., Mariano, T. M. & Laskin, J. D. (2003). UVB light stimulates production of reactive oxygen species unexpected role for catalase. *Journal of Biological Chemistry* **278**, 22432-22436.

Hessen, D. O. (2008). Solar radiation and the evolution of life. *Solar Radiation & Human Health* 123-136.

Hood, W. R., Zhang, Y., Mowry, A. V., Hyatt, H. W. & Kavazis, A. N. (2018). Life history trade-offs within the context of mitochondrial hormesis. *Integrative & Comparative Biology* **58**, 567-577.

Hu, M. C., Pavlicova, M. & Nunes, E. V. (2011). Zero-inflated and hurdle models of count data with extra zeros: examples from an HIV-risk reduction intervention trial. *American Journal of Drug & Alcohol Abuse* **37**, 367-75.

Hylander, S., Grenvald, J. C. & Kiørboe, T. (2014). Fitness costs and benefits of ultraviolet radiation exposure in marine pelagic copepods. *Functional* Ecology **28**, 149-158.

Kane, K. & Pomory, C. M. (2001). The effects of UV-B radiation on the reproduction and mortality of *Tigriopus californicus* (Copepoda: Harpacticoida). *Hydrobiologia* **444**, 213-215.

Karlsen, Ø., van der Meeren, T., Rønnestad, I., Mangor-Jensen, A., Galloway, T. F., Kjørsvik, E. & Hamre, K. (2015). Copepods enhance nutritional status, growth and development in Atlantic cod (Gadus morhua L.) larvae—can we identify the underlying factors? *PeerJ* **3**, 902.

Kimmerer, W. J. & McKinnon, A. D. (1990). High mortality in a copepod population caused by a parasitic dinoflagellate. *Marine Biology* **107**, 449-452.

Kirkwood, T. B. (1977). Evolution of ageing. *Nature* **270**, 301-304.

Lee, M. C., Park, J. C., Yoon, D. S., Han, J., Kang, S., Kamizono, S., Om, A. S., Shin, K. H., Hagiwara, A. & Lee, J. S. (2018). Aging extension and modifications of lipid metabolism in the monogonont rotifer *Brachionus koreanus* under chronic caloric restriction. *Scientific Reports* **8**, 1741.

Mattson, M. P. (2008). Hormesis defined. *Ageing Research Reviews* **7**, 1-7.

Munro, P. D., Henderson, R. J., Barbour, A. & Birkbeck, T. H. (1999). Partial decontamination of rotifers with ultraviolet radiation: the effect of changes in the bacterial load and flora of rotifers on mortalities in start-feeding larval turbot. *Aquaculture* **170**, 229-244.

Nussey, D. H., Kruuk, L. E., Donald, A., Fowlie, M. & Clutton-Brock, T. H. (2006). The rate of senescence in maternal performance increases with early-life fecundity in red deer. *Ecology Letters* **9**, 1342-1350.

Okkens, A. C., Teunissen, J. M., Van Osch, W., Van Den Brom, W. E., Dieleman, S. J. & Kooistra, H. S. (2001). Influence of litter size and breed on the duration of gestation in dogs. *Journal of Reproduction & Fertility – Supplement* **57**, 193-197.

Overholt, E. P., Hall, S. R., Williamson, C. E., Meikle, C. K., Duffy, M. A. & Cáceres, C. E. (2012). Solar radiation decreases parasitism in *Daphnia*. *Ecology Letters* **15**, 47-54.

Overholt, E. P., Rose, K. C., Williamson, C. E., Fischer, J. M. & Cabrol, N. A. (2016). Behavioral responses of freshwater calanoid copepods to the presence of ultraviolet radiation: avoidance and attraction. *Journal of Plankton Research* **38**, 16-26.

Paul, N. D. & Gwynn-Jones, D. (2003). Ecological roles of solar UV radiation: towards an integrated approach. *Trends in Ecology & Evolution* **18**, 48-55.

Puthumana, J., Lee, M. C., Park, J. C., Kim, H. S., Hwang, D. S, Han, J. & Lee, J. S. (2017). Ultraviolet B radiation induces impaired lifecycle traits and modulates expression of cytochrome P450 (CYP) genes in the copepod *Tigriopus japonicus*. *Aquatic Toxicology* **184**, 116-122.

R Core Team. (2018). R: A language and environment for statistical computing. R Foundation for Statistical Computing, Vienna, Austria. URL http://www.R-project.org/.

Radak, Z., Chung, H. Y., Koltai, E., Taylor, A. W. & Goto, S. (2008). Exercise, oxidative stress and hormesis. *Ageing Research Reviews* **7**, 34-42.

Raisuddin, S., Kwok, K. W., Leung, K. M., Schlenk, D. & Lee, J. S. (2007). The copepod *Tigriopus*: a promising marine model organism for ecotoxicology and environmental genomics. *Aquatic Toxicology* **83**, 161-173.

Ristow, M. (2014). Unraveling the truth about antioxidants: mitohormesis explains ROS-induced health benefits. *Nature Medicine* **20**, 709–711.

Rodríguez-Graña, L., Calliari, D., Tiselius, P., Hansen, B. W. & Sköld, H. N. (2010). Gender-specific ageing and non-Mendelian inheritance of oxidative damage in marine copepods. *Marine Ecology Progress Series* **401**, 1-13.

Scott, L. C. (1995). Survival and sex ratios of the intertidal copepod, *Tigriopus californicus*, following ultraviolet-B (290–320 nm) radiation exposure. *Marine Biology* **123**, 799-804.

Seki, H. & Fulton, J. (1969). Infection of marine copepods by Metschnikowia sp. *Mycopathologia et Mycologia Applicata* **38**, 61-70.

Setlow, R. B. & Setlow, J. K. (1962). Evidence that ultraviolet-induced thymine dimers in DNA cause biological damage. *Proceedings of the National Academy of Sciences of the United States of America* **48**, 1250-1257.

Shephard, A. M., Aksenov, V., Tran, J., Nelson, C. J, Boreham, D. R. & Rollo, C. D. (2018). Hormetic effects of early juvenile radiation exposure on adult reproduction and offspring performance in the cricket (*Acheta domesticus*). *Dose-Response* **16**, 1559325818797499.

Souza, M. S., Hansson, L. A., Hylander, S., Modenutti, B. & Balseiro, E. (2012). Rapid enzymatic response to compensate UV radiation in copepods. *PLoS ONE* **7**, e32046.

Speakman, J. R. (2008). The physiological costs of reproduction in small mammals. *Philosophical Transactions of the Royal Society B: Biological Sciences* **363**, 375-398.

Stearns, S. C. (2000). Life history evolution: successes, limitations, and prospects. *Naturwissenschaften* **87**, 476-486.

Venables, W. N. & Ripley, B. D. (2002). Modern applied statistics with S. 4th ed. New York: Springer.

Wickham, H. (2009). ggplot2: elegant graphics for data analysis. New York: Springer.

Williams, G. (1957). Pleiotropy, natural selection, and the evolution of senescence. *Evolution* **11**, 398-411.

Williams, G. C. (1966). Natural selection, the costs of reproduction, and a refinement of Lack's principle. *The American Naturalist* **100**, 687-690.

Williamson, C. E., Madronich, S., Lal, A., Zepp, R. G., Lucas, R. M., Overholt, E. P., Rose, K. C., Schladow, S. G. & Lee-Taylor, J. (2017). Climate change-induced increases in precipitation are reducing the potential for solar ultraviolet radiation to inactivate pathogens in surface waters. *Scientific Reports* **7**, 13033.

Williamson, C. E., Neale, P. J., Grad, G., De Lange, H. J. & Hargreaves, B. R. (2001). Beneficial and detrimental effects of UV on aquatic organisms: implications of spectral variation. *Ecological Applications* **11**, 1843-1857.

Williamson, C. E., Neale, P. J., Hylander, S., Rose, K. C., Figueroa, F. L., Robinson, S. A., Häder, D. P., Wängberg, S. Å. & Worrest, R. C. (2019). The interactive effects of stratospheric ozone depletion, UV radiation, and climate change on aquatic ecosystems. *Photochemical & Photobiological Sciences* **18**, 717-746.

Won, E. J., Han, J., Lee, Y., Kumar, K. S., Shin, K. H., Lee, S. J., Park, H. G. & Lee, J. S. (2015). In vivo effects of UV radiation on multiple endpoints and expression profiles of DNA repair and heat shock protein (Hsp) genes in the cycloid copepod *Paracyclopina nana*. *Aquatic Toxicology* **165**, 1-8.

Won, E. J., Lee, Y., Han, J., Hwang, U. K., Shin, K. H., Park, H. G. & Lee, J. S. (2014). Effects of UV radiation on hatching, lipid peroxidation, and fatty acid composition in the copepod *Paracyclopina nana*. *Comparative Biochemistry & Physiology Part C: Toxicology & Pharmacology* **165**, 60-66.

Yun, J. & Finkel, T. (2014). Mitohormesis. *Cell Metabolism* **19**, 757-766.

Zhang, Y., Brasher, A. L., Park, N. R., Taylor, H. A., Kavazis, A. N. & Hood, W. R. (2018). High activity before breeding improves reproductive performance by enhancing mitochondrial function and biogenesis. *Journal of Experimental Biology* **221**, 1-11.

Zhang, Y. & Hood, W. R. (2016). Current versus future reproduction and longevity: a re-evaluation of predictions and mechanisms. *Journal of Experimental Biology* **219**, 3177-3189.

Zhang, Y., Humes, F., Almond, G., Kavazis, A. N. & Hood, W. R. (2017). A mitohormetic response to pro-oxidant exposure in the house mouse. *American Journal of Physiology – Regulatory, Integrative & Comparative Physiology* **314**, 122-134.

Table 2.1. Mean, standard deviations, and sample sizes (*n*) of life history responses in copepods with respect to UV irradiation treatment. Under the longevity response, virgins represent females that did not mate, failed mating represents females that mated but did not produce clutches (egg sacs), and produced clutches represents females that mated and produced clutches.

Response	***n***	**Control**	**1-hr UV**	**3-hr UV**
Number of nauplii	41	20.8 ± 14.6	29.5 ± 10.9	27.8 ± 12.7
Gestation duration (days)	43	4.3 ± 1.3	3.5 ± 0.5	3.7 ± 0.9
Number of clutches	80	4.1 ± 5.3	3.2 ± 5.4	5.6 ± 6.6
Longevity (days)				
Virgins	64	61.3 ± 36.3	58.2 ± 40.1	57.1 ± 36.0
Failed mating	36	15.3 ± 16.2	8.5 ± 8.2	8.7 ± 5.9
Produced clutches	43	64.5 ± 34.1	54.4 ± 28.4	63.9 ± 27.5

Table 2.2. Results of GLMs predicting variation in the number of nauplii produced in the first clutch and the total number of clutches produced per female copepod. Mean estimates of gestation duration (appearance of an egg sac to hatching) and longevity are presented from LMs. *n* is sample size, Est. is the point estimate, and *SE* is the standard error of the estimate. Mean estimates for 1- and 3-hr UV irradiation treatments are estimated in comparison to controls. Longevity was modeled using two methods: one model with reproductive status (virgin, failed mating, and produced clutches) as a covariate and one model with the number of clutches that mating females produced as a covariate. Virgins and females that produced clutches are in comparison to females that mated but did not produce clutches (failed mating). Significance levels: #0.1, *0.05, **0.01, ***0.001, — not retained.

Response	**Predictor**	***n***	**Est. / *SE***
Number of nauplii[A]			
	1-hour UV	11	0.24 / 0.08**
	3-hour UV	15	0.20 / 0.07**
	Gestation duration	41	-0.13 / 0.03***
Gestation duration (days)[B]			
	1-hour UV	11	-0.16 / 0.09#
	3-hour UV	16	-0.13 / 0.08
Number of clutches[C]			
[1]*Count model*	1-hour UV	25	0.07 / 0.34
	3-hour UV	28	0.39 / 0.31
[2]*Zero-inf model*	1-hour UV	25	0.69 / 0.62
	3-hour UV	28	0.18 / 0.60
Longevity (days)[D]			
	1-hour UV	—	—
	3-hour UV	—	—
	Virgin	64	37.75 / 6.51***
	Produced clutches	43	37.72 / 7.26***
	Age	143	-12.68 / 3.09***
Longevity (days)[E]			
	1-hour UV	25	-0.93 / 0.40*
	3-hour UV	27	-0.71 / 0.41#
	Number of clutches	79	0.34 / 0.03***
	Age	79	-0.80 / 0.21***

Chapter 3: **Ultraviolet irradiation alters the density of inner mitochondrial membrane and proportion of inter-mitochondrial junctions in copepod myocytes**

Published with Nicholas M. Justyn, Geoffrey E. Hill, and Wendy R. Hood (2021) in *Mitochondrion* **56**, 82-90

INTRODUCTION

Explaining variation in whole-animal performance, which we define as the capacity to produce sufficient adenosine triphosphate (ATP) to support growth, self-maintenance, and reproduction, is a central goal of functional and physiological ecology (e.g., Drent & Daan, 1980; Kenagy *et al.*, 1990; Speakman *et al.*, 2015; Salin *et al.*, 2019). For complex animals, 90% of ATP is produced via oxidative phosphorylation in mitochondria, so the efficiency of the electron transport system (ETS) is a key determinant of energy production for most animals (Hill, 2019). In addition to ETS function, the behavior (position and communication within the cell) and morphology of mitochondria are also proposed to play key roles in the capacity of energy production (Heine & Hood, 2020). Past research has been successful in explaining how mitochondrial behavior and morphology impact the ability of mitochondria to produce energy efficiently (Zick *et al.*, 2009; Mannella *et al.*, 2013), as well as in characterizing variation in whole-animal performance (e.g., Speakman & Król, 2005). However, support for different hypotheses for how changes in mitochondrial behavior and structure impact animal performance (including stress responses) as a whole are equivocal.

Documented changes in the behavior and morphology of mitochondria suggest that they likely play formative roles in the energetic capacity of tissues. The density of inner mitochondrial membrane (IMM), proportion of inter-mitochondrial junctions (IMJs), and mitochondrial density have all been shown to increase with increased energetic demand. Moreover, the rates of mitochondrial fission and fusion will vary in relation to mitochondrial damage and dysfunction caused by an increase in the production of free radicals such as superoxide or hydroxyl radicals (see Heine & Hood, 2020 for a review). The IMM contains protein complexes I-IV of the ETS that create an

electrochemical gradient across the IMM, driving the production of ATP at complex V. Protons are actively pumped from the mitochondrial matrix into the inter-membrane space by complexes I, III, and IV, as complexes I and II deliver electrons to the quinone pool, and complex IV reduces oxygen to water. Protons flow down the electrochemical gradient through complex V to form ATP (Hatefi, 1985). A greater density of IMM can support more complexes of the ETS, leading to greater ATP production under increased energetic demand (Strohm & Daniels, 2003; Nielsen *et al.*, 2017). IMJs are electron-dense contacts between mitochondria. IMJs are more common in tissues with higher energetic demand, such as heart muscle (Picard *et al.*, 2015), and become more numerous when animals participate in energetically demanding behaviors such as running (Picard *et al.*, 2013*a*). Although the proximate function of these structures remains to be confirmed through empirical research, they have been proposed to facilitate the coordination of gene expression, as in bacteria (Ng & Bassler, 2009), and/or the transfer of electrochemical gradients (see Pacher & Hajnoczky, 2001; Santo-Domingo *et al.*, 2013). In turn, these changes may increase ATP production under increased energetic demand. Lastly, an increase in mitochondrial density in cells may increase the energetic capacity of organs (Hood *et al.*, 2019), irrespective of changes in mitochondrial morphology.

Several exogenous stressors, including ultraviolet (UV) radiation, are known to influence mitochondrial performance. UV-B radiation can produce reactive oxygen species (ROS) through interactions with cellular catalase (Heck *et al.*, 2003). In turn, ROS can impact cellular performance in both negative and positive ways, including damaging the cell (Finkel & Holbrook, 2000) or acting as signaling molecules to increase mitochondrial performance through the upregulation of antioxidants, mitochondrial biogenesis, or repair enzymes (Zhang *et al.*, 2017; Hood *et al.*, 2018). In addition to producing ROS, UV radiation can damage DNA directly (Cadet *et al.*, 2005). The impact of UV radiation on performance is particularly relevant for organisms that must energetically respond to variable levels of direct sunlight, including invertebrates that inhabit marine environments. Previous work has shown that UV radiation can both impact mitochondria (Han *et al.*, 2016) and increase reproductive performance in copepods (Hylander *et al.*, 2014; Heine *et al.*, 2019). Such energetically demanding changes to whole-animal performance likely stem from changes in mitochondrial

function, which could be mediated, in part, by changes in mitochondrial behavior and morphology. *Tigriopus californicus* copepods are an ideal model to study how radiation impacts mitochondrial structure and metabolic rate because this species lives in shallow splash pools and is exposed to varying levels of UV irradiation throughout any given day (Weaver *et al.*, 2018). Furthering our understanding of how UV irradiation impacts both the behavior and morphology of mitochondria, and metabolic rate, allows us to better understand how pervasive organisms such as copepods are able to function in such variable environments. Accordingly, this study sought to address the links between mitochondrial behavior, morphology, and animal performance in copepods, as mediated by UV irradiation.

We tested the hypothesis that UV irradiation influences: 1) whole-animal metabolic rate and 2) mitochondrial behavior and morphology—specifically the density of IMM and proportion of IMJs in myocytes of the copepod *T. californicus*. Copepods were exposed to zero, three, or six hours of UV-A/B irradiation (0.5 W/m^2), after which we recorded the metabolic rate of each copepod for one hour. Transmission electron microscopy (TEM) was completed on a subset of these individuals to quantify mitochondrial behavior and morphology. We predicted that UV irradiation would increase the density of IMM and proportion of IMJs since these traits have been linked to increased energetic demand. We also quantified mitochondrial area and density to assess any changes in mitochondrial fission or fusion, as well as mitochondrial aspect ratio (see Leduc-Gaudet *et al.*, 2015) which may impact mitochondrial performance.

MATERIALS AND METHODS

Copepod husbandry

This study was conducted from March to November 2019. All *Tigriopus californicus* copepods were acquired from Reef Nutrition, Campbell, CA in December 2018. Panmictic cultures of copepods were housed in 739 mL containers and were kept on a natural, ambient light cycle from laboratory windows at 20-22°C. All cultures were fed ad libitum *Isochrysis galbana* algae in artificial sea water of salinity S = 32.

Data collection

Male *T. californicus* copepods clasp virgin females until the female becomes sexually mature after completing her final copepodid molt; the male then inseminates the female and releases her (Burton, 1985). Mating pairs were collected from our cultures and placed into 60 x 15 mm petri dishes half-filled with artificial sea water of salinity S = 32 and ad libitum *I. galbana* algae. Males were removed from petri dishes and placed back into cultures once the male inseminated and released the female. Females were placed back into cultures once her first clutch hatched. Offspring of the first clutch (n = 15 controls from two mothers, 18 individuals from three mothers in the 3-hr UV treatment, and 19 individuals from one mother in the 6-hr UV treatment) were raised to 22 ± 3 days before irradiation treatments. These numbers of mothers and offspring were chosen to age-match the offspring as closely as possible to avoid any possible age-related effects in our study.

For irradiation treatments, each copepod was placed into a well of a 24-well plate half-filled with artificial sea water of salinity S = 32. The plate was place inside a black bin with either a full-spectrum light (Exo Terra Full Spectrum Natural Daylight Bulb; produces no UV-B; placed so that no UV-A was measured) or a UV-A/B light (Exo Terra 10.0 UVB Repti Glo Desert Terrarium Lamp; wavelengths ≥290 nm) above the bin. Both the lamps and bin were covered with a black drape to remove any effects of ambient lighting. For each set of animals, the UV lamp was secured approximately 0.5 m above the bottom of the bin. A Sper Scientific UV-A/B light meter was placed in the bin, and then the distance between the light and the meter was adjusted until the meter measured 0.5 W/m^2. The light meter was then replaced with the plate of copepods. All copepods were assigned to one of three treatments: a 1-hr control treatment, or a 3- or 6-hr UV irradiation treatment. The 1-hr control and 3-hr UV irradiation treatments were chosen based on previous work that showed an increase in size of the first clutch following the same 1-hr control and 3-hr UV irradiation treatments (Heine *et al.*, 2019; see also Han *et al.*, 2016). The 6-hr UV irradiation treatment was chosen to represent a higher dose of radiation than the 3-hr treatment which, we have previously shown, increases reproductive performance in copepods (Heine *et al.*, 2019); the impacts of the 6-hr treatment on reproductive performance are unknown.

Metabolic rate

Immediately following irradiation, each copepod was placed inside an 80 µL well of a 24-well fiber optics respirometer (PreSens, SDR SensorDish Reader, Loligo Systems) in the absence of food. We recorded change in dissolved oxygen for each copepod during one hour after a ~30-minute acclimation period. All assays were completed in autoclaved artificial sea water of S = 32 at 23°C room temperature. Metabolic rate (*R*) was calculated as:

$$R = | [[(DO)_{t2} - (DO)_{t1}] / \Delta t] / L |$$

where DO is dissolved oxygen in mmol/L, *t* is time in seconds (measured in 15 s increments), and L is body length (measured in mm). Measurements (and corresponding copepods) that did not yield a decrease in DO over time were excluded from the study (*n* = five controls, zero 3-hr UV treatments, and one 6-hr UV treatment); this is likely due to trapped air in the bottom of the well of the respirometer that was not seen by the operator, or an insufficient seal. Copepods were placed into primary fixative immediately following respiration assays. Once deceased, each copepod was photographed on a 1 x 1 mm grid under a dissecting microscope in the absence of fixative, and the length (mm) of each copepod was calculated as the distance from the center of the eyespot to the branch in the urosome. Length measurements were completed in ImageJ (Rueden *et al.*, 2017). After each copepod was photographed, the distal half of the urosome was removed to allow for the infiltration of fixative, and the copepod was placed back into primary fixative in a 3.5 mL glass vial and stored overnight at 4°C.

Transmission electron microscopy

Primary fixative was prepared at a final concentration of 12.5 mL of 0.2 M phosphate buffer, 6.25 mL of 10% glutaraldehyde, 5 mL of 10% formaldehyde, and 1.25 mL dH_2O. Tissue was washed for 30 minutes with 0.1 M phosphate buffer three times then placed into a secondary fixative of 2% osmium tetroxide in the dark at room temperature for one and a half hours. Tissue was then dehydrated through a seven-step series from 30, 50, 70, 80, to 90% EtOH at 30 min each, followed by two 45-minute washes in 95% EtOH, and two one-hour washes in 100% EtOH. Samples were then placed into a transitional solvent of propylene oxide (PO) for two 30-minute washes.

Tissue was then infiltrated with a PO/Epon resin mixture at a 2:1 ratio for three days, a 1:1 ratio for three days, a 1:2 ratio for three days, and lastly, pure resin for an additional three days. Expanding our infiltration to 12 days was the only means by which we obtained intact, well-preserved tissue (see Hopkins, 1978). Each copepod was embedded longitudinally in pure Epon resin and cured at 70°C for 24 hours. Ultra-thin, 80 nm longitudinal sections (cutting approximately one-fourth into the copepod to sample muscle tissue along the lateral surface of the prosome) of samples were ultramicrotomed and placed onto 200 mesh copper grids. Sections were then stained with uranyl acetate and lead citrate to increase contrast.

We then performed TEM using a ZEISS EM10 transmission electron microscope. We imaged, at random, three myocytes from the prosome of each copepod. For each myocyte, we collected one image at x8,000 to quantify mitochondrial density and the proportion of IMJs, and three images at a magnification of x25,000 to quantify mitochondrial aspect ratio, area, and the density of IMM. Measurements at x25,000 were completed only on mitochondria from which we could distinguish both inner and outer membrane. All images and measurements were completed only for mitochondria within the subsarcolemmal space of each myocyte (i.e., between the cell membrane and myofibrils).

Mitochondrial behavior and morphology measurements

All mitochondrial behavior and morphology measurements were completed using ImageJ. Measures of mitochondrial aspect ratio, area, and density of IMM were completed from all mitochondria that could be traced within the subsarcolemmal space of each image and averaged for each cell. This allowed us to correlate individual measures of mitochondrial behavior and morphology with measures of mitochondrial density and proportion of IMJs from each cell as a whole. We measured a total of 198 mitochondria (90 control, 40 3-hr, and 68 6-hr) from 45 myocytes (three myocytes from each copepod) of 15 copepods (the first five from each treatment group). This sample size of five copepods per group is comparable to other TEM studies (e.g., Picard *et al.*, 2013*a*; Leduc-Gaudet *et al.*, 2015). On average, we measured a total of 13 ± 5 mitochondria

from each copepod. Only one copepod contained less than eight measured mitochondria (see Nielsen *et al.*, 2017).

Mitochondrial density was quantified as the total number of mitochondria in the area (μm^2) of subsarcolemmal space. The proportion of IMJs was calculated as the total number of electron-dense (darker) contact sites divided by the total number of contacts between mitochondria (Picard *et al.*, 2015; see Heine & Hood, 2020 for further explanation of how IMJs are identified). Mitochondrial area was measured as the size (μm^2) of each mitochondrion by tracing the outer mitochondrial membrane. Mitochondrial aspect ratio was calculated as maximum Feret's diameter divided by minimum Feret's diameter (Marchi *et al.*, 2017), also measured by tracing the outer membrane. Maximum Feret's diameter represents the farthest distance between any two points of the mitochondrion, and minimum Feret's diameter represents the smallest distance between two parallel tangents of the mitochondrion. Density of IMM was quantified using a method adapted from Nielsen et al. (2017). Rows of parallel lines spaced 200 nm apart were overlaid perpendicular to the cristae of each mitochondrion. The total number of intersects between the lines and each crista was divided by the squared area (μm^2) of the mitochondrion. We also recorded the direction of each tissue section determined by the direction of the myofibrils (i.e., longitudinal or transverse).

Before use in the study, the method used to measure density of IMM was validated as follows. For all measured mitochondria from the first copepod of our control group, we quantified the density of IMM using two methods: first, we traced the cristae and divided the total length by the area of the mitochondrion (this gives us a more precise, although time-consuming, estimate of IMM density); second, we used the aforementioned method that estimates the density of IMM using a system of parallel lines. This method was much faster to estimate the density of IMM. Using a general linear regression, we were able to show that a statistically significant, positive linear relationship exists between the two methods (**Figure A1**).

The use of TEM to quantify changes in the three-dimensional behavior and morphology of mitochondria has limitations. In particular, the orientation of each muscle cell and mitochondrion when cut in a two-dimensional fashion will—to an extent—impact the values generated in this study. To control for these effects, we oriented and

microtomed each copepod in the same manner, included the direction of the myofibrils in each micrograph as a covariate in all behavioral and morphological models, included three cell replicates in our analysis of each copepod, and analyzed all measurable mitochondria from each cell.

Analytical design

All statistical analyses were completed using R version 3.5.0 (R Core Team, 2018). We used the "lme4" and "lmerTest" libraries for modeling (Bates *et al.*, 2014; Kuznetsova *et al.*, 2017) and the "ggplot2" package (Wickham, 2009) for graphical development.

The metabolic rate of each copepod was modeled using a general linear model (LM) with treatment (control, 3-hr, and 6-hr UV irradiation) as a categorical predictor. Including age as a random effect is synonymous with including mother ID as a random effect, given that each mother produced a clutch of a unique age. The inclusion of age as a random effect in the respiration model did not impact our estimates in any way, therefore, we chose to exclude age as a random effect in our models since all copepods were aged within six days of one another. The effects of UV irradiation on all behavioral and morphological traits were modeled using general linear mixed models (LMMs) with copepod ID retained as a random effect (random intercept) in each model; this allowed us to control for the non-independence of mean estimates among individual copepods since we sampled three myocytes from each individual. The density of IMM and proportion of IMJs were modeled with an interaction between treatment and mitochondrial density, an interaction between treatment and aspect ratio, and section of the tissue as fixed effects. This allowed us to see how mitochondrial density and aspect ratio affect the response variables while also being affected by the UV irradiation treatments themselves. Section was coded as a fixed effect, and not a random effect, since it was comprised of less than five groups (see Harrison *et al.*, 2018). Mitochondrial density was also modeled as a response variable since it was not retained in any of the former models after stepwise reduction (see below).

Mitochondrial area and mitochondrial density were modeled with treatment and section as fixed effects. Both response variables were cube-root transformed to achieve a

normal distribution of model residuals. The cube-root transformation brought the model residuals closer to normality than the square-root transformation for mitochondrial density, and the model residuals were not normally distributed when mitochondrial area was square-root transformed. Fully-saturated LMMs of mitochondrial behavior and morphology were reduced using the "step" function, but copepod ID was retained as a random effect in all LMMs. Model comparisons were completed using χ^2 analysis, and final models were validated by testing model residuals for normality using the Shapiro-Wilk test.

RESULTS

Descriptive statistics of each variable are presented in **Table 3.1**.

Metabolic rate

As an indication of whole-animal performance, we measured the metabolic rate of each copepod following irradiation. As expected, metabolic rate increased with body size in each treatment group (**Figure A2**). All copepods survived all irradiation treatments. The metabolic rate of copepods following the 3-hr UV irradiation treatment was maintained with respect to the control treatment (Est. = 0.01; *SE* = 0.02; $p = 0.58$). However, the metabolic rate of copepods exposed to the 6-hr UV irradiation treatment decreased significantly in reference to both the control (Est. = -0.05; *SE* = 0.02; $p = 0.03$) and 3-hr (Est. = -0.06; *SE* = 0.02; $p = 0.006$) treatment groups (**Figure 3.1**).

Mitochondrial behavior and morphology

To quantify mitochondrial behavior and morphology, we measured several structural components of individual mitochondria (mitochondrial aspect ratio, mitochondrial area, and density of IMM), as well as behavioral aspects of mitochondria within the subsarcolemmal space of the myocyte as a whole (mitochondrial density and proportion of IMJs). We found that the density of IMM increased markedly in both the 3- and 6-hr UV irradiation treatments in comparison to the control group (**Figure 3.2**; **Table 3.2**), however, the density of IMM from the 6-hr treatment did not differ significantly from the 3-hr treatment (Est. = 12.03; *SE* = 7.21; $p = 0.12$).

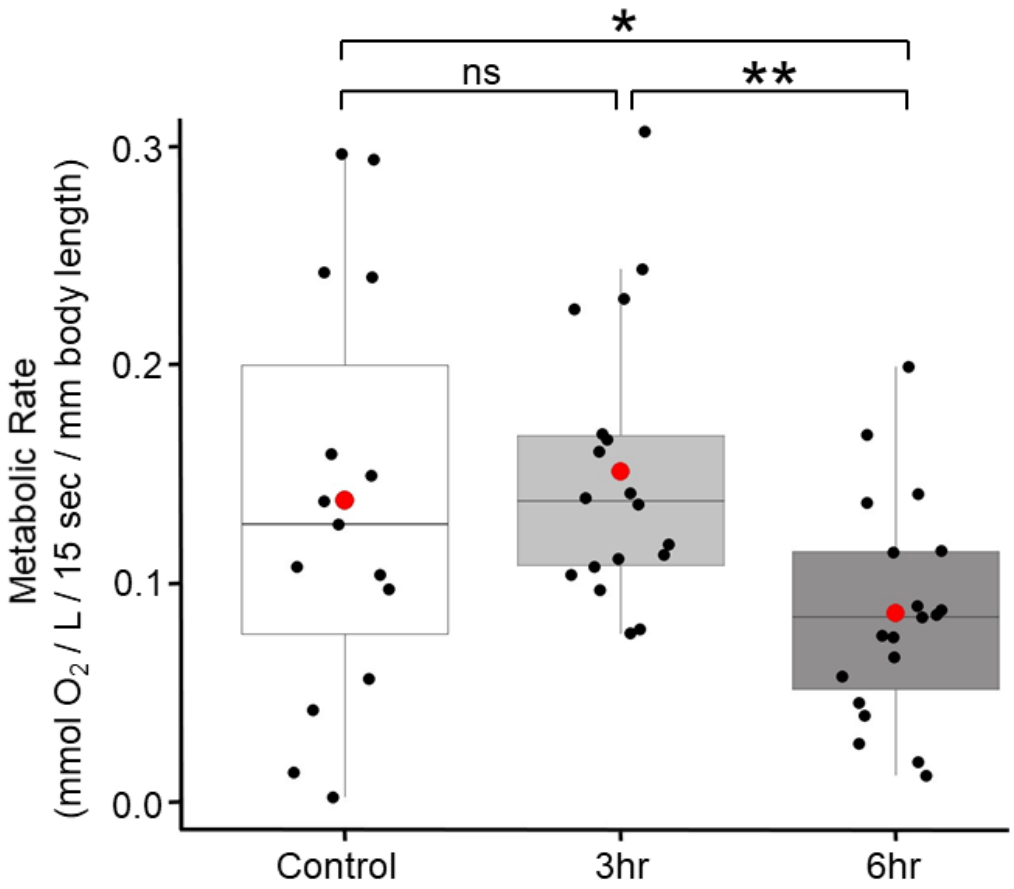

Figure 3.1. Effects of UV irradiation on whole-animal metabolic rate. Boxplots showing the effects of UV irradiation on size-adjusted metabolic rates of individual copepods. Large, red dots represent mean estimates. Significance codes: *0.05, **0.01, ns - not significant.

The majority of cristae in mitochondria from the UV-treated groups were exceedingly narrow, and few mitochondria had cristae with intermembrane space that was visible (e.g., **Figure A3**). The proportion of IMJs increased significantly with increasing aspect ratio in both UV irradiation treatments (**Figure 3.3**; **Table 3.2**), but the proportion of IMJs with increasing aspect ratio did not differ significantly between the 3- and 6-hr treatment groups (Est. = -0.15; *SE* = 0.16; $p = 0.34$). Mitochondrial density increased significantly following both three and six hours of UV irradiation (**Figure 3.4A**; **Table 3.2**), however, there was no difference in mitochondrial density of the 6-hr UV irradiation treatment with respect to the 3-hr treatment (Est. = -0.06; *SE* = 0.08; $p = 0.46$). Lastly, mitochondrial size (area) decreased significantly under the 6-hr UV irradiation treatment but not the 3-hr treatment in reference to the control (**Figure 3.4B**;

Table 3.2). The area of mitochondria following six hours of UV irradiation did not differ significantly from the 3-hr treatment group (Est. = -0.01, *SE* = 0.04; *p* = 0.73).

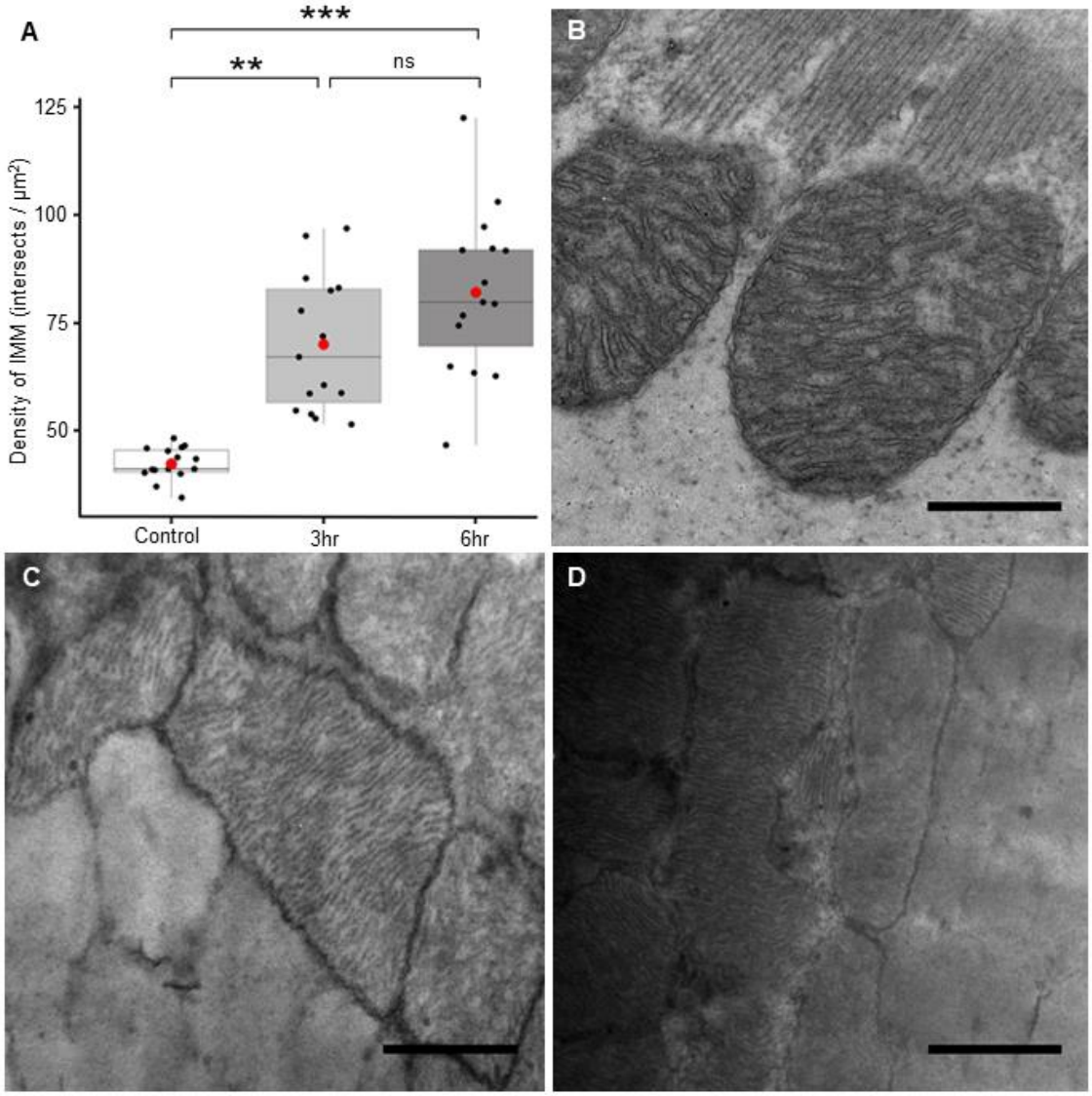

Figure 3.2. Effects of UV irradiation on the density of inner mitochondrial membrane. Boxplots showing the (A) effects of UV irradiation on the density of IMM in mitochondria within the subsarcolemmal space of copepod myocytes. Large, red dots represent mean estimates. Significance codes: **0.01, ***0.001, ns - not significant. Transmission electron micrographs show (B) cristae that are wide and distantly spaced from one another within mitochondria from the control treatment, (C) cristae that are narrow and densely packed within mitochondria from the 3-hr UV irradiation treatment, and (D) cristae that are narrow and densely packed within mitochondria from the 6-hr UV irradiation treatment. All scale bars are 500nm.

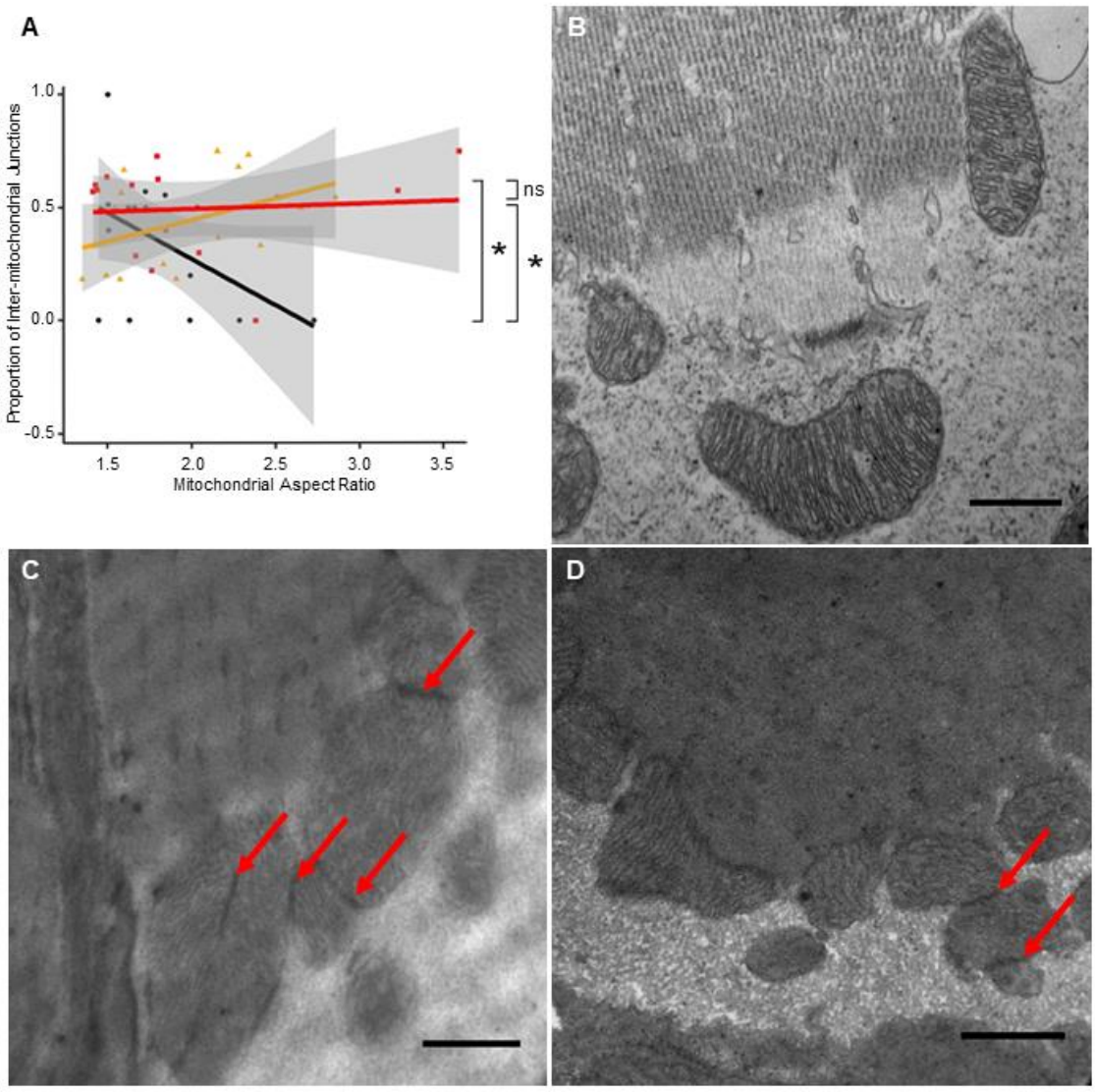

Figure 3.3. Effects of UV irradiation on the proportion of inter-mitochondrial junctions. Scatterplot showing the (A) effects of UV irradiation on the proportion of IMJs with increasing aspect ratio between mitochondria within the subsarcolemmal space of copepod myocytes. Gray shading denotes 95% confidence intervals. Black circles, orange triangles, and red squares represent the control, 3-hr, and 6-hr treatment groups, respectively. Significance codes: *0.05, ns - not significant. Transmission electron micrographs show (B) a low proportion of IMJs between elongated mitochondria from the control treatment, (C) a high proportion of IMJs (red arrows) between elongated mitochondria from the 3-hr UV irradiation treatment, and (D) a high proportion of IMJs between elongated mitochondria from the 6-hr UV irradiation treatment. All scale bars are 500nm.

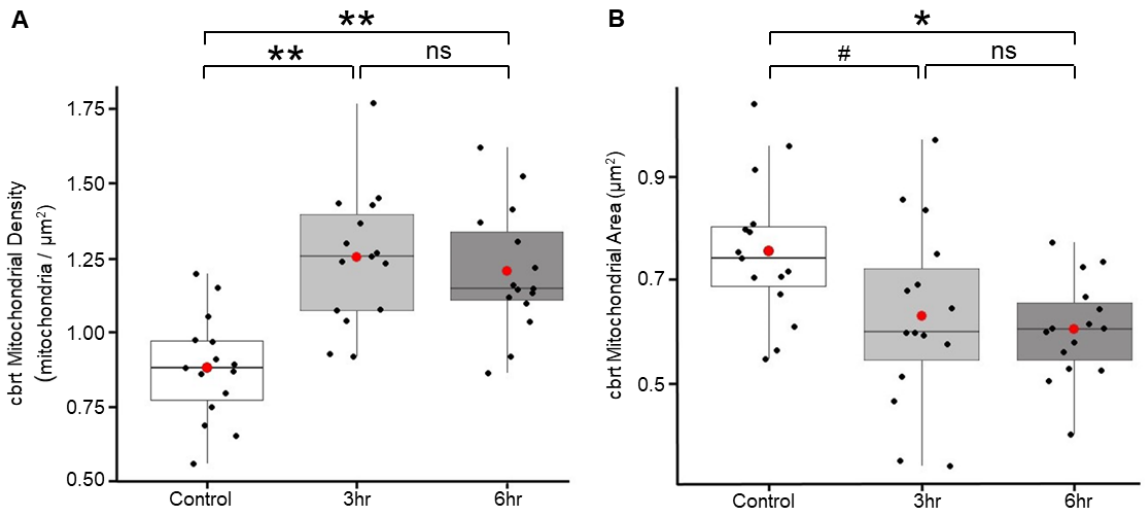

Figure 3.4. Effects of UV irradiation on mitochondrial density and area. Boxplots showing the effects of UV irradiation on (A) mitochondrial density and (B) mitochondrial area of mitochondria within the subsarcolemmal space of copepod myocytes. Note the cube-root transformation of both response variables. Large, red dots represent mean estimates. Significance codes: #0.1, *0.05, **0.01, ns - not significant.

DISCUSSION

Bilaterian animals derive the majority of their energy from oxidative phosphorylation in mitochondria, and much of the research directed toward understanding the role of energy production in animal performance has necessarily focused on the function of the ETS. However, the behavior and morphology of mitochondria can also play key roles in the capacity for energy production. Previous work demonstrated that mitochondrial behavior and morphology influence mitochondrial performance under increased energetic demand, and the literature has also described a large amount of variation that exists in whole-animal performance, both within populations and between taxa (Heine & Hood, 2020). Accordingly, our study aimed to determine how UV radiation influences mitochondrial behavior and morphology at the cellular level, as well as respiratory performance at the organismal level, in myocytes of *Tigriopus californicus* copepods. We hypothesized that UV irradiation induces changes in mitochondrial behavior and morphology, possibly to impact whole-animal metabolic rate under increased energetic demand by increasing the density of IMM and proportion of IMJs.

In copepod myocytes, we found that the density of IMM increased under both three and six hours of UV irradiation, and the proportion of IMJs increased with increasing mitochondrial aspect ratio under UV irradiation. An increase in mitochondrial density and a decrease in mitochondrial size suggest that UV irradiation may induce mitochondrial biogenesis and/or fission. Additionally, copepod metabolic rate was maintained under three hours of UV irradiation but decreased under six hours of exposure. These results indicate that an increase in the density of IMM and proportion of IMJs (along with increased mitochondrial biogenesis and/or fission) may allow animals to maintain metabolic rate, but this capacity for compensation may be lost at higher levels of UV irradiation. These results have broad implications for understanding variation in whole-animal performance.

Animals must produce enough energy in a cost-effective manner to support survival and reproduction. Recent advances in cell and molecular biology have linked increases in the density of IMM with increased energetic demand (Nielsen *et al.*, 2017), but few studies have evaluated this relationship in an ecological context (e.g., Strohm & Daniels, 2003). As the density of IMM increases within the mitochondrion, the number of protein complexes within the IMM may increase, which could lead to greater (or more efficient) ATP production. Thus, mitochondria can potentially respond to increased demand for energy by increasing the density of cristae, but eventually the quantity of IMM will become so high that cristae can no longer maintain an effective electrochemical gradient (Willis *et al.*, 2016). Accordingly, it is important that we begin to delineate when the IMM should increase in response to environmental stressors and how such an increase impacts animal performance.

UV irradiation can increase the energetic demand of the cell by damaging DNA, lipids, and proteins (Setlow & Setlow, 1962), making energy production within mitochondria less efficient. However, the ROS produced by UV irradiation can act as a cellular signal to upregulate beneficial aspects of mitochondrial behavior such as mitochondrial biogenesis (Zhang *et al.*, 2017), or increase antioxidant production (Han *et al.*, 2016). Such changes have the potential to impact the longevity and reproductive success of the animal as a whole (Ristow & Schmeisser, 2011; Zhang & Hood, 2016; Heine *et al.*, 2019). Consistent with these ideas, we observed that mitochondria increase

the density of IMM in response to UV irradiation. While protein markers of biogenesis were not evaluated, an increase in mitochondrial number appears to be a common response to damage that plays a role in rescuing mitochondrial performance (Westermann, 2010). Furthermore, we observed that the respiratory performance of copepods is maintained under lower levels of UV irradiation but decreased under higher levels of UV irradiation. The observed increase in density of the IMM in our study may be the result of mitochondrial repair mechanisms, initiated through mitochondrial fission, that act to discard damaged regions of mitochondria. Consequently, we are left with images of more continuous, intact IMM that are more densely packed into a given area possibly to counteract the damaging effects of UV irradiation. This effort has the potential to fail under higher levels of radiation if efficiency of the mitochondrion decreases when the density of IMM becomes too great in comparison to the volume of mitochondrial matrix and surface area of the outer mitochondrial membrane (Mannella, 2006; see also Navratil *et al.*, 2008). The lower metabolic rates of copepods in the 6-hr treatment group could be interpreted as beneficial (i.e., they do not need to consume as much oxygen to produce ATP), however, we interpret this decrease in metabolic rate as a detriment, provided that the energetic demand of the cell should increase under increasing UV irradiation. Additionally, Han et al. (2016) has previously shown that the same 3- and 6-hr UV irradiation treatments increase both ROS production and antioxidant enzyme activity in other species of *Tigriopus* copepods. Therefore, a decrease in metabolic rate may indicate greater rates of mitochondrial repair and more efficient metabolism, however, other work has also shown an increase in mortality when metabolic rates decrease following UV irradiation in other copepods (Ma *et al.*, 2013). Further work is needed to determine the extent to which the density of IMM varies with ROS production, oxidative damage, and tissue-specific metabolic rates.

The proportion of IMJs within a cell may facilitate communication between mitochondria and, therefore, the efficiency with which ATP is produced. As such, an increase in energetic demand should be met with more IMJs to upregulate (or maintain) energy production as needed. Since higher levels of UV radiation are known to decrease respiratory performance in copepods (Ma *et al.*, 2013), mitochondria should respond both behaviorally and morphologically to counteract this negative effect. One way that

mitochondria can respond to increased energetic demand and/or oxidative stress is to upregulate mitochondrial biogenesis (Zhang *et al.*, 2017), although we found no evidence that the expression of IMJs is linked to mitochondrial density. In both of our UV irradiation treatments, we did observe an increase in the proportion of IMJs in copepod myocytes. However, this increase occurred with increasing aspect ratio of the mitochondria; namely, we observed a greater proportion of IMJs between mitochondria with a lower aspect ratio in our control group, in comparison to more junctions between more elongate mitochondria in our UV-treated groups. If mitochondria became smaller as a result of mitochondrial fission, induced by UV radiation, then elongation is one mechanism by which they could retain a high number of IMJs. Previous work has demonstrated a higher mitochondrial aspect ratio of intermyofibrillar mitochondria than subsarcolemmal mitochondria (Picard *et al.*, 2013*b*), which may be a product of both the mitochondrion's environment (located between myofibrils versus open space between the myofibrils and cell membrane) or differences in energetic demand at different locations within the cell. Also, previous work in rat soleus muscle has shown significant spreading of mitochondria below the sarcolemma following endurance training (Müller, 1976) and an increase in mitochondrial length in mouse embryonic fibroblasts two to three hours after exposure to UV-C (Tondera *et al.*, 2009). Similarly, our study demonstrates that mitochondria can become more elongate within the subsarcolemmal space of the myocyte, possibly to facilitate communication between mitochondria as energetic demand increases (Heine & Hood, 2020) with increasing oxidative stress (Han *et al.*, 2016). Continuous networks of mitochondria (Kirkwood *et al.*, 1986) within the subsarcolemmal space may also result from the movement of mitochondria towards the intermyofibrillar space (see Picard *et al.*, 2013*b*) or mitochondrial fission.

We found that UV irradiation increased mitochondrial density in both of our UV irradiation treatments but decreased the size of subsarcolemmal mitochondria only in the 6-hr treatment group. An increase in small mitochondria may indicate either an increase in mitochondrial fission or an upregulation of mitochondrial biogenesis (or both; see Westermann, 2010; Zhang *et al.*, 2017) within our UV-treated groups. Mitochondrial fission may be an adaptive response to avert apoptosis (Meyer *et al.*, 2017) following an increase in the production of free radicals, and one way to counteract a reduction in

mitochondrial size following fission may be to increase mitochondrial biogenesis (Dorn *et al.*, 2015). A decrease in mitochondrial size can result from the cleavage of damaged regions of mitochondria, however, this effect was observed only in the 6-hr UV irradiation group. Therefore, a reduction in size may be merely a byproduct of the fission process but not a direct response to an increase in UV irradiation (i.e., smaller mitochondria are not necessarily more efficient at producing ATP). Previous work in mammalian cell lines has demonstrated instances of stress-induced mitochondrial hyperfusion following UV-C irradiation (Tondera *et al.*, 2009), but the mitochondria in our study showed an increase, not a decrease, in density and were exposed to UV-A/B light. Increasing the number of mitochondria within the cell can increase the overall function of smaller mitochondrial populations as a whole or compensate for the oxidative damage imposed to individual mitochondria. The maintenance of efficient ATP production is likely a delicate balance between mitochondrial biogenesis and fission following an increase in oxidative stress. Overall, an increase in mitochondrial density and/or fission, a greater proportion of IMJs between mitochondria, and a more densely packed IMM within mitochondria, may facilitate more efficient ATP production to counteract the damaging effects of UV irradiation. These processes appear to act concurrently in the myocytes of *T. californicus* copepods but are likely stressor and tissue dependent.

In the wild, *T. californicus* copepods live in shallow splash pools above the intertidal zone throughout the west coast of North America (Burton *et al.*, 1979). As with most aquatic organisms, the amount of UV radiation to which copepods are exposed on any given day will vary depending on the taxon and habitat in which they thrive (Overholt *et al.*, 2016). Because they live in shallow pools of water, *T. californicus* copepods are likely exposed to higher levels of radiation than most other species of lake- or ocean-dwelling copepods. Accordingly, our study demonstrates that copepod mitochondria can change their behavior and morphology in response to increasing levels of UV radiation, which may allow them to maintain metabolic rate at lower levels of UV radiation and potentially reduce the costs of maintenance. The same 3-hr UV irradiation treatment in this study was previously shown to increase the reproductive performance of *T. californicus* copepods (Heine *et al.*, 2019). It is plausible that changes in mitochondrial

behavior and morphology impact reproductive performance, however, such effects need to be addressed in larger model organisms where the tissue-specific metabolic rates of reproductive tissues can be sampled in conjunction with TEM assays. Also, further work is required to assess the tissue-dependent responses of mitochondria to varying levels of UV radiation in copepods that reside in different environments.

In this study, we demonstrated that UV irradiation can impact whole-animal metabolic rate, possibly through changes in the behavior and morphology of mitochondria. These results illustrate a potential mechanism for how variation in animal function can arise in the face of an exogenous stressor. Additionally, our results show that morphological changes within the cell have the potential to impact metabolic rate even when we do not observe changes in animal function as a whole (i.e., we observed changes in mitochondrial behavior and morphology in the 3-hr UV treatment, but respiratory performance was maintained). Our study suggests that increases in the density of IMM and proportion of IMJs (along with mitochondrial biogenesis and/or fission) in copepod myocytes may allow copepods to maintain metabolic rate under lower levels of radiation. Generally, future work on whole-animal performance should continue to address the proximate causes of variation in energy production at the cellular level, as opposed to only characterizing variation of the organism as a whole. By exploring how mitochondrial behavior and morphology respond to energetic challenges and stressors, we will gain a more thorough understanding of how animals support the processes that underlie survival and reproductive success (Heine & Hood, 2020).

REFERENCES

Bates, D., Mächler, M., Bolker, B. & Walker, S. (2014). Fitting linear mixed-effects models using lme4. arXiv:1406.5823.

Burton, R. S. (1985). Mating system of the intertidal copepod *Tigriopus californicus*. *Marine Biology* **86**, 247-252.

Burton, R. S., Feldman, M. W. & Curtsinger, J. W. (1979). Population genetics of *Tigriopus californicus* (Copepoda: Harpacticoida): I. Population structure along the central California coast. *Marine Ecology Progress Series* **1**, 29-39.

Cadet, J., Sage, E. & Douki, T. (2005). Ultraviolet radiation-mediated damage to cellular DNA. *Mutation Research* **571**, 3-17.

Dorn, G. W., Vega, R. B. & Kelly, D. P. (2015). Mitochondrial biogenesis and dynamics in the developing and diseased heart. *Genes & Development* **29**, 1981-1991.

Drent, R. H. & Daan, S. (1980). The prudent parent: energetic adjustments in avian breeding. *Ardea* **68**, 225-252.

Finkel, T. & Holbrook, N. J. (2000). Oxidants, oxidative stress and the biology of ageing. *Nature* **408**, 239-247.

Han, J., Puthumana, J., Lee, M. C., Kim, S. & Lee, J. S. (2016). Different susceptibilities of the Antarctic and temperate copepods *Tigriopus kingsejongensis* and *T. japonicus* to ultraviolet (UV) radiation. *Marine Ecology Progress Series* **561**, 99-107.

Harrison, X. A., Donaldson, L., Correa-Cano, M. E., Evans, J., Fisher, D. N., Goodwin, C. E., Robinson, B. S., Hodgson, D. J. & Inger, R. (2018). A brief introduction to mixed effects modelling and multi-model inference in ecology. *PeerJ* **6**, e4794.

Hatefi, Y. (1985). The mitochondrial electron transport and oxidative phosphorylation system. *Annual Review of Biochemistry* **54**, 1015-1069.

Heck, D. E., Vetrano, A. M., Mariano, T. M. & Laskin, J. D. (2003). UVB light stimulates production of reactive oxygen species unexpected role for catalase. *Journal of Biological Chemistry* **278**, 22432-22436.

Heine, K. B. & Hood, W. R. (2020). Mitochondrial behaviour, morphology, and animal performance. *Biological Reviews* **95**, 730-737.

Heine, K. B., Powers, M. J., Kallenberg, C., Tucker, V. L. & Hood, W. R. (2019). Ultraviolet irradiation increases size of the first clutch but decreases longevity in a marine copepod. *Ecology & Evolution* **9**, 9759-9767.

Hill, G. E. (2019). *Mitonuclear ecology*. Oxford, UK: Oxford University Press.

Hood, W. R., Zhang, Y., Mowry, A. V., Hyatt, H. W. & Kavazis, A. N. (2018). Life history trade-offs within the context of mitochondrial hormesis. *Integrative & Comparative Biology* **58**, 567-577.

Hood, W. R., Zhang, Y., Taylor, H. A., Park, N. R., Beatty, A. E., Weaver, R. J., Yap, K. N. & Kavazis, A. N. (2019). Prior reproduction alters how mitochondria respond to an oxidative event. *Journal of Experimental Biology* **222**, jeb195545.

Hopkins, C. C. E. (1978). The male genital system, and spermatophore production and function in *Euchaeta norvegica* Boeck (Copepoda: Calanoida). *Journal of Experimental Marine Biology & Ecology* **35**, 197-231.

Hylander, S., Grenvald, J. C. & Kiørboe, T. (2014). Fitness costs and benefits of ultraviolet radiation exposure in marine pelagic copepods. *Functional Ecology* **28**, 149-158.

Kenagy, G. J., Masman, D., Sharbaugh, S. M. & Nagy, K. A. (1990). Energy expenditure during lactation in relation to litter size in free-living golden-mantled ground squirrels. *Journal of Animal Ecology*. **59**, 73-88.

Kirkwood, S. P., Munn, E. A. & Brooks, G. A. (1986). Mitochondrial reticulum in limb skeletal muscle. *American Journal of Physiology-Cell Physiology* **251**, C395-C402.

Kuznetsova, A., Brockhoff, P. B. & Christensen, R. H. B. (2017). lmerTest package: tests in linear mixed effects models. *Journal of Statistical Software* **82**, 1-26.

Leduc-Gaudet, J. P., Picard, M., Pelletier, F. S. J., Sgarioto, N., Auger, M. J., Vallée, J., Robitaille, R., St-Pierre, D. H. & Gouspillou, G. (2015). Mitochondrial morphology is altered in atrophied skeletal muscle of aged mice. *Oncotarget* **6**, 17923.

Ma, Z., Li, W. & Gao, K. (2013). Impacts of UV radiation on respiration, ammonia excretion, and survival of copepods with different feeding habits. *Hydrobiologia* **701**, 209-218.

Mannella, C. A. (2006). The relevance of mitochondrial membrane topology to mitochondrial function. *Biochimica et Biophysica Acta* **1762**, 140-147.

Mannella, C. A., Lederer, W. J. & Jafri, M. S. (2013). The connection between inner membrane topology and mitochondrial function. *Journal of Molecular & Cellular Cardiology* **62**, 51-57.

Marchi, S., Bonora, M., Patergnani, S., Giorgi, C. & Pinton, P. (2017). Methods to assess mitochondrial morphology in mammalian cells mounting autophagic or mitophagic responses. In *Methods in Enzymology* **588**, 171-186. Academic Press.

Meyer, J. N., Leuthner, T. C. & Luz, A. L. (2017). Mitochondrial fusion, fission, and mitochondrial toxicity. *Toxicology* **391**, 42-53.

Müller, W. (1976). Subsarcolemmal mitochondria and capillarization of soleus muscle fibers in young rats subjected to an endurance training. *Cell & Tissue Research* **174**, 367-389.

Navratil, M., Terman, A. & Arriaga, E. A. (2008). Giant mitochondria do not fuse and exchange their contents with normal mitochondria. *Experimental Cell Research* **314**, 164-172.

Ng, W. L. & Bassler, B. L. (2009). Bacterial quorum-sensing network architectures. *Annual Review of Genetics* **43**, 197-222.

Nielsen, J., Gejl, K. D., Hey-Mogensen, M., Holmberg, H. C., Suetta, C., Krustrup, P., Elemans, C. P. H. & Ørtenblad, N. (2017). Plasticity in mitochondrial cristae density allows metabolic capacity modulation in human skeletal muscle. *The Journal of Physiology* **595**, 2839-2847.

Overholt, E. P., Rose, K. C., Williamson, C. E., Fischer, J. M. & Cabrol, N. A. (2016). Behavioral responses of freshwater calanoid copepods to the presence of ultraviolet radiation: Avoidance and attraction. *Journal of Plankton Research* **38**, 16–26.

Pacher, P. & Hajnoczky, G. (2001). Propagation of the apoptotic signal by mitochondrial waves. *EMBO J.* **20**, 4107-4121.

Picard, M., Gentil, B. J., McManus, M. J., White, K., Louis, K. S., Gartside, S. E., Wallace, D. C. & Turnbull, D. M. (2013a). Acute exercise remodels mitochondrial membrane interactions in mouse skeletal muscle. *Journal of Applied Physiology* **115**, 1562-1571.

Picard, M., White, K. & Turnbull, D. M. (2013b). Mitochondrial morphology, topology, and membrane interactions in skeletal muscle: a quantitative three-dimensional electron microscopy study. *Journal of Applied Physiology* **114**, 161-171.

Picard, M., McManus, M. J., Csordás, G., Várnai, P., Dorn, G. W. II, Williams, D., Hajnóczky, G. & Wallace, D. C. (2015). Trans-mitochondrial coordination of cristae at regulated membrane junctions. *Nature Communications* **6**, 6259.

R Core Team (2018). *R: A language and environment for statistical computing*. Vienna, Austria: R Foundation for Statistical Computing.

Ristow, M. & Schmeisser, S. (2011). Extending life span by increasing oxidative stress. *Free Radical Biology & Medicine* **51**, 327-336.

Rueden, C. T., Schindelin, J., Hiner, M. C., DeZonia, B. E., Walter, A. E., Arena, E. T. & Eliceiri, K. W. (2017). ImageJ2: ImageJ for the next generation of scientific image data. *BMC Bioinformatics* **18**, 529.

Salin, K., Villasevil, E. M., Anderson, G. J., Lamarre, S. G., Melanson, C. A., McCarthy, I... & Metcalfe, N. B. (2019). Differences in mitochondrial efficiency explain

individual variation in growth performance. *Proceedings of the Royal Society B* **286**, 20191466.

Santo-Domingo, J., Giacomello, M., Poburko, D., Scorrano, L. & Demaurex, N. (2013). OPA1 promotes pH flashes that spread between contiguous mitochondria without matrix protein exchange. *The EMBO Journal* **32**, 1927-1940.

Setlow, R. B. & Setlow, J. K. (1962). Evidence that ultraviolet-induced thymine dimers in DNA cause biological damage. *Proceedings of the National Academy of Sciences U. S. A.* **48**, 1250-1257.

Speakman, J. R. & Król, E. (2005). Limits to sustained energy intake IX: a review of hypotheses. *Journal of Comparative Physiology B* **175**, 375-394.

Speakman, J. R., Blount, J. D., Bronikowski, A. M., Buffenstein, R., Isaksson, C., Kirkwood, T. B... & Carr, S. K. (2015). Oxidative stress and life histories: unresolved issues and current needs. *Ecology & Evolution* **5**, 5745-5757.

Strohm, E. & Daniels, W. (2003). Ultrastructure meets reproductive success: performance of a sphecid wasp is correlated with the fine structure of the flight–muscle mitochondria. *Proceedings of the Royal Society B* **270**, 749-754.

Tondera, D., Grandemange, S., Jourdain, A., Karbowski, M., Mattenberger, Y., Herzig, S… & Ehses, S. (2009). SLP-2 is required for stress-induced mitochondrial hyperfusion. *The EMBO Journal* **28**, 1589-1600.

Weaver, R. J., Wang, P., Hill, G. E. & Cobine, P. A. (2018). An in vivo test of the biologically relevant roles of carotenoids as antioxidants in animals. *Journal of Experimental Biology* **221**.

Westermann, B. (2010). Mitochondrial fusion and fission in cell life and death. *Nature Reviews Molecular Cell Biology* **11**, 872-884.

Wickham, H. 2009 *ggplot2: Elegant graphics for data analysis*. New York, NY: Springer.

Willis, W. T., Jackman, M. R., Messer, J. I., Kuzmiak-Glancy, S. & Glancy, B. (2016). A simple hydraulic analog model of oxidative phosphorylation. *Medicine & Science in Sports & Exercise* **48**, 990-1000.

Zhang, Y. & Hood, W. R. (2016). Current versus future reproduction and longevity: a re-evaluation of predictions and mechanisms. *Journal of Experimental Biology* **219**, 3177-3189.

Zhang, Y., Humes, F., Almond, G., Kavazis, A. N. & Hood, W. R. (2017). A mitohormetic response to pro-oxidant exposure in the house mouse. *American*

Journal of Physiology – Regulatory, Integrative, & Comparative Physiology **314**, 122-134.

Zick, M., Rabl, R. & Reichert, A. S. (2009). Cristae formation—linking ultrastructure and function of mitochondria. *Biochimica et Biophysica Acta* **1793**, 5-19.

Table 3.1. Mean estimates, standard deviations, and sample sizes (*n*) of mitochondrial behavior and morphology traits measured according to UV irradiation treatment.

Variable	*n*	Control	3-hr UV	6-hr UV
Metabolic rate (mmol O_2 / L / 15 sec / mm body length)	52	0.13 ± 0.09	0.15 ± 0.06	0.08 ± 0.05
Density of IMM (intersects / μm^2)	45	42.1 ± 3.76	69.8 ± 15.7	81.9 ± 18.8
Proportion of IMJs (IMJs / total contacts)	45	0.34 ± 0.30	0.44 ± 0.21	0.49 ± 0.20
Mitochondrial density (mitochondria / μm^2)	45	0.75 ± 0.43	2.13 ± 1.20	1.89 ± 1.01
Mitochondrial area (μm^2)	45	0.47 ± 0.26	0.30 ± 0.24	0.23 ± 0.10
Aspect ratio	45	1.81 ± 0.34	1.98 ± 0.46	2.00 ± 0.65

Table 3.2. Results of LMMs predicting variation in the density of IMM, proportion of IMJs, mitochondrial density, and mitochondrial area. Estimates of mitochondrial density and mitochondrial area are cube-root transformed. Est. is the point estimate, *SE* is the standard error of the estimate, *n* is sample size, and *SD* is the standard deviation of the random effect. Estimates for 3- and 6-hr UV irradiation treatments are in comparison to the control treatment, and transverse sections are in comparison to longitudinal sections. Significance codes: #0.1, *0.05, **0.01, ***0.001, — not retained.

Response	**Predictor**	***n***	**Est. / *SE***	***SD* (Copepod ID)**
Density of IMM				9.26
	3-hr UV	15	27.7 / 7.21**	
	6-hr UV	15	39.7 / 7.21***	
	Mitochondrial density	—	—	
	Aspect Ratio	—	—	
	Transverse	—	—	
Proportion of IMJs				0.04
	3-hr UV	15	-1.00 / 0.42*	
	6-hr UV	15	-0.64 / 0.38	
	Mitochondrial density	—	—	
	Aspect Ratio	45	-0.40 / 0.17*	
	Transverse	—	—	
	3-hr UV : Aspect Ratio	15	0.58 / 0.22*	
	6-hr UV : Aspect Ratio	15	0.43 / 0.20*	
Mitochondrial density				0.09
	3-hr UV	15	0.32 / 0.08**	
	6-hr UV	15	0.26 / 0.08**	
	Transverse	19	0.21 / 0.05***	
Mitochondrial area				0.01
	3-hr UV	15	-0.09 / 0.04#	
	6-hr UV	15	-0.10 / 0.04*	
	Transverse	19	-0.16 / 0.03***	

Chapter 4: **Copepod respiration increases by 7% per °C increase in temperature: A meta-analysis**

Published with Ash Abebe, Alan E. Wilson, and Wendy R. Hood (2019) in *Limnology and Oceanography Letters* **4**(3), 53-61

INTRODUCTION

The rate of chemical reactions is generally known to increase with increasing temperature (Arrhenius law). Thus, studies focused on physiological adaptation commonly evaluate changes in metabolism with changes in thermal environments. More than 90 studies have evaluated the relation between temperature and respiration in copepods, with most either measuring temperature and respiration rates concurrently to evaluate the mechanisms that underlie environmental adaptation (e.g., Anraku, 1964; Auel *et al.*, 2005) or evaluate individual responses to acclimation treatments (e.g., Pascal & Chong, 2016; Liu & Ban, 2017). Yet, despite the large number of experimental and observational measurements, we have a limited understanding of how the energetic demands of copepods respond to increasing temperature.

Respiration rates of animals are influenced by several intrinsic and extrinsic variables, including temperature, body size, and food availability (Nakamura & Turner, 1997; Ikeda *et al.*, 2001; Ikeda *et al.*, 2007; Pedersen *et al.*, 2014; Morata & Søreide, 2015). The speed by which substrates interact with enzymes in the mitochondrial matrix and electron transport system increases with increasing temperature (Packard *et al.*, 1971; Bode *et al.*, 2013) due to the chemical nature of respiratory processes that use oxygen to produce ATP, carbon dioxide, and water. This can be seen experimentally when copepods are acclimated to different temperatures in the lab (e.g., Raymont, 1959; Pascal & Chong, 2016; Liu & Ban, 2017), as well as when respiration is measured in both warm and cold temperatures in the field (e.g., Li *et al.*, 2004; Teuber *et al.*, 2013; Cass & Daly, 2014). Given the vital role of oxygen in the respiratory process, it is important to understand the environmental and intrinsic factors that influence rate of oxygen consumption in key primary consumers such as copepods.

Larger organisms exhibit higher respiration rates due to the greater energetic demand of maintaining more tissue but lower respiration rates per unit mass (Bode *et al.*, 2013). Differences in size and respiration rate may also be tied to sex and age in species with sexual dimorphism and indeterminate growth (Weymouth *et al.*, 1944; Fenchel, 1974). Additionally, food intake provides substrate for oxidative phosphorylation. Thus, the availability of phytoplankton will influence the ability of copepods to sustain respiration (Cruz *et al.*, 2013). Such studies examine the magnitude (mean values) of respiration rates between select temperatures; however, the rate (slope) by which copepods accomplish this increase in respiration across multiple temperatures is more obscure (**Figure A4**).

The effect of temperature on respiration is often examined by calculating Q_{10} values (e.g., Gaudy *et al.*, 2000; Kiko *et al.*, 2016). Q_{10} measurements are typically based on change in the rate of reaction or respiration at two temperatures. The limited scope of these measurements limits an investigator's ability to accurately extrapolate changes in respiration beyond two temperatures. Thus, measuring percent change in respiration rate (rate $\cdot$ $^{\circ}C^{-1}$) across numerous points on a log-linear scale should provide a more accurate prediction (see "Effect size: percent change in respiration" for an explanation of rate calculation in exponential and log-linear models).

The aim of this study was to explain how copepod respiration (dissolved oxygen) may respond to warming waters as a result of climate change. We asked the specific question: how much do copepod respiration rates change with a degree change in water temperature for calanoid, cyclopoid, and harpacticoid copepods? We also examined the effect of fasting on copepod respiration rates. To determine if copepod respiration rates increase significantly with temperature, we conducted a formal, random-effects meta-analysis without moderators. The method used to measure dissolved oxygen, food availability, and whether or not studies scaled respiration rates by copepod dry weight (DW) were included as categorical moderators in meta-analytical mixed-effects models to further delineate heterogeneity in respiration. If copepod respiration rates display a plastic response to water temperature, we expect the rate of change in respiration rates to increase significantly (a non-zero increase) with increasing temperature. We also expect studies that fed copepods prior to respiration measurements to display higher rates of

change in oxygen consumption with increasing temperature in comparison to studies that fasted copepods.

METHODS

Literature search

Following the Preferred Reporting Items of Systematic reviews and Meta-Analyses (PRISMA) recommendations (Moher *et al.*, 2009), we used two databases to quantify respiration rates across a range of temperatures for three orders of copepods while controlling for the method used to measure dissolved oxygen, food availability, and the incorporation of DW into respiration measurements. We searched Google Scholar and Web of Science using the search term "copepod respiration" from 02 to 13 February 2018. Most studies were not useful; therefore, we refined our searches accordingly. We used the search criteria "in title" to search Google Scholar, returning 47 articles (10 collected); "all topics" was used to search Web of Science, returning 407 articles (72 collected). Both databases were also searched using "copepod oxygen" on 17 February 2018. We used "in title" to search both databases, returning 38 articles for Google Scholar (three collected) and 39 for Web of Science (one collected). We also searched the literature cited of acquired articles for appropriate studies (five collected).

To be included in our analyses, each study must have reported—at a minimum—organismal oxygen consumption across two or more temperatures. We excluded studies that reported respiration rates at only one temperature or across temperatures with a range not greater than 1°C. We did not include review papers, but acquired appropriate papers from reviews to directly calculate effect sizes. The search criteria yielded an initial collection of 86 articles, of which we screened based on the following criteria (**Figure A5**).

Studies that reported mean oxygen consumption across an uncertain range of temperatures (e.g., 1-5°C) were excluded. Suboptimal or exceedingly high temperatures known to denature or damage proteins (Somero, 1995) were excluded from our calculations. We also excluded studies that failed to report the number of replicates per mean value.

We only included studies that measured oxygen consumption at the organismal level and not CO_2 production, N consumption, C : O ratios, or oxygen consumption based on electron transport activity. We did not feel that attempts to convert said values to organismal oxygen consumption would be accurate (Glazier, 2005). Studies that measured oxygen consumption per unit of DW were coded separately from those that did not incorporate DW.

Effect size estimation

Given the rate of change in oxygen consumption across temperatures is often identical between sexes, only differing in magnitude (Weymouth *et al.*, 1944; Isla & Perissinotto, 2004; Liu & Ban, 2017), we combined male and female data and reported the life history stage of individuals (i.e., nauplius, copepodid, and adult), in addition to whether studies included DW if applicable, to control for size. Single data points of a different life history stage in comparison to the rest of the study were removed when calculating effect sizes to accurately represent body size.

We reported the family and order of copepods to account for phylogenetic non-independence. Separate effect sizes were calculated for each species where applicable. We also recorded the method used to measure dissolved oxygen. Studies that used polarography to measure oxygen but did not specify using Clark-type electrodes were coded as using "polarographic electrodes."

Both experimental and observational studies were used to be as inclusive as possible.

Data acquisition

We calculated 78 effect sizes from 32 studies from 1939 to 2017, including 50 species from three copepod orders. Several studies reported functions of data graphed with *y*-axes fit to either $\log_{10}$, ln, or exponential scaling; for these studies, we extracted data from graphs using ImageJ (Schindelin *et al.*, 2012) and transformed the measured values to the original data using $(10^{Y}) \cdot 100^{-1}$ for ln graphs and $(10^{Y}) \cdot 10^{-1}$ for $\log_{10}$ graphs. These values, and measures taken directly from exponential graphs, were transformed to natural log values to acquire variance estimates. Our line estimate of $\log_{10}$

respiration differed from that reported in McAllen et al. (1999), although our graph coincided with that of the study. In this one instance, we used the β_1 estimate of 0.0971 acquired from our extracted data.

Most studies reported mean respiration rates for a given value of temperatures. In these cases, we used the mean, reported error estimate (SD or SE), and *n* number of replicates per mean to calculate β_1 and the original sampling variance of the raw data (see "Effect size: percent change in respiration"). For studies that reported mean values and range (no SD or SE available), we calculated the SD using (range $\cdot$ 4^{-1}), assuming a small number of replicates that were normally distributed per mean. If only the range and median using boxplots were reported, we calculated the mean using ((min + 2(median) + max) $\cdot$ 4^{-1}), for sample sizes < 25 (Hozo *et al.*, 2005).

Effect size: Percent change in respiration

For each species within each study, we calculated percent change in respiration per one-unit increase in temperature. Given that respiration increases exponentially with temperature, we used β_1 of the exponential function $R = \beta_0 \cdot e^{\beta_1 T}$ to calculate our effect size. Here, β_1 coincides with β_1 of the log-linear respiration model, expressed as $\ln R = \ln\beta_0 + \beta_1 T$. We calculated percent change in respiration as:

$$\%\text{change} = (e^{\beta_1} - 1) \cdot 100$$

Variance in percent change (V) was calculated using the delta method (Ver Hoef, 2012):

$$V = (100)^2 \cdot e^{2\beta_1} \cdot (\text{SE})^2$$

where SE is the standard error of the log-linear respiration model.

For studies that did not report the SE and β_1 of the log-linear or exponential model but only mean values at given temperatures, we calculated the original sampling variance of the log-linear model slope as:

$$\text{SE}^2 = \frac{(\sigma_1^2 + \sigma_2^2)/(\sum n - 2)}{\sum(n \cdot (x - \bar{x})^2)}$$

where σ_1^2 is $\sum((n-1)\cdot\sigma_{\mathrm{LM}}^2)$, σ_2^2 is $\sum(n\cdot(\ln R-\ln f)^2)$, n is a vector containing the number of replicates for each mean at a given temperature x, and $\bar{x}$ is $\sum(n\cdot x)/\sum n$. σ_{LM}^2 is the variance of a given mean ln respiration rate at temperature x, ln$R$ is the natural log respiration rates, and ln$f$ is the fitted values of the log-linear model. For studies that reported the standard error of mean rates (σ_{M}), we first calculated σ_{LM} using ($\sigma_{\mathrm{M}}\cdot \mathrm{mean}^{-1}$); this was derived using the delta method (Ver Hoef, 2012). This σ_{LM}^2 was then used in the calculation of SE^2.

Random-effects meta-analyses and mixed modeling

Using a Bayesian approach, we conducted formal, random-effects meta-analyses without moderators to quantify percent change in copepod respiration rates per degree change in temperature across calanoid, cyclopoid, and harpacticoid copepod orders and calanoid families. To further examine the heterogeneity in copepod respiration with increasing temperature, we conducted meta-analytical mixed-effects modeling with methodology, food availability, or DW as categorical moderators.

A common concern of meta-analysis is non-independent effect sizes within and between studies; examples include calculating effect sizes of identical taxa or calculating multiple effect sizes from one study (Nakagawa *et al.*, 2017). We conducted random-effects meta-analyses with authorship and ultrametric phylogenies of either Calanoida families or Calanoida, Cyclopoida, and Harpacticoida orders as random effects. We also included species as a random effect to account for non-independence when calculating mean effects for each family- or order-level phylogeny. Relatedness of copepod orders was obtained from Khodami et al. (2017), and family-level relatedness was determined from Blanco-Bercial et al. (2010) and Bradford-Grieve et al. (2010). Model priors of V = 1 and nu (degree of belief) = 1 were used for all random effects. Model parameters were based on posterior distributions of 5,000 samples.

Meta-analytical mixed-effects models included food availability, the method used to measure dissolved oxygen, or whether studies scaled respiration by DW, as categorical moderators; these models also included the random effects listed above. Both newer (fiber optics) and older (Winkler titration) dissolved oxygen measurement methods were

included as reference groups. We did not have enough replicates to include life history stage or water salinity as moderators in our analyses, nor examine moderator effects within Harpacticoida or Cyclopoida (see **Table A6** for variable descriptions). One study did not report the taxon of copepods.

Copepod respiration is known to increase with temperature, however, several of our effect size estimates show negative percent changes in this relationship (i.e., respiration rates decrease as temperature increases). We ran sensitivity analysis by removing these unexpected, negative effects and re-analyzing percent changes at the family level since all negative effect sizes stemmed from Calanoida. To test for publication bias, we qualitatively examined funnel plot asymmetry, as well as a bubble plot of effect sizes plotted against publication year. Funnel plots portray effect size estimates plotted against the standard error of those estimates. Asymmetry in the plot, or estimates that fall outside the confidence intervals, indicate possible publication bias. Bias and overall effect size heterogeneity was assessed by modeling author (categorical) and publication year (continuous) as moderators using Restricted Maximum Likelihood "REML" in "metafor." All phylogenetic meta-analyses were completed using the package "MCMCglmm" (Hadfield, 2010; Hadfield & Nakagawa, 2010) and "ape" (Paradis *et al.*, 2004) in R version 3.4.4 (R Core Team, 2018). We used "ggplot2" (Wickham, 2002) and "metafor" (Viechtbauer, 2010) for graphical development.

RESULTS

Effects of temperature on copepod respiration

Although copepod respiration is known to increase exponentially with temperature, we have yet to determine if the increase is significant (non-zero) and the rate (function slope) of such an increase. While including authorship, order-level phylogeny, and species as random effects, we determined that respiration exhibited a significant, non-zero increase of 7.51% per one-unit increase in temperature (**Table 4.1**). Order-level relatedness with corresponding meta-analytical means and 95% credible intervals (CIs) are presented in **Figure 4.1**.

We included authorship, family-level phylogeny, and species as random effects in our analysis of calanoid copepods and found that respiration increased by 6.67% per one-

unit increase in temperature (**Table 4.1**). Family-level relatedness with corresponding meta-analytical means and 95% CIs are presented in **Figure 4.2**. Effects with 95% CIs that do not overlap zero are considered statistically significant ($\alpha = 0.05$).

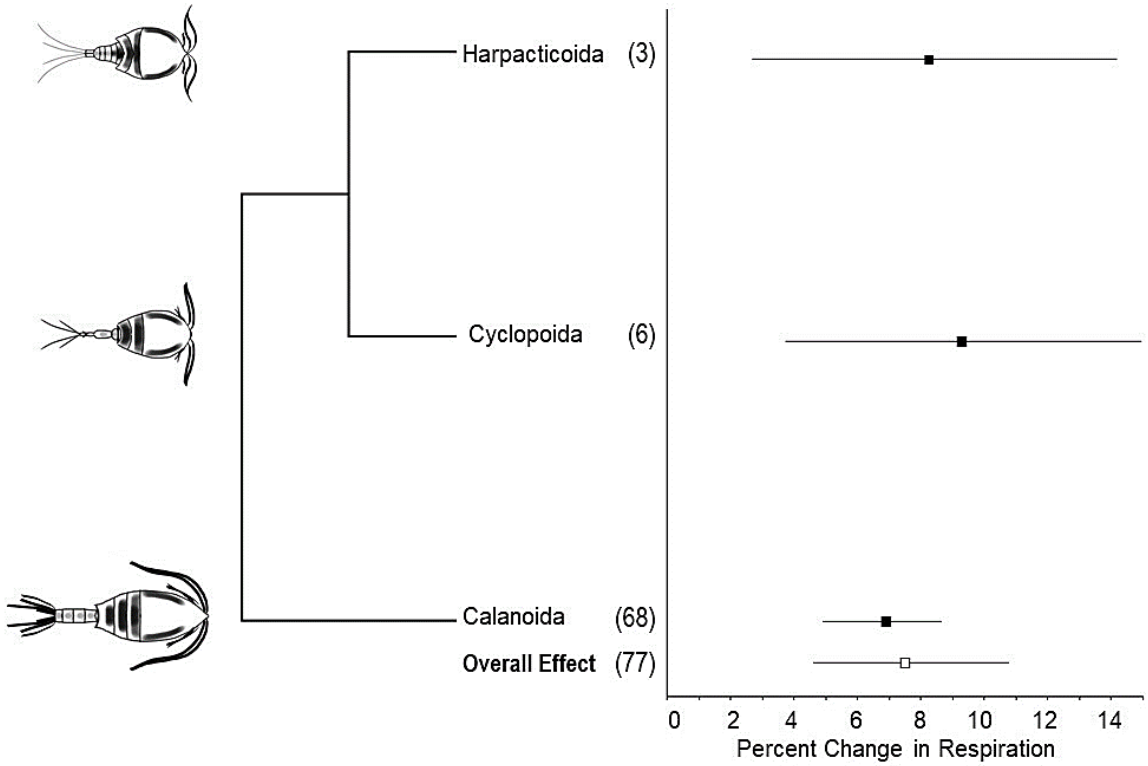

Figure 4.1. Meta-analytical, mean percent changes in respiration with 95% CIs of Calanoida, Cyclopoida, and Harpacticoida copepod orders. Overall effect represents the collective effect of all three orders. Number of effect sizes per order is in parentheses. Effect size estimates with CIs that do not overlap zero are considered statistically significant ($\alpha = 0.05$).

Methodology, food availability, and DW

Upon further examining the heterogeneity in respiration, we found that the method used to measure dissolved oxygen significantly influenced effect size estimates across all three orders of copepods. Both newer (fiber optics) and older (gas chromatography) methods produced significantly smaller percent changes in respiration when compared to the commonly-used Winkler titration method. We also found that Winkler titration produced significantly larger percent changes in respiration with increasing temperature than polarographic electrodes (**Table 4.1**). In other words,

copepod respiration increased at a significantly higher rate with temperature as measured by Winkler titration.

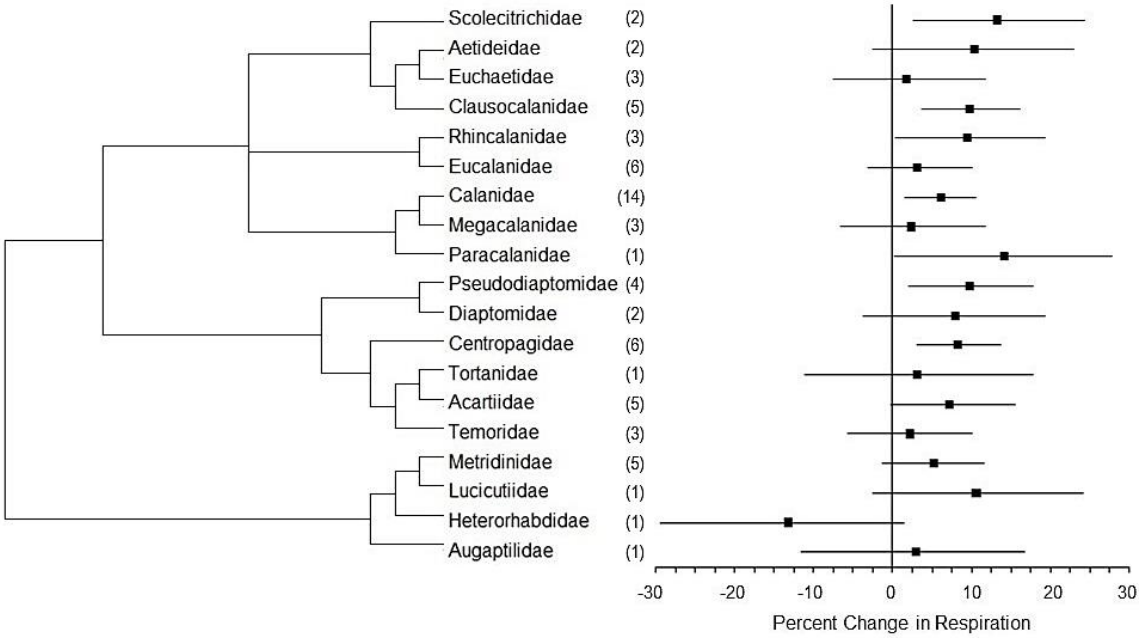

Figure 4.2. Meta-analytical, mean percent changes in respiration with 95% CIs of Calanoida copepod families. Number of effect sizes per family is in parentheses. Effect size estimates with CIs that do not overlap zero are considered statistically significant ($\alpha = 0.05$).

Fiber optic meters are becoming increasingly popular in respiration research, nevertheless, Clark-type electrodes are used routinely. Effect size estimates using fiber optics did not differ significantly from those obtained using Clark-type electrodes, nor from older methods such as Cartesian divers or manometers (**Table 4.1**). We did not have enough replicates to assess the impact of methodology at the family level.

Provided that food intake supplies a greater amount of available substrate for oxidative phosphorylation, we hypothesized that the respiration rates of copepods fed prior to respiration measurements would increase at a higher rate in response to increasing temperature than copepods that were fasted. However, the presence of food did not affect the manner in which respiration responded to increasing temperature in the order- or family-level models (**Table 4.1**).

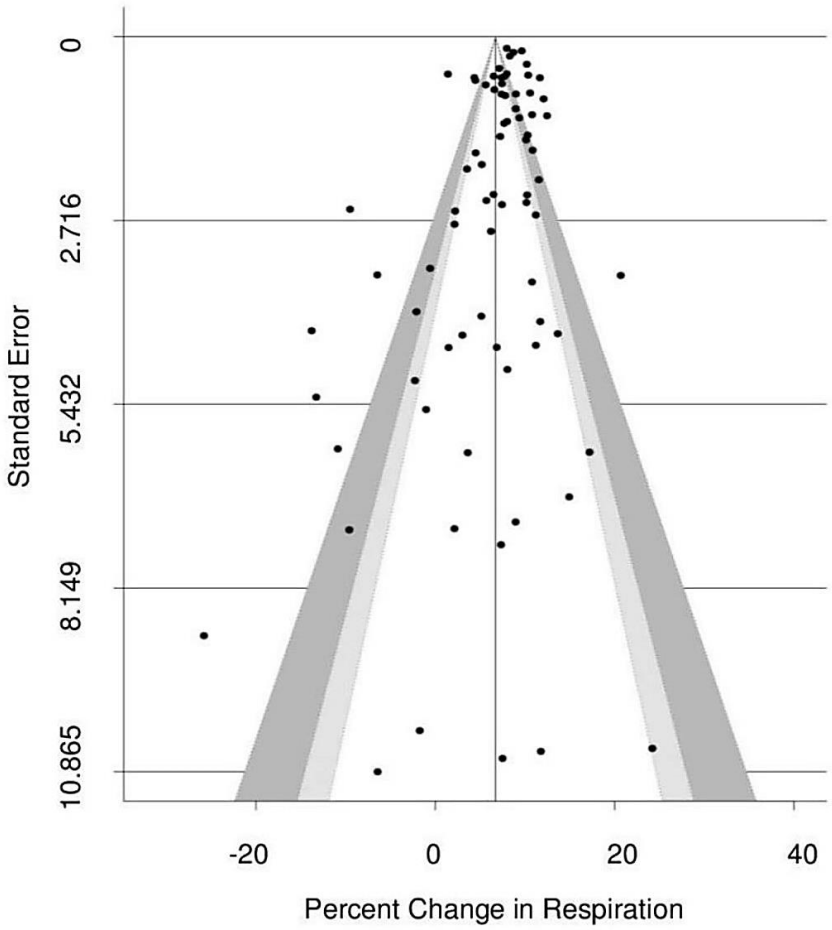

Figure 4.3. Funnel plot of effect sizes plotted against standard error to assess asymmetry and publication bias. Point estimates that display asymmetry in the plot or fall outside the confidence intervals indicate possible publication bias. White, light gray, and dark gray shading correspond to 90%, 95%, and 99% confidence intervals.

Lastly, several studies have scaled respiration by copepod DW to account for greater respiration rates of larger copepods. We found no difference between effect size estimates that did or did not scale respiration by DW (**Table 4.1**).

Sensitivity analysis

Given the positive relationship between respiration and temperature, not including exceedingly high or low temperatures, we did not anticipate finding negative percent changes in the literature. Therefore, we ran sensitivity analysis at the family level by removing all negative effects from our model. This provides a further understanding of how studies that calculated decreases in respiration with increasing temperature

influenced our results. With family-level phylogeny, authorship, and species as random effects, we found that respiration increased by 7.97% with increasing temperature (l-CI 95% = 6.01, u-CI 95% = 9.96, $p < 0.001$).

Publication bias

We qualitatively analyzed funnel plot asymmetry of effect sizes and standard error and found that several effect sizes fell outside the 95% and 99% confidence intervals (**Figure 4.3**). We also examined publication bias as a function of publication year using a bubble plot (**Figure A7**). Several negative effects were deemed outliers, confirming our decision to remove these values in our sensitivity analysis. We found no significant effect of authorship or publication year on effect size estimates ($p > 0.05$). Heterogeneity between study effect sizes was estimated at $I^2 = 96.9\%$.

DISCUSSION

The rate of increase of copepod respiration across a broad range of temperatures varies greatly among published studies. We calculated percent change in respiration rates across 32 studies (Appendix **List A8**) and addressed the question: how much do copepod respiration rates change with a degree change in water temperature for calanoid, cyclopoid, and harpacticoid copepods? Respiration rate increased by 7.51% among these three orders, and 6.67% within Calanoida. However, when negative effects were removed from our family-level model, percent change in Calanoida respiration increased from 6.67% to 7.97%.

Commonly used Q_{10} values limit an investigator's capacity to predict copepod respiration rates across a broad range of temperatures because Q_{10} values are based on two temperatures. Furthermore, Q_{10} values must be interpreted through comparison to other Q_{10} values. The effect size of 7% reported here demonstrates how respiration rates change across the full range of published temperatures across which copepods are viable. Because these equations are based on many temperatures, we believe that percent change is more accurate in predicting respiration rates than Q_{10}.

We examined the effect of fasting on copepod respiration rates and hypothesized that percent change in respiration of fed copepods would be greater than fasted copepods.

We found no support for this hypothesis. This result does not imply that the respiration rates of fed copepods are similar to starved copepods, but concludes that food availability does not affect how copepod respiration responds to increasing temperature. Although larger organisms exhibit higher organismal respiration rates on average than smaller organisms (Bode *et al.*, 2013), copepod studies have been inconsistent in their decision to scale respiration measurements to copepod DW. Given this dichotomy in study design, we compared effect sizes between these studies but found no significant difference in percent change in respiration.

Recent technological advances, such as fiber optics, allow researchers to measure respiration non-invasively without consuming oxygen in the process (Preininger *et al.*, 1994). We compared effect sizes across studies that used recent advances (fiber optics) with older methods that are still in use (Winkler titration). Winkler titration produced significantly larger percent changes in respiration with increasing temperature than fiber optics, gas chromatography, and polarography.

Several inquiries have been conducted regarding the accuracy of Winkler titration and optical oxygen sensors. Optical oxygen sensors are largely variable in their response time—influenced by stirring—and therefore, membrane thickness and material should be selected carefully in accordance with stirring (Markfort & Hondzo, 2009). This contrasts with possible inaccuracies of Winkler titration, including the oxygen contribution of reagents (Carpenter, 1965). Provided that Winkler titration has a greater accuracy (Markfort & Hondzo, 2009) and is used to calibrate other oxygen sensors, future research needs to further develop the accuracy and response time of non-Winkler methods as a function of increasing temperature.

Percent change in respiration of 6% to 7% corroborates the results of Green (1975), Teare and Price (1979), Gaudy et al. (2000), Li et al. (2015), Kiko et al. (2016), and Svetlichny (2017). However, studies such as Isla and Perissinotto (2004), Castellani et al. (2005), and Teuber et al. (2013) reported increasingly large changes in respiration with increasing temperature, whereas Raymont (1959) and Castellani and Altunbas (2014) reported exceedingly small or negative relationships (Raymont, 1959; Ikeda, 1979; Teuber *et al.*, 2013). Although investigators may not expect respiration to decrease

with increasing temperature, it is important that researchers discuss these relationships to determine why studies measure such trends (e.g., taxonomic relatedness).

Organisms respond in vastly different ways to increasing water temperature; therefore, it is important to understand the physiological responses of organisms including primary consumers such as copepods. Previous studies have demonstrated that certain species of *Calanus* and *Oithona*, for example, withstand a relatively large increase in water temperature from -1.7°C to 8°C from June to July during seasonal vertical migrations (Darnis & Fortier, 2014). Our study elaborates on such findings by characterizing the ability of copepods to increase their respiration rates in response to increasing water temperature. We conclude that copepod respiration rates increase significantly with temperature (a non-zero increase) by 7% per °C. This result is a crucial first step in understanding the physiological response of copepods to increasing water temperature; however, the effects of other environmental factors such as ocean acidification (Vehmma *et al.*, 2013) and increasing CO_2 (Runge *et al.*, 2016) warrant further investigation.

REFERENCES

Anraku, M. (1964). Influence of the Cape Cod Canal on the hydrography and on the copepods in Buzzards Bay and Cape Cod Bay, Massachusetts. II. Respiration and feeding. *Limnology & Oceanography* **2**, 195-206.

Auel, H., Hagen, W., Ekau, W. & Verheye, H. M. (2005). Metabolic adaptations and reduced respiration of the copepod *Calanoides carinatus* during diapause at depth in the Angola-Benguela Front and northern Benguela upwelling regions. *African Journal of Marine Science* **3**, 653-7.

Blanco-Bercial, L., Bradford-Grieve, J. & Bucklin, A. (2010). Molecular phylogeny of the Calanoida (Crustacea: Copepoda). *Molecular Phylogenetics & Evolution* **1**, 103-13.

Bode, M., Schukat, A., Hagen, W. & Auel, H. (2013). Predicting metabolic rates of calanoid copepods. *Journal of Experimental Marine Biology & Ecology* **444**, 1-7.

Bradford-Grieve, J. M., Boxshall, G. A., Ahyong, S. T. & Ohtsuka, S. (2010). Cladistic analysis of the calanoid Copepoda. *Invertebrate Systematics* **3**, 291-321.

Carpenter, J. H. (1965). The accuracy of the Winkler method for dissolved oxygen analysis. *Limnology & Oceanography* **10**, 135-140.

Cass, C. J. & Daly, K. L. (2014). Eucalanoid copepod metabolic rates in the oxygen minimum zone of the eastern tropical north Pacific: Effects of oxygen and temperature. *Deep-Sea Research, Part* I **94**, 137-49.

Castellani, C. & Altunbaş, Y. (2014). Seasonal change in acclimatised respiration rate of *Temora longicornis*. *Marine Ecology Progress Series* **500**, 83-101.

Castellani, C., Robinson, C., Smith, T. & Lampitt, R. S. (2005). Temperature affects respiration rate of *Oithona similis*. *Marine Ecology Progress Series* **285**, 129-35.

Cruz, J., Garrido, S., Pimentel, M. S., Rosa, R., Santos, A. M. & Ré, P. (2013). Reproduction and respiration of a climate change indicator species: effect of temperature and variable food in the copepod *Centropages chierchiae*. *Journal of Plankton Research* **5**, 1046-58.

Darnis, G. & Fortier, L. (2014). Temperature, food and the seasonal vertical migration of key arctic copepods in the thermally stratified Amundsen Gulf (Beaufort Sea, Arctic Ocean). *Journal of Plankton Research* **4**, 1092-108.

Fenchel, T. (1974). Intrinsic rate of natural increase: the relationship with body size. *Oecologia* **4**, 317-26.

Gaudy, R., Cervetto, G. & Pagano, M. (2000). Comparison of the metabolism of *Acartia clausi* and *A. tonsa*: influence of temperature and salinity. *Journal of Experimental Marine Biology & Ecology* **1**, 51-65.

Glazier, D. S. (2005). Beyond the '3/4-power law': variation in the intra-and interspecific scaling of metabolic rate in animals. *Biological Reviews* **4**, 611-62.

Green, J. D. (1975). Feeding and respiration in the New Zealand copepod *Calamoecia lucasi* Brady. *Oecologia* **4**, 345-58.

Hadfield, J. D. (2010). MCMC methods for multi-response generalized linear mixed models: The MCMCglmm R package. *Journal of Statistical Software* **33**, 1-22.

Hadfield, J. D. & Nakagawa, S. (2010). General quantitative genetic methods for comparative biology: Phylogenies, taxonomies and multi-trait models for continuous and categorical characters. *Journal of Evolutionary Biology* **23**, 494-508.

Hozo, S. P., Djulbegovic, B. & Hozo, I. (2005). Estimating the mean and variance from the median, range, and the size of a sample. *BMC Medical Research Methodology* **1**, 13.

Ikeda, T. (1979). Respiration rates of copepod larvae and a ciliate from a tropical sea. *Journal of Oceanography* **1**, 1-8.

Ikeda, T., Kanno, Y., Ozaki, K. & Shinada, A. (2001). Metabolic rates of epipelagic marine copepods as a function of body mass and temperature. *Marine Biology* **3**, 587-96.

Ikeda, T., Sano, F. & Yamaguchi, A. (2007). Respiration in marine pelagic copepods: a global-bathymetric model. *Marine Ecology Progress Series* **339**, 215-9.

Isla, J. A. & Perissinotto, R. (2004). Effects of temperature, salinity and sex on the basal metabolic rate of the estuarine copepod *Pseudodiaptomus hessei*. *Journal of Plankton Research* **5**, 579-83.

Khodami, S., McArthur, J. V., Blanco-Bercial, L. & Arbizu, P. M. (2017). Molecular phylogeny and revision of copepod orders (Crustacea: Copepoda). *Scientific Reports* **1**, 9164.

Kiko, R., Hauss, H., Buchholz, F. & Melzner, F. (2016). Ammonium excretion and oxygen respiration of tropical copepods and euphausiids exposed to oxygen minimum zone conditions. *Biogeosciences* **8**, 2241-55.

Li, C., Sun, S., Wang, R. & Wang, X. (2004). Feeding and respiration rates of a planktonic copepod (*Calanus sinicus*) oversummering in Yellow Sea Cold Bottom Waters. *Marine Biology* **1**, 149-57.

Li, W., Han, G., Dong, Y., Ishimatsu, A., Russell, B. D. & Gao, K. (2015). Combined effects of short-term ocean acidification and heat shock in a benthic copepod *Tigriopus japonicus* Mori. *Marine Biology* **9**, 1901-12.

Liu, X. & Ban, S. (2017). Effects of acclimatization on metabolic plasticity of *Eodiaptomus japonicus* (Copepoda: Calanoida) determined using an optical oxygen meter. *Journal of Plankton Research* **1**, 111-21.

Markfort, C. D. & Hondzo, M. (2009). Dissolved oxygen measurements in aquatic environments: the effects of changing temperature and pressure on three sensor technologies. *Journal of Environmental Quality* **38**, 1766-1774.

McAllen, R., Taylor, A. C. & Davenport, J. (1999). The effects of temperature and oxygen partial pressure on the rate of oxygen consumption of the high-shore rock pool copepod *Tigriopus brevicornis*. *Comparative Biochemistry & Physiology Part A: Molecular & Integrative Physiology* **2**, 195-202.

Moher, D., Liberati, A., Tetzlaff, J., Altman, D. G. & The PRISMA Group. (2009). Preferred reporting items for systematic reviews and meta-analyses: the PRISMA statement. *PLoS Medicine* **6**, e1000097.

Morata, N. & Søreide, J. E. (2015). Effect of light and food on the metabolism of the Arctic copepod *Calanus glacialis*. *Polar Biology* **1**, 67-73.

Nakagawa, S., Noble, D. W., Senior, A. M. & Lagisz, M. (2017). Meta-evaluation of meta-analysis: ten appraisal questions for biologists. *BMC Biology* **1**, 18.

Nakamura, Y. & Turner, J. T. (1997). Predation and respiration by the small cyclopoid copepod *Oithona similis*: How important is feeding on ciliates and heterotrophic flagellates? *Journal of Plankton Research* **9**, 1275-88.

Packard, T. T., Healy, M. L. & Richards, F. A. (1971). Vertical distribution of the activity of the respiratory electron transport system in marine plankton. *Limnology & Oceanography* **1**, 60-70.

Paradis, E., Claude, J. & Strimmer, K. (2004). APE: analyses of phylogenetics and evolution in R language. *Bioinformatics* **20**, 289-290.

Pascal, L. & Chong, V. C. (2016). Does developmental temperature modulate copepods respiratory activity through adult life? *Journal of Plankton Research* **5**, 1215-24.

Pedersen, S. A., Håkedal, O. J., Salaberria, I., Tagliati, A., Gustavson, L. M., Jenssen, B. M., Olsen, A. J. & Altin, D. (2014). Multigenerational exposure to ocean acidification during food limitation reveals consequences for copepod scope for growth and vital rates. *Environmental Science & Technology* **20**, 12275-84.

Preininger, C., Klimant, I. & Wolfbeis, O. S. (1994). Optical fiber sensor for biological oxygen demand. *Analytical Chemistry* **11**, 1841-6.

R Core Team. (2018). R: A language and environment for statistical computing. R Foundation for Statistical Computing, Vienna, Austria. https://www.R-project.org/.

Raymont, J. E. (1959). The respiration of some planktonic copepods. *Limnology & Oceanography* **4**, 479-91.

Runge, J. A., Fields, D. M., Thompson, C. R., Shema, S. D., Bjelland, R. M., Durif, C. M., Skiftesvik, A. B. & Browman, H. I. (2016). End of the century CO2 concentrations do not have a negative effect on vital rates of *Calanus finmarchicus*, an ecologically critical planktonic species in North Atlantic ecosystems. *ICES Journal of Marine Science* **3**, 937-50.

Schindelin, J., Arganda-Carreras, I., Frise, E., Kaynig, V., Longair, M., Pietzsch, T., Preibisch, S., Rueden, C., Saalfeld, S., Schmid, B. & Tinevez, J. Y. (2012). Fiji: an open-source platform for biological-image analysis. *Nature Methods* **7**, 676.

Somero, G. N. (1995). Proteins and temperature. *Annual Review of Physiology* **57**, 43-68.

Svetlichny, L., Hubareva, E. & Isinibilir, M. (2017). Comparative trends in respiration rates, sinking and swimming speeds of copepods *Pseudocalanus elongatus* and *Acartia clausi* with comments on the cost of brooding strategy. *Journal of Experimental Marine Biology & Ecology* **488**, 24-31.

Teare, M. & Price, R. (1979). Respiration of the meiobenthic harpacticoid copepod, *Tachidius discipes* Giesbrecht, from an estuarine mudflat. *Journal of Experimental Marine Biology & Ecology* **1**, 1-8.

Teuber, L., Kiko, R., Séguin, F. & Auel, H. (2013). Respiration rates of tropical Atlantic copepods in relation to the oxygen minimum zone. *Journal of Experimental Marine Biology & Ecology* **448**, 28-36.

Vehmma, A., Hogfors, H., Gorokhova, E., Brutemark, A., Holmborn, T. & Engström-Öst, J. (2013). Projected marine climate change: effects on copepod oxidative status and reproduction. *Ecology & Evolution* **13**, 4548-57.

Ver Hoef, J. M. (2012). Who invented the delta method? *The American Statistician* **2**, 124-7.

Viechtbauer, W. (2010). Conducting meta-analyses in R with the metafor package. *Journal of Statistical Software* **3**, 1-48.

Weymouth, F. W., Crismon, J. M., Hall, V. E., Belding, H. S. & Field, J. (1944). Total and tissue respiration in relation to body weight a comparison of the kelp crab with other crustaceans and with mammals. *Physiological Zoology* **1**, 50-71.

Wickham, H. (2002). ggplot2: elegant graphics for data analysis. Springer-Verlag New York.

Table 4.1. Results of random-effects meta-analyses and mixed-effects models of Calanoida, Cyclopoida, and Harpacticoida orders and Calanoida families. Includes DW, food availability, and methodology modeled as categorical moderators. Author, family/order-level phylogeny, and species were included as random effects in all models. *n* represents the number of effect sizes. Significant *p* values are in bold. [1]In comparison to DW excluded in study measurements. [2]In comparison to copepods fed during study measurements. [3]Winkler titration as reference level. [4]Fiber optics as reference level.

Level	Model	*n*	Mean (% Change)	Lower CI (95%)	Upper CI (95%)	*p*
Order	**Random effects**	77	7.51	4.59	10.80	< **0.01**
	DW					
	Included[1]	42	-0.13	-2.46	2.23	0.91
	Food					
	Starved[2]	61	-1.06	-6.79	4.11	0.69
	Method[3]					
	Cartesian diver	4	-2.45	-10.70	5.20	0.55
	Clark-type	16	-1.29	-4.64	1.89	0.42
	Fiber optics	24	-4.36	-8.14	-0.62	< **0.05**
	Gas chromatography	10	-6.01	-12.10	-0.28	< **0.05**
	Manometer	5	-4.57	-9.26	0.64	0.06
	Polarography	2	-9.02	-14.29	-4.55	< **0.001**
	Method[4]					
	Cartesian diver	4	1.91	-6.67	9.77	0.63
	Clark-type	16	3.07	-0.60	6.58	0.09
	Gas chromatography	10	-1.65	-7.49	4.37	0.57
	Manometer	5	-0.23	-5.56	5.20	0.94
	Polarography	2	-4.71	-9.78	0.42	0.07
	Winkler titration	16	4.30	0.58	8.12	< **0.05**
Family	**Random effects**	68	6.67	3.81	9.37	< **0.01**
	DW					
	Included[1]	38	-0.48	-2.97	2.09	0.70
	Food					
	Starved[2]	58	-2.06	-9.95	5.30	0.57

Chapter 5: **Density, morphology, and performance of the inner mitochondrial membrane**

In revision with Wendy R. Hood

INTRODUCTION

Mitochondria play a formative role in the evolution of complex life (Lane, 2006). Most energy produced in eukaryotic organisms stems from the use of adenosine triphosphate (ATP) that is produced by oxidative phosphorylation within mitochondria. The relative capacity of cells and tissues to produce energy is dependent on the number of mitochondria within each cell and the capacity of the mitochondrial population to use oxygen and convert adenosine diphosphate (ADP) to ATP. This process, known as oxidative phosphorylation, is driven by chemiosmosis where the transfer of electrons by electron transport system (ETS) complexes facilitates the movement of ions across the semipermeable inner mitochondrial membrane (IMM). The movement of ions into the inter-membrane space (IMS) forms a proton gradient (i.e., the proton motive force (pmf)) that ultimately powers the phosphorylation of ADP at ATP synthase (Mitchell, 1961). The efficiency of this process is determined by the availability of oxygen and electron-donating substrates, the enzymatic activity and density of ETS complexes, and the morphology of mitochondria (e.g., Mannella, 2020).

To understand variation in mitochondrial efficiency, investigators commonly measure mitochondrial density and coupling, complex density and activity, proteins that regulate mitochondrial biogenesis and repair, variables that contribute to or directly indicate mitochondrial damage, among others (Marcinek *et al.*, 2005; Zhang *et al.*, 2013; Hyatt *et al.*, 2019; Roca-Portoles & Tait, 2021). An increasing number of studies have also considered markers of mitochondrial fission and fusion, also known as mitochondrial dynamics (e.g., Picard *et al.*, 2013). With a few notable exceptions (e.g., Strohm & Daniels, 2003; Nielsen *et al.*, 2017), few studies have also quantified density of the IMM.

Respiratory complexes are typically distributed uniformly within the IMM along flattened segments of cristae (Hackenbrock & Hammon, 1975; Suarez *et al.*, 2000), yet they are not typically found within the inner boundary membrane or along crista tips,

other than complex V that bends the IMM at the crista tip. Thus, density of the IMM within a mitochondrion determines the number of ETS complexes, as well as the volume of IMS and matrix, within each organelle (Suarez, 1998). While IMM density was thought to be held constant (see Nielsen *et al.*, 2017 and references therein), an increasing number of studies have shown that IMM density increases in response to increasing energetic demand or energetic strain on the mitochondrion (e.g., Suarez *et al.*, 2000; Strohm & Daniels, 2003; Heine *et al.*, 2021). We propose that changes in density of the IMM alter the capacity of mitochondria to produce energy, and thus, can represent an adaptive response to changing energetic demand (Heine & Hood, 2020).

The goal of this review is to outline support for the idea that variation in density and morphology of the IMM influence performance of the ETS, and as a result, the capacity of mitochondria to produce ATP. We start by briefly reviewing evidence that variation in mitochondrial morphology is linked to variation in mitochondrial performance. Given this evidence, we describe how changes in morphology are expected to equate to change in the efficiency of ATP production. Specifically, we describe the relationship between IMM density and capacity to build and maintain a pmf. We outline how the structure and angle of ATP synthase dimers influence the proton gradient within cristae and, therefore, oxygen consumption and the rate of ATP synthesis. We briefly suggest how the formation of crista junctions and lamellar versus tubular cristae impact proton gradients and crista function. We then address possible links between density of the IMM and mitochondrial density. Finally, we conclude with suggestions for how we can better understand roles of the IMM in mitochondrial performance across diverse taxa.

RESPONSE TO CHANGE IN ENERGETIC DEMAND AND MITOCHONDRIAL DECLINE

The IMM is a lipid bilayer that folds in on itself to form distinct compartments (cristae) that act as individual proton capacitors. The shape and volume of cristae determine the number of ions required to maintain the pmf (Lee, 2020). Studies have shown that IMM density and cristae area change relative to intensity of energetic demand. Nielsen et al. (2017) found that human athletes subject to long-term endurance training display higher mitochondrial cristae densities than recreationally active and

sedentary obese individuals. Further, the density of cristae in skeletal muscle mitochondria is a better predictor of maximum oxygen uptake by the individual than muscle mitochondrial volume. Reproduction is typically associated with a sustained increase in energy utilization, whether associated with territorial defense or parental care. In the European beewolf, *Philanthus triangulum*, females paralyze and carry honeybees to their nest to feed their developing young, a feat that requires females to regularly perform flights while carrying an object that more than doubles the females' weight (Strohm & Linsenmair, 1997). Strohm and Daniels (2003) found that the provisioning rate, and ultimately reproductive success, correlated with IMM density within the flight muscles of this species. Given that persistent endurance training and reproduction are both associated with sustained increases in energy expenditure, but less intense recreational exercise is not associated with a change in IMM density, we suggest that a sustained change in energy expenditure is likely necessary to increase density of the IMM in the absence of an oxidative event as describe below.

IMM density has also been shown to change with reduced mitochondrial activity. When the availability of ETS substrate is limited due to a 40% caloric restriction, the density of IMM in hepatocyte mitochondria is greater than in age-matched animals consuming ad libitum food (Khraiwesh *et al.*, 2014). Hibernating frogs display a change in IMM confirmation with hibernation. The cristae of active frogs cross mitochondria longitudinally within mitochondria of kidney cells, but hibernating frogs display transverse cristae (Karnovsky, 1963). The impact of this reorientation on density of the IMM, relative IMS, and capacity to maintain a pmf are unknown, but could be a response to reduced substrate availability and a reduced proton concentration within the IMS.

A reduction in mitochondrial capacity across organ systems is a hallmark of aging. These changes are exemplified by a reduction in mitochondrial respiratory performance, a reduction in mitochondrial density and the signal for mitochondrial biogenesis (PGC-1α), a reduced capacity for repair, and both fission and fusion, among others (Sastre *et al.*, 2000; López-Lluch *et al.*, 2008). Some investigators have also noted a reduction in IMM between young and old individuals. Jiang et al. (2017) found that flight muscle of long-lived fruit flies displayed an increase in the proportion of mitochondria that display cristae vacuolation and disintegration, and a sparce distribution

of ATP synthase. Changes in cardiac myocyte mitochondria with aging have been described in multiple studies (e.g., Terman & Brunk, 2005). These post-mitotic cells display increased variation in mitochondrial size with aging. While, on average, changes in IMM density have not always been observed in cardiomyocytes when young and old animals are compared (Riva *et al.*, 2006), extremely enlarged mitochondria appear to be exclusively found in aged individuals (Terman & Brunk, 2005; Seo *et al.*, 2010). Giant mitochondria display a loss of cristae and IMM, and thus, are assumed to have a limited ability to produce ATP and ultimately, an inability to maintain a pmf (Tandler & Hoppel, 1986).

DENSITY OF THE INNER MITOCHONDRIAL MEMBRANE AND MITOCHONDRIAL MORPHOLOGY

The IMM is populated by complexes I-V of the ETS that contribute to the transfer of electrons from NADH and $FADH_2$ at complexes I and II, respectively, to complex IV where oxygen is reduced to water in the mitochondrial matrix. This transfer of electrons leads to the pumping of protons across the IMM and into the IMS by complexes I, III, and IV. The protons pumped into the IMS flow down their electrochemical gradient and through ATP synthase to phosphorylate ADP to ATP (Hatefi, 1985). Aside from increasing the rate of respiration (Heine *et al.*, 2019), mitochondria can upregulate or maintain their function by increasing density of the IMM (Kilarski *et al.*, 1996; Strohm & Daniels, 2003; Nielsen *et al.*, 2017; Heine *et al.*, 2021). By increasing density of the IMM, the mitochondrion can support more ETS complexes per unit mitochondrial volume, including ATP synthases and supercomplexes (Strohm & Daniels, 2003; Berndtsson *et al.*, 2020). Although such morphological changes have the potential to meet increasing energetic demands of the cell (Mannella, 2020), there are likely limits to how much IMM can exist within a mitochondrion without decreasing mitochondrial function / performance of the IMM.

Empirical evidence for a limit to the benefits of increased IMM density on mitochondrial respiratory performance comes from recent work by Heine et al. (2021). Heine et al. (2021) showed that when *Tigriopus californicus* copepods are exposed to ultraviolet (UV) radiation (0.5 W/m^2), the metabolic rate of individual copepods was

maintained at three hours of UV irradiation but decreased after six hours of exposure. Subsarcolemmal mitochondria within the copepod myocytes displayed an increased IMM density in both irradiation treatments, suggesting that more IMM may be a proximate response to increased oxidative stress from UV light but may ultimately fail to maintain metabolic rate at exceedingly high levels of UV radiation. Accordingly, increases in density of the IMM can alter mitochondrial performance depending on the ratio of IMM to the aforementioned traits (**Figure 5.1**) and can, therefore, be viewed as having both beneficial and detrimental effects.

Theoretically, a disproportionate change in IMM surface area relative to mitochondrial volume will impact the volume of the IMS and volume of the matrix. A change in volume of the IMM (i.e., intracristal space) is expected to alter effort required to maintain the concentration of protons within cristae and, thus, the capacity of the mitochondrion to maintain the pmf (see Willis *et al.*, 2016; Lee, 2020). This change can impact the efficiency of ATP phosphorylation at ATP synthase (Davies *et al.*, 2011). Thus, when energetic demand increases or when oxygen diffusion decreases, a higher IMM density will decrease the number of protons pumped per complex for a given number of protons. As a result, both the relative efficiency and capacity for oxidative phosphorylation may both be enhanced. The number of protons required to maintain the pmf, however, will depend on (i) proton consumption by ATP synthase and (ii) proton leak of the IMM. Work by Kilarski et al. (1996) showed that crucian carp (*Carassius carassius*) acclimated to 5^{o}C for six weeks, following collection from warm late-summer waters (20^{o}C), displayed a near two-fold increase in IMM area relative to mitochondrial volume in muscle tissue. Because the oxygen content of water increases while diffusion rates across membranes and through solutions drop at lower temperatures, it is assumed that the change in IMM density increases oxygen delivery when diffusion rates are low (Kilarski *et al.*, 1996). We predict that this effect also allows mitochondria to concentrate protons within the IMS, reduce proton diffusion distance, and increase the efficiency of oxidative phosphorylation. However, see Hackenbrock et al. (1971) for how ATP synthesis increases as mitochondria change from orthodox to condensed conformations. Further, increases in IMM area may allow mitochondria to maintain the pmf if they

become damaged, associated with increased oxidant exposure as described by Heine at al. (2020).

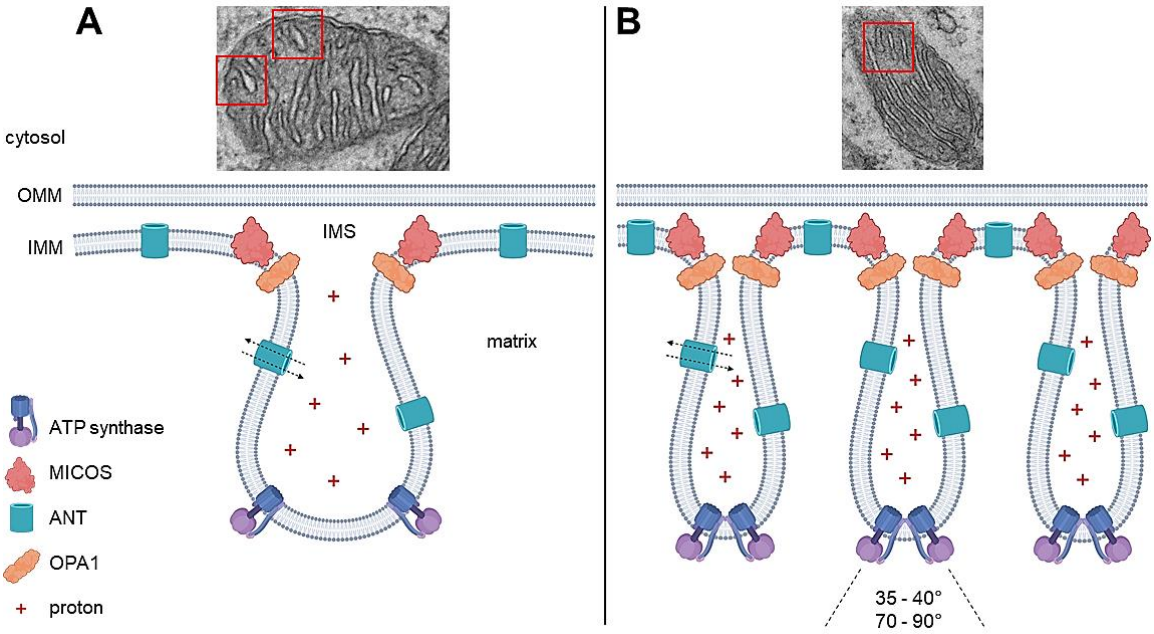

Figure 5.1. Illustration of how crista morphology changes with density of the inner mitochondrial membrane (IMM) and relation to other morphological traits. **A** Depiction of an enlarged, aberrant crista with ATP synthase complexes that have dissociated into monomers. Widened cristae and/or a lower density of IMM may result in a lower concentration of protons, altered crista junctions associated with OPA1 and MICOS (depending on size of the matrix), and fewer adenine nucleotide translocase (ANT) per unit volume within the mitochondrion. **B** Depiction of narrow, densely-packed cristae with ATP synthase complexes that are associated as dimers. Narrow cristae and/or a greater density of IMM may result in a greater concentration of protons, altered crista junctions (depending on size of the matrix), and more ANT per unit volume within the mitochondrion. **B** is likely to result in greater ATP production under increased energetic demand. The angle of dimers will depend on the organism, tissue, aging process, and possibly the energetic demand of the mitochondrion and cell. See Section 4 regarding the control of cristae shape and Section 6 regarding the relationship between cristae density and mitochondrial density. The aforementioned differences between **A** and **B** will fundamentally change the ratios of IMM to outer mitochondrial membrane, inter-membrane space, and matrix, altering mitochondrial function—provided the overall volume of the mitochondrion (i.e., enclosed within the outer membrane) remains constant. Micrographs are of mitochondria within myocytes of *Tigriopus californicus* copepods.

In contrast, an exceedingly high density of IMM could have several negative impacts on mitochondrial performance, such as more diffusion bottlenecks and reduced

flux of ATP synthase (Afzal *et al.*, 2021). When IMM density is exceedingly high, a high density of ETS complexes and limited IMS should result in the mitochondrion to quickly exceed its optimal proton concentration. When this occurs, ETS complexes can no longer efficiently move new protons into the IMS, and electrons can backup within ETS complexes I-III instead of being passed to oxygen as the terminal electron acceptor (Willis *et al.*, 2016). This backup allows electrons to escape the ETS and generate reactive oxygen species (ROS). Thus, a very high density of IMM is predicted to be associated with low mitochondrial efficiency and increased ROS production, and as a result, potentially an increase in oxidative damage. Alternatively, mitochondrial capacity could be reduced because a reduction in matrix volume may decrease the capacity of the mitochondrion to support the citric acid cycle and produce the electron-donating substates necessary to power the ETS. This is largely speculation on our part and warrants further experimental and quantitative evaluation.

In Heine et al.'s copepod study (2021), the mitochondria in myocytes were likely damaged from high UV irradiation, and consequently, high ROS exposure (see also Han *et al.*, 2016). In this case, we believe that the exceptional IMM densities that were observed were a consequence of mitochondria attempting to maintain ATP production despite oxidative damage to lipids and proteins that may have punctured membranes and rendered ETS complexes dysfunctional. In this case, a greater density of IMM may have helped to maintain the pmf, concentrate matrix substrates, and increase the density of functional ETS complexes, but appears to have not been sufficient to maintain mitochondrial capacity under prolonged UV radiation exposure, as indicated by a reduced metabolic rate.

As density of the IMM increases and matrix volume decreases, more substrates could be imported, and more products exported, through an increase in adenine nucleotide translocase (ANT, located within the IMM; Metelkin *et al.*, 2006). Such an increase in IMM could drive an increase in oxygen diffusion and ATP export, although this will depend largely on the ability of the outer mitochondrial membrane and matrix to import and store substrates and export products of the ETS. The fraction of ANT localized to the inner boundary membrane (IMM located adjacent to the outer membrane and not involved in the formation of cristae) and crista membrane determines how well

the mitochondrion can sense changes in energetic demand, in addition to how efficiently ATP is exported to the cytosol (Afzal *et al.*, 2021).

Last, as density of the IMM increases, the ratio of outer membrane to IMM should decrease if size of the mitochondrion remains constant. As a result, there is likely a point where the transport of substrates into the mitochondrion becomes inefficient to feed oxidative phosphorylation. This is likely one reason why cells contain thousands of smaller mitochondria and not very few large mitochondria, provided that mitochondrial function can decrease once density of the IMM becomes too great (i.e., as mitochondrial size increases, volume of the organelle and density of the IMM increase at a far greater rate than surface area of the outer mitochondrial membrane).

ATP SYNTHASE BENDS THE INNER MITOCHONDRIAL MEMBRANE

ATP synthase, or complex V, phosphorylates ADP to ATP within the crista membrane. This complex is comprised of numerous subunits that make up the proton pore within the IMM, the rotor ring, and the stalk of the complex (Boyer, 1997). ATP synthase first form as monomers within the IMM, which then dimerize. Due to long-range attractive forces, these dimers spontaneously associate to form rows that exist along the curved edges of cristae (Anselmi *et al.*, 2018). Recent work by Flygaard et al. (2020) has also shown the tetramerization of ATP synthase dimers in cultivated protozoan cells, where an extended subunit-*a* forms an association between neighboring dimers. Associated dimers form tetramers that result in a helically twisted row of ATP synthase dimers along the curved edge of cristae. One of the most crucial aspects of ATP synthase function—and dimerization—is the degree at which dimers are angled to bend the IMM and form cristae compartments.

The angle at which ATP synthase dimers bend the IMM directly influences the concentration of protons within the IMS (Strauss *et al.*, 2008), and the angle varies between taxa, tissue types, and even within an individual organism over time (Dudkina *et al.*, 2006; Davies *et al.*, 2012; Kühlbrandt, 2015). Generally speaking, ATP synthase forms both wide-angle dimers (70-90°, shown in algal mitochondria) and small-angle dimers (35-40°, shown in *Bos taurus* heart mitochondria); small-angle dimers may be considered “pseudo-dimers” and form through the association of monomers from

neighboring dimers that are no longer associated as “true-dimers” (Minauro-Sanmiguel *et al.*, 2005; Dudkina *et al.*, 2005, 2006). The formation of lamellar cristae in bovine heart and club-shaped cristae in green algae (Blum *et al.*, 2019) may result from the formation of small- versus large-angle dimers, respectively. Provided that complex animals, such as bovines, have a greater energetic demand than less-complex protists such as algae, small angle dimers in animal mitochondria may bend the IMM less to allow for more protons to be stored within the IMS. In protists, we see the IMM is bent to a greater extent by large-angle dimers, concentrating fewer protons within a smaller IMS. A concentration of fewer protons within a smaller IMS can be ideal for lower rates of ATP synthesis, whereas concentrating more protons within a larger IMS can drive higher rates of ATP synthesis.

If the formation of different angled dimers influences the concentration of protons within the IMS, and therefore oxygen diffusion and ATP synthesis, then how the IMM is bent will also influence density of the IMM and associated morphological traits of the mitochondrion. For instance, if the formation of small-angle dimers in more complex animals leads to the development of cristae with a larger volume, then the mitochondrion will need to adjust how substrates that feed oxidative phosphorylation are taken into a smaller volume of matrix if size of the organelle remains constant. The formation of small-angle dimers and larger cristae will allow for the storage of more protons within the IMS, but the products of oxidative phosphorylation (ATP, water) may need to be stored in greater quantities within the matrix (or shuttled out of the matrix at a greater rate). This relationship will likely result in a trade-off and delicate balance between how the angle of ATP synthase dimers influences cristae morphology and size of the mitochondrial matrix.

Although the formation of monomeric ATP synthase does not eliminate mitochondrial function altogether, it has been shown to decrease mitochondrial membrane potential and organism growth in yeast (Bornhövd *et al.*, 2006). Therefore, the formation of ATP synthase dimers, and bending of the IMM, is critical for efficient performance of the ETS and cellular function (**Figure 5.1**). Whether or not complex V forms large- or small-angle dimers seems to be dependent on the organism, tissue, and the aging process.

CRISTAE AND CRISTA JUNCTION MORPHOLOGY

The structure and proper formation of cristae and crista junctions is crucial to mitochondrial performance. ATP production directly depends on the ability of cristae to import substrates, store protons, and export energy produced from oxidative phosphorylation. This is done largely through crista junctions and changes to the morphology of cristae (e.g., lamellar and tubular conformations). Cristae shape varies between species (but can also vary within a mitochondrion, to an extent) and is influenced by the presence of ATP synthase and function of crista junctions. Some species have cristae that are predominately long thin tubes that are suspended in the matrix, i.e. tubular cristae, that may or may not connect to the inner boundary membrane. Other species predominately display sheet-like lamellar cristae that attach to the inner boundary membrane (e.g., Prince, 2002; **Figure 5.2**).

One of the largest differences in function between tubular and lamellar cristae is the relative abundance of complex IV, or cytochrome c oxidase (COX). In *Drosophila* muscle, each sheet of lamellar cristae appears to carry many COX4 proteins (a protein unique to COX; Jiang *et al.*, 2020). In contrast, COX4, and thus COX, is not detectable in each of the tubular cristae, although Jiang et al. (2020) refers to these as "reticular structures" and not tubular cristae. It is unclear whether cristae without COX must fuse with cristae that contain COX or form crista junctions to complete oxidative phosphorylation. Thus, because mitochondrial efficiency is reduced when the distance that electrons must be transferred is greater, cristae morphology is expected to have a direct impact on the efficiency of oxidative phosphorylation. Furthermore, the presence of COX plays a direct role in the formation of supercomplexes. Recent work in yeast by Berndtsson et al. (2020) showed that the formation of supercomplexes may decrease the distance required for electron transport by cytochrome *c* between complexes III and IV, making the transfer of electrons more efficient. If this is the case, then the presence of COX4 in predominantly lamellar cristae points to a significant difference in ETS efficiency between tubular and lamellar cristae. Such differences can have implications for how quickly oxygen can be reduced and how quickly ATP can be produced. COX has also been shown to operate near max capacity with increased enzyme turnover in the flight muscle of honeybees (Suarez *et al.*, 2000). A greater density of COX was

concurrent with increased IMM and mitochondrial density. Such work underlines the importance of density of the IMM in mitochondrial performance and may have implications for understanding how the metabolic rate of ectotherms increases with temperature (e.g., Heine *et al.*, 2019). This suggests that the performance of oxidative phosphorylation is not only dependent on the rate of chemical reactions within the ETS but mitochondrial morphology.

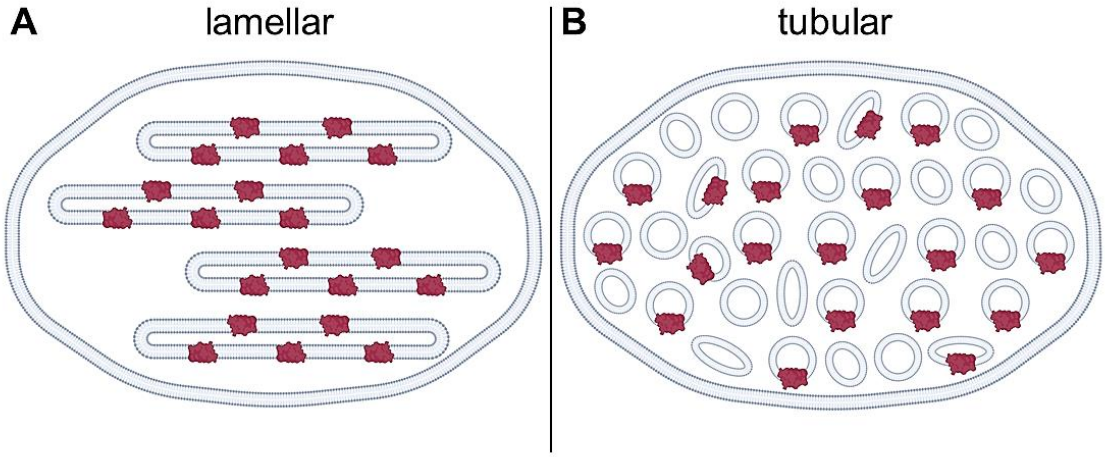

Figure 5.2. Illustration of how the density of cytochrome *c* oxidase (COX), shown in red, is greater in lamellar (A) versus tubular (B) cristae, or reticular structures. Lamellar cristae are thin, sheet-like folds of the inner mitochondrial membrane, whereas tubular cristae are rounded, tube-like folds. Such differences are important to measure and observe via microscopy due to the fact that tissue samples can contain the same density of COX (as shown between **A** and **B**) but differ in the number of cristae, cristae morphology, and/or performance of the inner mitochondrial membrane. Figure based on Jiang et al. (2020).

At least two species adapted to the hypoxic conditions of high altitude have been shown to display increased COX efficiency. Zhang et al. (2013) has shown that Tibetan locusts at higher altitudes tolerate hypoxia better than lowland locusts, largely due to an increased efficiency of COX and its affinity to cytochrome *c* in flight muscle. Likewise, Scott et al. (2011) showed that bar-headed geese flying at high altitudes have an amino acid substitution in COX3, which likely results in a change in enzyme kinetics and, ultimately, more efficient O_2 transport in cardiomyocytes. If such changes to the efficiency of oxygen transport are not due to a mere increase in protein content, another possibility may be the presence of fewer lamellar cristae as opposed to a greater number

of tubular cristae if COX4 is associated more with the former (**Figure 5.2**); this would result in no change in protein density but could impact cristae function if the concentration of protons is influenced by cristae architecture (see Jiang *et al.*, 2020). As a result, the volume of mitochondrial matrix can change with cristae size and morphology, influencing the import of substrates and export of products of the ETS (i.e., cells that are more efficient at reducing oxygen may have mitochondria with few lamellar cristae with the same concentration of COX4 as cells containing mitochondria with many tubular cristae). Further research is needed to support this idea, which is largely speculation on our part. Although little evidence exists that tubular cristae may exist in greater numbers than lamellar cristae due to the presence of COX4, densely-packed tubular cristae are regularly observed in marmoset Leydig cells, where distantly-spaced lamellar cristae are a more common feature of mitochondria in most cell types (Prince, 2002). Furthermore, crista junctions influence the size of cristae, as both lamellar and tubular cristae morphologies can fluctuate in volume.

The swelling of cristae is impacted by crista junction size and function and, in part, by size and swelling of the matrix. Crista junctions function in stabilizing inner membrane curvature, regulating enzymes within cristae, and creating contacts between the inner and outer mitochondrial membranes (Rampelt *et al.*, 2017). In turn, cristae can swell and put pressure on the outer membrane—causing it to rupture—which is a prelude to apoptosis (Mannella, 2020). Given that crista junctions influence the presence and concentration of enzymes within the IMS and IMM, crista junctions are functionally and structurally related to the mitochondrial matrix, which holds the electron donors and products of the ETS. Crista junctions are primarily circular and relatively constant in size when the matrix is enlarged. However, when the matrix is condensed (contracted), crista junctions become larger and non-circular (Renken *et al.*, 2002). Although, Perkins and Ellisman (2010) have found that condensed mitochondria within the axoplasm (neuron cytoplasm) of rats contain narrow crista junctions, where narrow crista junctions are usually common in mitochondria with an expanded matrix. Although a contracted mitochondrial matrix may allow for less storage of substrates and products of the ETS, narrow crista junctions may be indicative of a high rate of ATP production in fewer, high-performing cristae (see Matsuhashi *et al.*, 2017).

The MICOS (mitochondrial contact site and cristae organizing system) complex also plays an important role in crista junction organization and cristae dynamics. This complex is comprised of seven subunits and serves to stabilize crista junctions and form contacts between the inner boundary membrane and the outer membrane. The MICOS complex is also involved in the regulation of cristae biogenesis, fission, and fusion. See Anand et al. (2021) for a recent, extensive review of roles of the MICOS complex in cristae dynamics.

CRISTAE DENSITY AND MITOCHONDRIAL DENSITY

Increased mitochondrial density may support some of the most energetically-demanding aspects of animal performance, such as flight. Mathieu-Costello et al. (1992), for example, found that relatively high mitochondrial densities per muscle fiber, upwards of 39% of the fiber volume, are typical in the supracoracoideus (the muscle supporting the upstroke) in hummingbirds (*Selaphorus rufus*); Suarez et al. (1991) found that mitochondria occupy ~35% of the muscle fiber volume in hummingbird flight muscles. Furthermore, the location of mitochondria within cells also improves efficiency. For example, mitochondria in the muscle of high-altitude deer mice localize to cell walls that are adjacent to capillaries. This behavior reduces the distance for oxygen diffusion (Mahalingam *et al.*, 2017). However, recent work shows that increases in density of the IMM may accompany, or occur in place of, increases in mitochondrial density (e.g., Nielsen *et al.*, 2017).

Increasing density of the IMM may be an efficient, alternative means for mitochondria to meet increasing energetic demands in addition to increasing mitochondrial density. Nielsen et al. (2017) found not only that both IMM density and mitochondrial density increased in human skeletal muscle following long-term endurance training, but cristae density in particular was a better predictor of VO_2 max than mitochondrial density. Both mitochondrial density and density of the IMM increased in myocytes when *T. californicus* copepods were exposed to varying levels of UV radiation (Heine *et al.*, 2021). The effect sizes in the latter study were consistent between treatment groups for both mitochondrial density and density of the IMM in copepods. These results

would be expected if mitochondrial density and morphology work in concert to maintain metabolic rate.

The aforementioned studies demonstrate how efficient performance of the IMM can be accomplished through numerous mechanisms including, but not limited to, increases in mitochondrial density and density of the IMM. However, other changes such as an increase in capillary density and the location of mitochondria near the cell sarcolemma (Scott *et al.*, 2009) likely play formative roles in both mitochondrial and cellular performance. Further work is needed to determine the extent to which trade-offs may exist between mitochondrial density and density of the IMM to influence mitochondrial performance. One benefit of increasing density of the IMM over increasing mitochondrial density may be an increase in the presence ANT within individual mitochondria.

ANT exists within both the inner boundary membrane and crista membrane (Chen *et al.*, 2004; Brenner *et al.*, 2011; Afzal *et al.*, 2021) and may increase significantly when density of the IMM increases (**Figure 5.1**). If more cristae form to meet the increasing energetic demands of the organelle, that demand needs to be met by a greater influx of ADP and efflux of ATP, which can be handled by more ANT transporters within the inner boundary and crista membranes (Mannella *et al.*, 2013). Such an increase in transport may be more difficult to implement (and decrease mitochondrial function) in mitochondria with fewer cristae when the demand for ATP is high but the surface area of IMM is insufficient to transport metabolites for oxidative phosphorylation.

CONCLUSIONS AND FUTURE DIRECTIONS

The fields of physiological ecology and mitochondrial biology have made significant strides in understanding variation in whole-animal performance (e.g., López-Lluch *et al.*, 2008) and how mitochondrial morphology impacts mitochondrial performance (e.g., Mannella, 2020), respectively. By integrating theory and techniques common to these fields, we will gain a better understanding of the mechanisms responsible for the many fascinating and diverse adaptations to energetic challenges that have evolved among eukaryotes. Density and morphology of the IMM influence variation in energy production within mitochondria; however, few studies have evaluated the roll

of change in IMM density and its relation to other mitochondrial traits under different energetic constraints. This review outlines our current understanding of these relationships as a crucial step towards understanding variation in mitochondrial performance.

In particular, we review how mitochondrial performance is influenced by: 1) the relationship between density of the IMM and other morphological traits of the mitochondrion, 2) bending of the IMM by ATP synthase, 3) cristae and crista junction morphology, and 4) possible relationships between density of the IMM and mitochondrial density. The aforementioned traits interact concurrently to influence oxygen consumption, energy production, and ROS production within individual and populations of mitochondria. Last, few studies (e.g., Heine *et al.*, 2021; Afzal *et al.*, 2021) have evaluated the limitations and possible detrimental effects of exceedingly high levels of IMM density. Such work shows that although increasing density of the IMM may be sufficient to maintain function when mitochondria are compromised, or to increase oxygen consumption and/or ATP production under increased energetic demand, there is likely a point where exceedingly high levels of IMM density decrease mitochondrial performance due to a significant decrease in matrix volume and an increase in ROS production.

To further understand how density and morphology of the IMM can influence mitochondria and, therefore, whole-animal performance, studies should include microscopy alongside measures of mitochondrial physiology and a relevant measure of organ or organism capacity. This approach may initially be most informative by investigating differences in mitochondrial phenotypes between extreme life history traits and environmental change. For example, mitochondrial morphology and respiratory capacity can be measured in migrating and non-migrating birds, in animals subject to extreme differences in temperature, and between protists and complex animals. Migrating birds will maintain flight and, thus, sustain a high metabolic rate and mitochondrial respiratory performance for longer periods than non-migrating birds (McWilliams *et al.*, 2004), especially those that undergo non-stop, transoceanic migration. It is not clear what is different about the mitochondrial morphology and IMM structure of birds that must produce such extraordinary amounts of energy. As previously mentioned, changes to

density and morphology of the IMM may play a significant role in metabolic plasticity among ectotherms, however, this field of inquiry is scarce. The respiration rates of crustaceans such as copepods increase significantly with temperature (e.g., Heine *et al.*, 2019), but the proportion of this increase that is due to increases in enzyme activity versus changes to morphology of the IMM is unknown. It is also prudent to understand how density and morphology of the IMM differ between exceedingly small eukaryotes such as protists and larger eukaryotes, including plants, animals, and fungi.

Understanding differences in mitochondrial morphology under different energetic challenges may begin to shed light on adaptive mechanisms that have evolved in different eukaryotes. While we assume that morphological responses to energetic demand are under selection, the genetic basis of variation in mitochondrial morphology is poorly understood. We predict that the energetic optima for each tissue will vary by taxa and, thus, the combination of mitochondrial, physiological, and morphological solutions and reaction norms for each morphological variable will also vary, suggesting that there will not be a common mechanism to maximize energetic capacity in all circumstances.

Future work may benefit from investigating variation in density and morphology of the IMM to understand variation in mitochondrial performance. Doing so can further our understanding of why we observe large amounts of variation in mitochondrial function between organisms, tissues, and life-history strategies (Heine & Hood, 2020). We hope this work encourages the integration of mitochondrial behavior and morphology with studies of whole-animal performance in ecology and evolutionary biology.

REFERENCES

Afzal, N., Lederer, W. J., Jafri, M. S. & Mannella, C. A. (2021). Effect of crista morphology on mitochondrial ATP output: A computational study. *Current Research in Physiology* **4**, 163-176.

Anand, R., Reichert, A. S. & Kondadi, A. K. (2021). Emerging roles of the MICOS complex in cristae dynamics and biogenesis. *Biology* **10**, 600.

Anselmi, C., Davies, K. M. & Faraldo-Gómez, J. D. (2018). Mitochondrial ATP synthase dimers spontaneously associate due to a long-range membrane-induced force. *Journal of General Physiology* **150**, 763-770.

Berndtsson, J., Aufschnaiter, A., Rathore, S., Marin-Buera, L., Dawitz, H., Diessl, J. ... & Ott, M. (2020). Respiratory supercomplexes enhance electron transport by decreasing cytochrome *c* diffusion distance. *EMBO Reports* **21**, e51015.

Blum, T. B., Hahn, A., Meier, T., Davies, K. M. & Kühlbrandt, W. (2019). Dimers of mitochondrial ATP synthase induce membrane curvature and self-assemble into rows. *Proceedings of the National Academy of Sciences* **116**, 4250-4255.

Bornhövd, C., Vogel, F., Neupert, W. & Reichert, A. S. (2006). Mitochondrial membrane potential is dependent on the oligomeric state of F1F0-ATP synthase supracomplexes. *Journal of Biological Chemistry* **281**, 13990-13998.

Boyer, P. D. (1997). The ATP synthase—a splendid molecular machine. *Annual Review of Biochemistry* **66**, 717-749.

Brenner, C., Subramaniam, K., Pertuiset, C. & Pervaiz, S. (2011). Adenine nucleotide translocase family: four isoforms for apoptosis modulation in cancer. *Oncogene* **30**, 883-895.

Chen, C., Ko, Y., Delannoy, M., Ludtke, S. J., Chiu, W. & Pedersen, P. L. (2004). Mitochondrial ATP synthasome: three-dimensional structure by electron microscopy of the ATP synthase in complex formation with carriers for Pi and ADP/ATP. *Journal of Biological Chemistry* **279**, 31761-31768.

Davies, K. M., Anselmi, C., Wittig, I., Faraldo-Gómez, J. D. & Kühlbrandt, W. (2012). Structure of the yeast F1Fo-ATP synthase dimer and its role in shaping the mitochondrial cristae. *Proceedings of the National Academy of Sciences* **109**, 13602-13607.

Davies, K. M., Strauss, M., Daum, B., Kief, J. H., Osiewacz, H. D., Rycovska, A. ... & Kühlbrandt, W. (2011). Macromolecular organization of ATP synthase and complex I in whole mitochondria. *Proceedings of the National Academy of Sciences* **108**, 14121-14126.

Dudkina, N. V., Heinemeyer, J., Keegstra, W., Boekema, E. J. & Braun, H. P. (2005). Structure of dimeric ATP synthase from mitochondria: an angular association of monomers induces the strong curvature of the inner membrane. *FEBS Letters* **579**, 5769-5772.

Dudkina, N. V., Sunderhaus, S., Braun, H. P. & Boekema, E. J. (2006). Characterization of dimeric ATP synthase and cristae membrane ultrastructure from *Saccharomyces* and *Polytomella* mitochondria. *FEBS Letters* **580**, 3427-3432.

Flygaard, R. K., Mühleip, A., Tobiasson, V. & Amunts, A. (2020). Type III ATP synthase is a symmetry-deviated dimer that induces membrane curvature through tetramerization. *Nature Communications* **11**, 1-11.

Hackenbrock, C. R., Rehn, T. G., Weinbach, E. C. & Lemasters, J. J. (1971). Oxidative phosphorylation and ultrastructural transformation in mitochondria in the intact ascites tumor cell. *Journal of Cell Biology* **51**, 123-137.

Hackenbrock, C. R. & Hammon, K. M. (1975). Cytochrome c oxidase in liver mitochondria. Distribution and orientation determined with affinity purified immunoglobulin and ferritin conjugates. *Journal of Biological Chemistry* **250**, 9185-9197.

Han, J., Puthumana, J., Lee, M. C., Kim, S. & Lee, J. S. (2016). Different susceptibilities of the Antarctic and temperate copepods *Tigriopus kingsejongensis* and *T. japonicus* to ultraviolet (UV) radiation. *Marine Ecology Progress Series* **561**, 99-107.

Hatefi, Y. (1985). The mitochondrial electron transport and oxidative phosphorylation system. *Annual Review of Biochemistry* **54**, 1015-1069.

Heine, K. B., Abebe, A., Wilson, A. E. & Hood, W. R. (2019). Copepod respiration increases by 7% per° C increase in temperature: A meta-analysis. *Limnology & Oceanography Letters* **4**, 53-61.

Heine, K. B. & Hood, W. R. (2020). Mitochondrial behaviour, morphology, and animal performance. *Biological Reviews* **95**, 730-737.

Heine, K. B., Justyn, N. M., Hill, G. E. & Hood, W. R. (2021). Ultraviolet irradiation alters the density of inner mitochondrial membrane and proportion of inter-mitochondrial junctions in copepod myocytes. *Mitochondrion* **56**, 82-90.

Hyatt, H. W., Zhang, Y., Hood, W. R. & Kavazis, A. N. (2019). Changes in metabolism, mitochondrial function, and oxidative stress between female rats under nonreproductive and 3 reproductive conditions. *Reproductive Sciences* **26**, 114-127.

Jiang, Y. F., Lin, S. S., Chen, J. M., Tsai, H. Z., Hsieh, T. S. & Fu, C. Y. (2017). Electron tomographic analysis reveals ultrastructural features of mitochondrial cristae architecture which reflect energetic state and aging. *Scientific Reports* **7**, 1-11.

Jiang, Y. F., Lin, H. L., Wang, L. J., Hsu, T. & Fu, C. Y. (2020). Coordinated organization of mitochondrial lamellar cristae and gain of COX function during mitochondrial maturation in *Drosophila. Molecular Biology of The Cell* **31**, 18-26.

Karnovsky, M. J. (1963). The fine structure of mitochondria in the frog nephron correlated with cytochrome oxidase activity. *Experimental & Molecular Pathology* **2**, 347-366.

Khraiwesh, H., López-Domínguez, J. A., del Río, L. F., Gutierrez-Casado, E., López-Lluch, G., Navas, P. ... & González-Reyes, J. A. (2014). Mitochondrial ultrastructure and markers of dynamics in hepatocytes from aged, calorie restricted mice fed with different dietary fats. *Experimental Gerontology* **56**, 77-88.

Kilarski, W. M., Romek, M., Kozlowska, M. & Gorlich, A. (1996). Short-term thermal acclimation induces adaptive changes in the inner mitochondrial membranes of fish skeletal muscle. *Journal of Fish Biology* **49**, 1280-1290.

Kühlbrandt, W. (2015). Structure and function of mitochondrial membrane protein complexes. *BMC Biology* **13**, 89.

Lane, N. (2006). *Power, sex, suicide: mitochondria and the meaning of life*. Oxford University Press.

Lee, J. W. (2020). Protonic Capacitor: Elucidating the biological significance of mitochondrial cristae formation. *Scientific Reports* **10**, 1-14.

López-Lluch, G., Irusta, P. M., Navas, P. & de Cabo, R. (2008). Mitochondrial biogenesis and healthy aging. *Experimental Gerontology* **43**, 813-819.

Mahalingam, S., McClelland, G. B. & Scott, G. R. (2017). Evolved changes in the intracellular distribution and physiology of muscle mitochondria in high-altitude native deer mice. *The Journal of Physiology* **595**, 4785-4801.

Mannella, C. A. (2020). Consequences of folding the mitochondrial inner membrane. *Frontiers in Physiology* **11**, 536.

Mannella, C. A., Lederer, W. J. & Jafri, M. S. (2013). The connection between inner membrane topology and mitochondrial function. *Journal of Molecular & Cellular Cardiology* **62**, 51-57.

Marcinek, D. J., Schenkman, K. A., Ciesielski, W. A., Lee, D. & Conley, K. E. (2005). Reduced mitochondrial coupling in vivo alters cellular energetics in aged mouse skeletal muscle. *The Journal of Physiology* **569**, 467-473.

Mathieu-Costello, O., Suarez, R. K. & Hochachka, P. W. (1992). Capillary-to-fiber geometry and mitochondrial density in hummingbird flight muscle. *Respiration Physiology* **89**, 113-132.

Matsuhashi, T., Sato, T., Kanno, S. I., Suzuki, T., Matsuo, A., Oba, Y. ... & Abe, T. (2017). Mitochonic Acid 5 (MA-5) facilitates ATP synthase oligomerization and cell survival in various mitochondrial diseases. *EBioMedicine* **20**, 27-38.

McWilliams, S. R., Guglielmo, C., Pierce, B. & Klaassen, M. (2004). Flying, fasting, and feeding in birds during migration: a nutritional and physiological ecology perspective. *Journal of Avian Biology* **35**, 377-393.

Metelkin, E., Goryanin, I. & Demin, O. (2006). Mathematical modeling of mitochondrial adenine nucleotide translocase. *Biophysical Journal* **90**, 423-432.

Minauro-Sanmiguel, F., Wilkens, S. & García, J. J. (2005). Structure of dimeric mitochondrial ATP synthase: novel F0 bridging features and the structural basis of mitochondrial cristae biogenesis. *Proceedings of the National Academy of Sciences* **102**, 12356-12358.

Mitchell, P. (1961). Coupling of phosphorylation to electron and hydrogen transfer by a chemi-osmotic type of mechanism. *Nature* **191**, 144-148.

Nielsen, J., Gejl, K. D., Hey-Mogensen, M., Holmberg, H.C., Suetta, C., Krustrup, P., Elemans, C. P. H. & Ørtenblad, N. (2017). Plasticity in mitochondrial cristae density allows metabolic capacity modulation in human skeletal muscle. *Journal of Physiology* **595**, 2839-2847.

Perkins, G. A. & Ellisman, M. H. (2010). Mitochondrial configurations in peripheral nerve suggest differential ATP production. *Journal of Structural Biology* **173**, 117-127.

Picard, M., White, K. & Turnbull, D. M. (2013). Mitochondrial morphology, topology, and membrane interactions in skeletal muscle: a quantitative three-dimensional electron microscopy study. *Journal of Applied Physiology* **114**, 161-171.

Prince, F. P. (2002). Lamellar and tubular associations of the mitochondrial cristae: unique forms of the cristae present in steroid-producing cells. *Mitochondrion* **1**, 381-389.

Rampelt, H., Zerbes, R. M., van der Laan, M. & Pfanner, N. (2017). Role of the mitochondrial contact site and cristae organizing system in membrane architecture and dynamics. *Biochimica et Biophysica Acta (BBA)-Molecular Cell Research* **1864**, 737-746.

Renken, C., Siragusa, G., Perkins, G., Washington, L., Nulton, J., Salamon, P. & Frey, T. G. (2002). A thermodynamic model describing the nature of the crista junction: a structural motif in the mitochondrion. *Journal of Structural Biology* **138**, 137-144.

Riva, A., Tandler, B., Lesnefsky, E. J., Conti, G., Loffredo, F., Vazquez, E. & Hoppel, C. L. (2006). Structure of cristae in cardiac mitochondria of aged rat. *Mechanisms of Ageing & Development* **127**, 917-921.

Roca-Portoles, A. & Tait, S. W. (2021). Mitochondrial quality control: from molecule to organelle. *Cellular & Molecular Life Sciences*, **78**, 3853-3866.

Sastre, J., Pallardó, F. V., García de la Asunción, J. & Viña, J. (2000). Mitochondria, oxidative stress and aging. *Free Radical Research* **32**, 189-198.

Scott, G. R., Egginton, S., Richards, J. G. & Milsom, W. K. (2009). Evolution of muscle phenotype for extreme high altitude flight in the bar-headed goose. *Proceedings of the Royal Society B: Biological Sciences* **276**, 3645-3653.

Scott, G. R., Schulte, P. M., Egginton, S., Scott, A. L., Richards, J. G. & Milsom, W. K. (2011). Molecular evolution of cytochrome c oxidase underlies high-altitude adaptation in the bar-headed goose. *Molecular Biology & Evolution* **28**, 351-363.

Seo, A. Y., Joseph, A. M., Dutta, D., Hwang, J. C., Aris, J. P. & Leeuwenburgh, C. (2010). New insights into the role of mitochondria in aging: mitochondrial dynamics and more. *Journal of Cell Science* **123**, 2533-2542.

Strauss, M., Hofhaus, G., Schröder, R. R. & Kühlbrandt, W. (2008). Dimer ribbons of ATP synthase shape the inner mitochondrial membrane. *The EMBO Journal* **27**, 1154-1160.

Strohm, E. & Daniels, W. (2003). Ultrastructure meets reproductive success: performance of a sphecid wasp is correlated with the fine structure of the flight–muscle mitochondria. *Proceedings of the Royal Society of London. Series B: Biological Sciences* **270**, 749-754.

Strohm, E. & Linsenmair, K. E. (1997). Female size affects provisioning and sex allocation in a digger wasp. *Animal Behaviour* **54**, 23-34.

Suarez, R. K. (1998). Oxygen and the upper limits to animal design and performance. *Journal of Experimental Biology* **201**, 1065-1072.

Suarez, R. K., Lighton, J. R., Brown, G. S. & Mathieu-Costello, O. (1991). Mitochondrial respiration in hummingbird flight muscles. *Proceedings of the National Academy of Sciences* **88**, 4870-4873.

Suarez, R. K., Staples, J. F., Lighton, J. R. & Mathieu-Costello, O. (2000). Mitochondrial function in flying honeybees (*Apis mellifera*): respiratory chain enzymes and electron flow from complex III to oxygen. *Journal of Experimental Biology* **203**, 905-911.

Tandler, B. & Hoppel, C. L. (1986). Studies on giant mitochondria. *Annals of the New York Academy of Sciences* **488**, 65-81.

Terman, A. & Brunk, U. T. (2005). The aging myocardium: roles of mitochondrial damage and lysosomal degradation. *Heart, Lung & Circulation* **14**, 107-114.

Willis, W. T., Jackman, M. R., Messer, J. I., Kuzmiak-Glancy, S. & Glancy, B. (2016). A simple hydraulic analog model of oxidative phosphorylation. *Medicine & Science in Sports & Exercise* **48**, 990.

Zhang, Z. Y., Chen, B., Zhao, D. J. & Kang, L. (2013). Functional modulation of mitochondrial cytochrome c oxidase underlies adaptation to high-altitude hypoxia in a Tibetan migratory locust. *Proceedings of the Royal Society B: Biological Sciences* **280**, 20122758.

Concluding remarks

Animals have evolved a vast number of ways to survive and reproduce successfully in different environments, and successful survival and reproduction require substantive amounts of energy to be produced efficiently. Approximately 90% of this energy is produced via oxidative phosphorylation in mitochondria. In turn, mitochondrial function is influenced by mitochondrial behavior (i.e., communication and movement) and morphology (structure). As such, this body of work investigates how mitochondrial behavior and morphology influence mitochondrial performance and, therefore, whole-animal performance—particularly under various environmental stressors.

The fields of physiological ecology and mitochondrial biology have been successful at outlining variation in animal performance and how mitochondrial structure influences mitochondrial performance, respectively. However, these two fields of research would benefit from integration with one another. Provided that mitochondrial behavior and morphology are responsible, in part, for variation in mitochondrial function, understanding said relationship can further our understanding of variation in whole-animal performance (i.e., energetically demanding aspects of animal growth, survival, and reproduction). Understanding how the environment influences mitochondria can further our knowledge of animal performance.

Climate change is rapidly altering the natural world, including the physiology and life history of aquatic organisms. Two ecologically relevant, environmental stressors are temperature and ultraviolet (UV) radiation. These two exogenous factors are readily shown to influence the metabolic rate and life history of aquatic organisms, including pervasive zooplankton such as copepods that are important to aquatic ecosystems. There is currently a growing body of literature that shows how increasing temperature and UV radiation influence whole-animal performance, but the mechanisms by which this occurs are obscure. Here, we demonstrate how UV radiation and temperature influence the behavior, morphology, and performance of mitochondria in the copepod *Tigriopus californicus,* as well as copepod life history; we also develop new ideas surrounding the impact of mitochondrial behavior and morphology on mitochondrial performance.

UV radiation is known to decrease the metabolic rate of copepods and impede critical life history traits of animals, such as survival and reproduction. Few studies have

evaluated both beneficial and detrimental effects—hormetic responses—that radiation can have on mitochondrial physiology. For the first time, we show that, under hormetic theory, low levels of UV irradiation not only decrease the longevity of copepods but increase their short-term reproductive performance (i.e., first clutch size). This study was followed by examining the effects of similar radiation exposure on the behavior and morphology of mitochondria and metabolic rate of copepods. The latter study demonstrates that mitochondria not only undergo fission but increase density of the inner mitochondrial membrane and proportion of inter-mitochondrial junctions (with increasing mitochondrial aspect ratio) to maintain metabolic rate under UV light stress. Collectively, these two studies reveal how UV radiation can both benefit and curtail life history traits, as well as the mechanisms by which this may occur through linking an environmental stressor with whole-animal metabolic rate. Further work is needed to determine additional mechanisms that may be involved in such relationships (e.g., oxidative damage, additional environmental stressors).

Much attention is given to the positive, exponential increase in copepod respiration with increasing temperature. However, the average rate of change (slope) in copepod respiration across more than two temperatures is not well characterized. Meta-analysis is becoming an increasingly useful and powerful tool for answering long-standing, complex questions in ecology and evolutionary biology. Quantitative, systematic reviews allow authors to address important questions surrounding problems that have been previously studied by numerous labs that have used various methods and model organisms in their research. We developed a new effect size that we refer to as Percent Change to conduct a meta-analysis across 78 years of copepod physiological research to answer the question: how much does copepod respiration increase per one degree increase in temperature? We determined that copepod respiration increases by approximately 7% per °C increase in temperature across the three copepod orders Calanoida, Cyclopoida, and Harpacticoida. This work not only answers an enduring question regarding the extent to which temperature impacts the respiration rates of an important aquatic poikilotherm, but it presents a new (and more accurate) way of quantifying the relationship between temperature and respiration. Future work may find it prudent to adopt this effect size in physiological studies in ecology and evolutionary

biology to describe the relationship between temperature and respiration, provided that the commonly-used Q_{10} value is limited by its pairwise calculations across only two temperatures.

Last, we outline the importance of density and morphology of the IMM in performance of the IMM. Various morphological traits of the mitochondrion impact mitochondrial performance, including how ATP synthase bends the IMM, cristae and crista junction morphology, mitochondrial density, and IMM density. Although increasing density of the IMM has been attributed to increased energy production to meet increasing energetic demands, few studies have evaluated the possible negative effects of this mechanism on mitochondrial performance. There is likely a ceiling on increasing density of the IMM, as numerous other morphological traits of the organelle change when density of the IMM increases. Future work should consider this ceiling in studies of mitochondrial morphology as it relates to mitochondrial performance if we are to gain a more thorough understanding of how mitochondrial function influences whole-animal performance.

Collectively, this body of work unites the fields of physiological ecology and mitochondrial biology to further our understanding of whole-animal performance. If we can begin to understand how increasing temperatures and UV radiation can impact the mitochondria of important zooplankton such as copepods, we can begin to understand (and possibly predict) how climate change may affect our world's ecosystems. I hope this work inspires the integration of mitochondrial behavior and morphology in studies of whole-animal performance in ecology and evolutionary biology.

Appendix

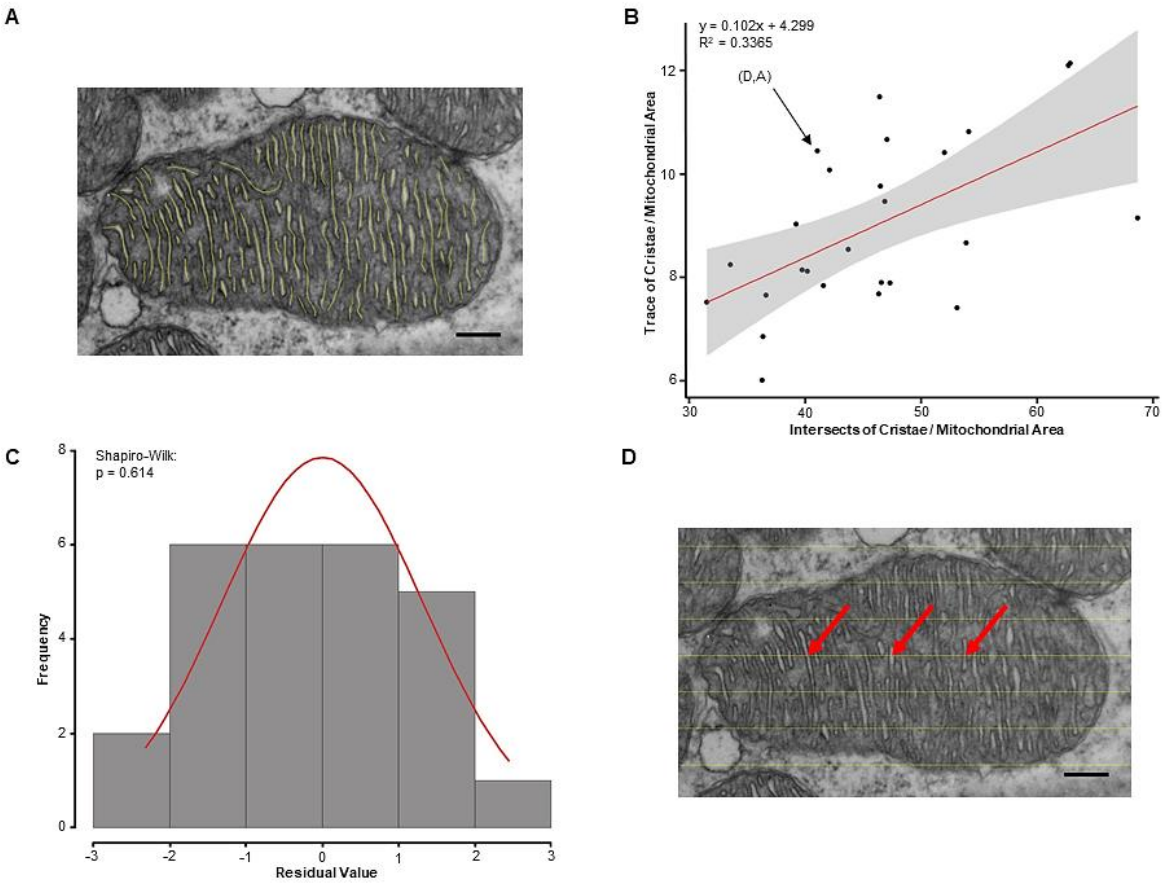

Figure A1. Comparison between the two methods used to quantify density of the inner mitochondrial membrane. (A) tracing each crista, (B) a general linear regression showing a positive, linear relationship between the two methods and the individual value (x,y) for the two example measurements in (D) and (A), (C) a frequency histogram showing the normal distribution of model residuals from the regression model, and (D) the use of a transect to quantify density of the inner mitochondrial membrane as used in our study. Red arrows indicate examples of where the intersects between cristae and the lines would be counted. Scale bars are 250nm.

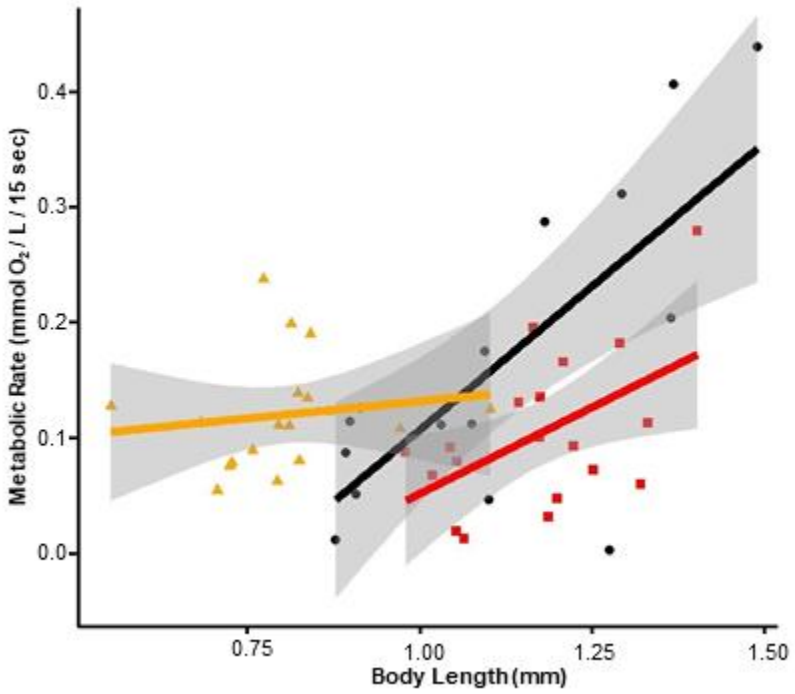

Figure A2. Scatterplot showing the metabolic rates of individual copepods plotted against copepod body length for each treatment group. Black circles, orange triangles, and red squares represent the control, 3-hr, and 6-hr treatment groups, respectively. Gray shading denotes 95% confidence intervals.

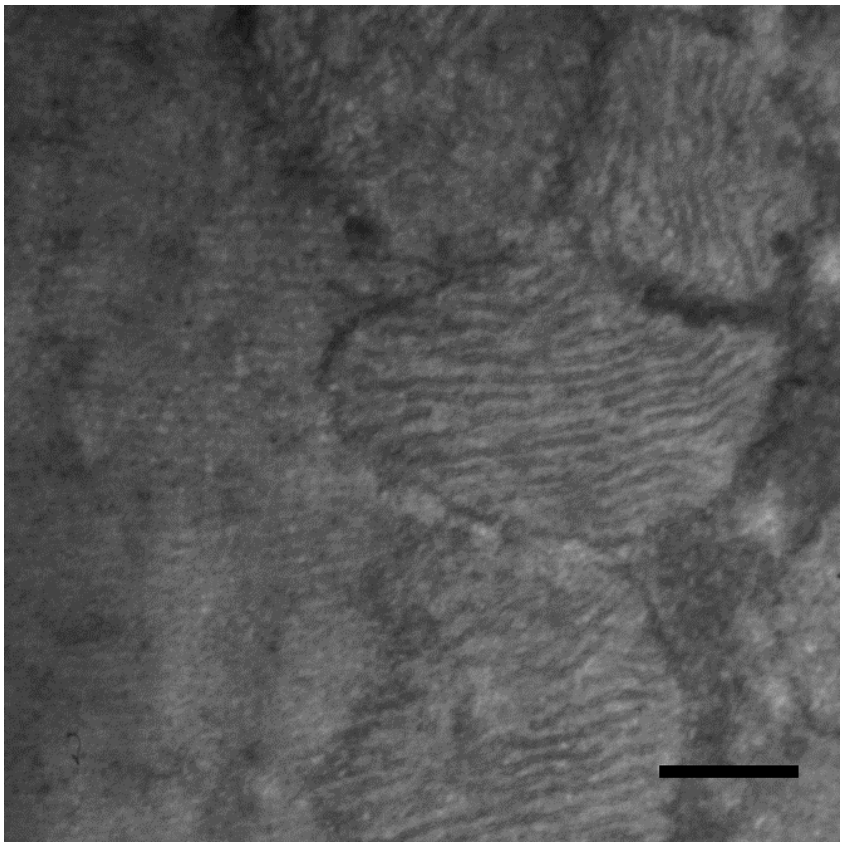

Figure A3. Transmission electron micrograph of a mitochondrion from the 3-hr UV irradiation treatment. Little to no inter-membrane space is visible. Scale bar is 250nm.

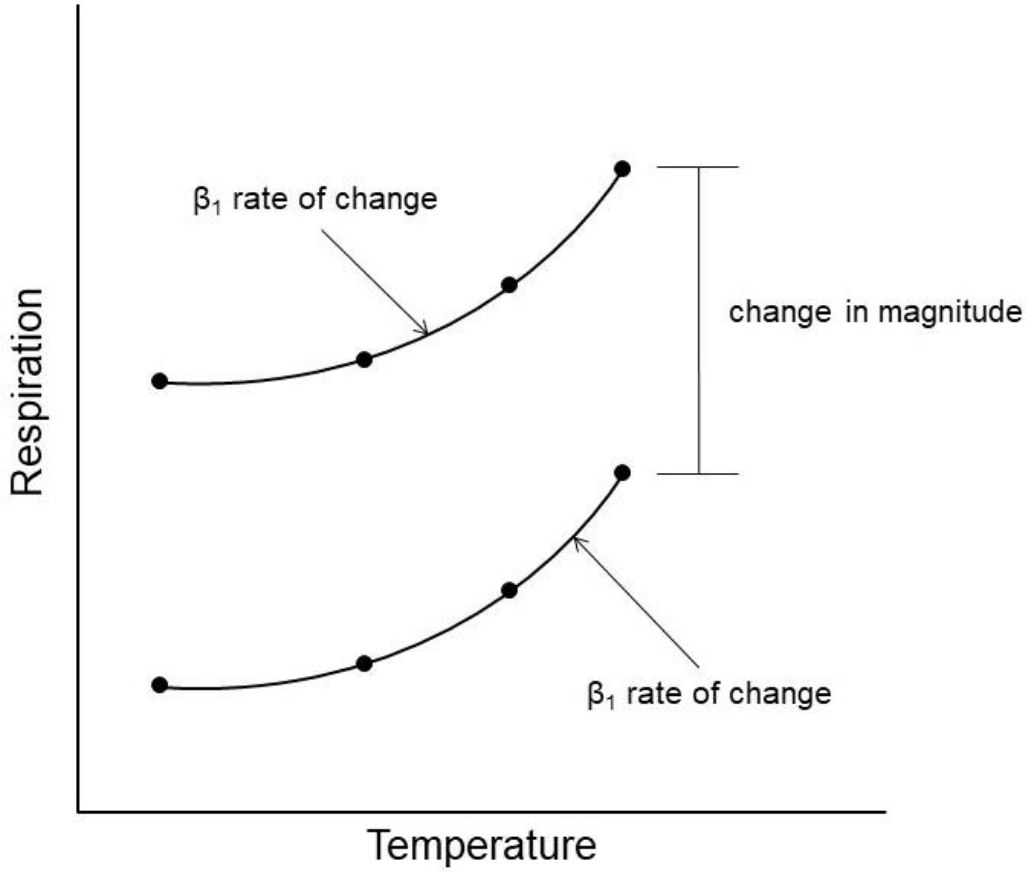

Figure A4. Change in magnitude between respiration at each temperature versus β_1 used in our study to calculate percent change. Our study does not assess differences in mean respiration rates at select temperatures as indicated by the change in magnitude, but assesses differences in the rate of change in respiration rates with increasing temperature (slope) as indicated by the β_1 rate of change.

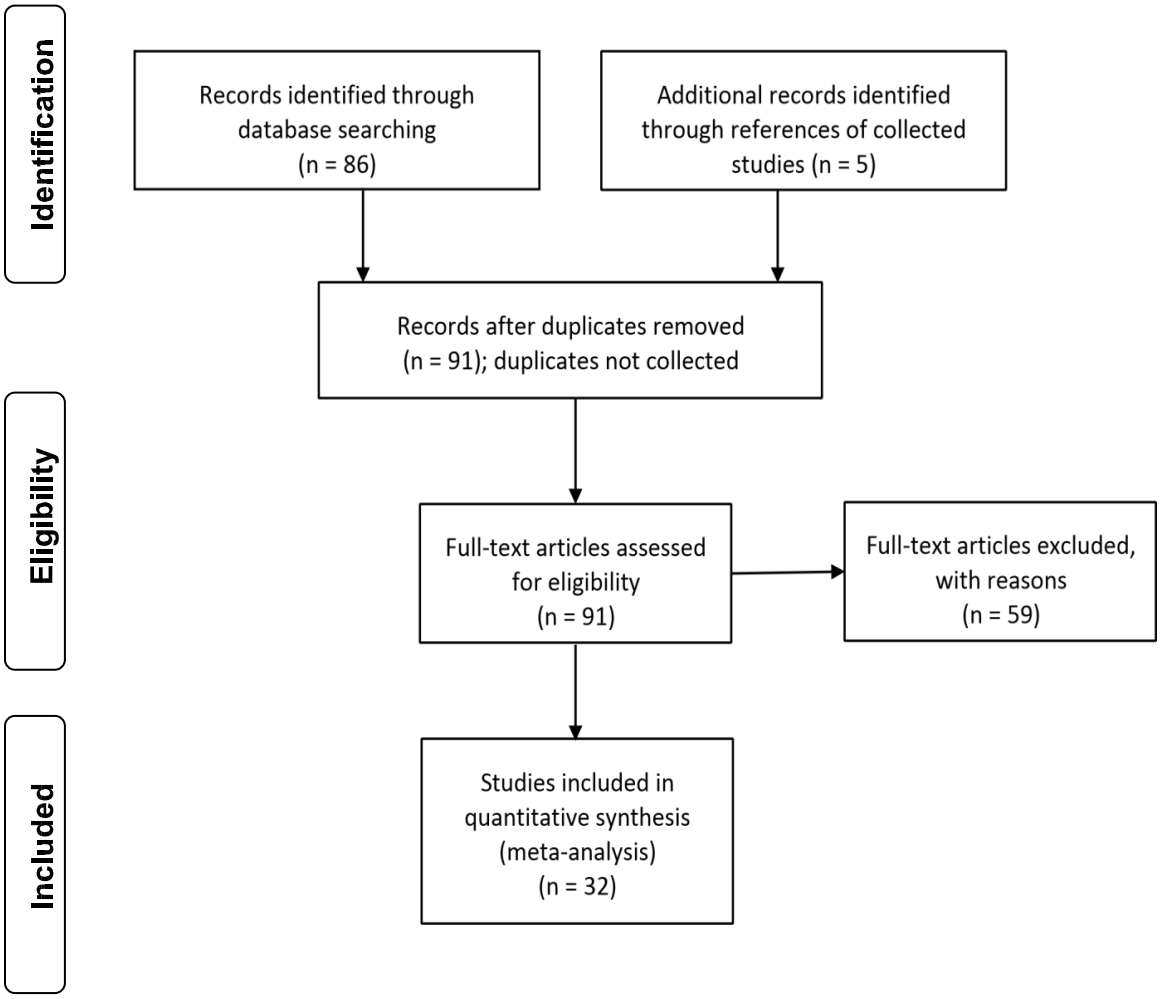

Figure A5. Flow diagram of study identification, eligibility screening, and inclusion.

Table A6. Table summary of variables included in meta-analytical models and how each was coded, as well as the levels within each variable if applicable.

Variable	Coded	Levels
Dry weight	Factor	Yes, No
Family, Order	Factor	*Taxon*, *Taxon*
Food	Factor	Fed, Starved
Lead author	Factor	*Name*
Method	Factor	Cartesian diver, Clark-type electrode, fiber optic meter, gas chromatography, manometer, polarographic electrode, Winkler titration
Percent change	Numeric	*Continuous*
Publication year	Numeric	*Continuous*
Species	Factor	*Taxon*
Variance	Numeric	*Continuous*

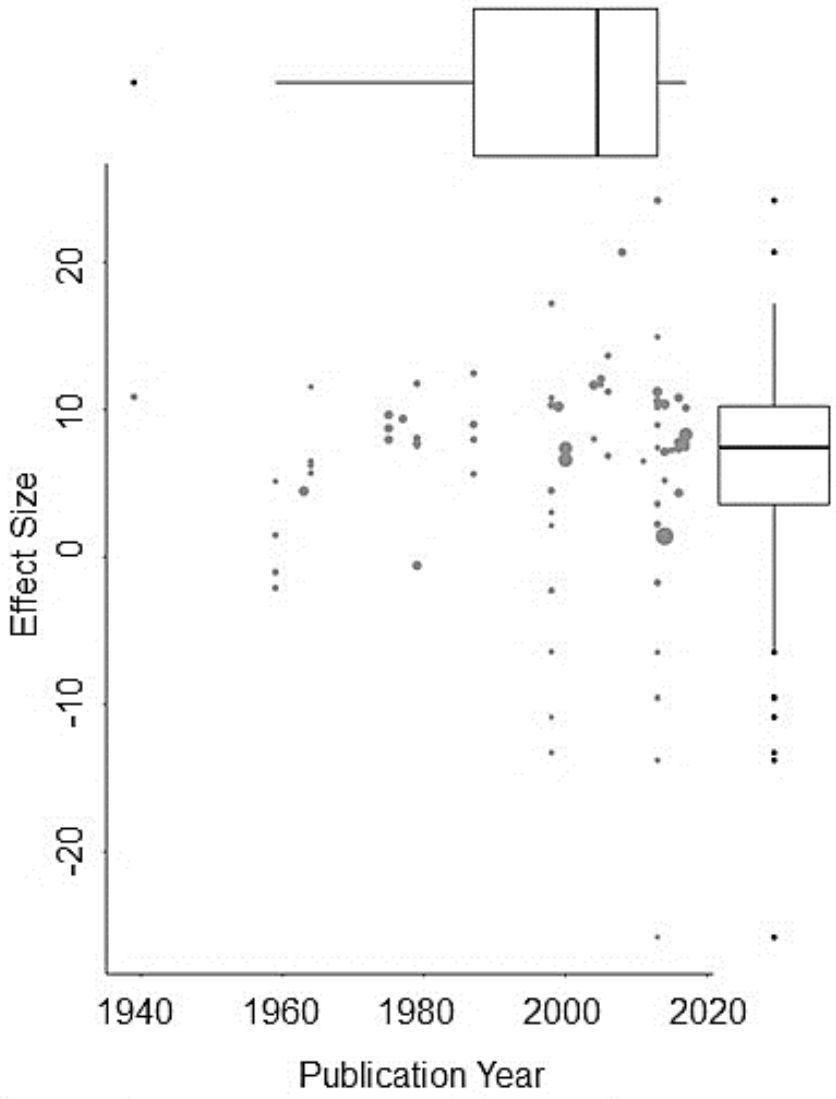

Figure A7. Bubble plot of publication year plotted against effect size to assess outliers and possible publication bias. Point size corresponds to the number of replicates per effect size.

List A8. Citations of studies used in the meta-analysis.

Almeda, R., Alcaraz, M., Calbet, A. & Saiz, E. (2011). Metabolic rates and carbon budget of early developmental stages of the marine cyclopoid copepod *Oithona davisae*. *Limnology & Oceanography* **1**, 403-14.

Anraku, M. (1964). Influence of the Cape Cod Canal on the hydrography and on the copepods in Buzzards Bay and Cape Cod Bay, Massachusetts. II. Respiration and feeding. *Limnology & Oceanography* **2**, 195-206.

Auel, H., Hagen, W., Ekau, W. & Verheye, H. M. (2005). Metabolic adaptations and reduced respiration of the copepod *Calanoides carinatus* during diapause at depth in the Angola-Benguela Front and northern Benguela upwelling regions. *African Journal of Marine Science* **3**, 653-7.

Cass, C. J. & Daly, K. L. (2014). Eucalanoid copepod metabolic rates in the oxygen minimum zone of the eastern tropical north Pacific: Effects of oxygen and temperature. *Deep-Sea Research Part I* **94**, 137-49.

Castellani, C. & Altunbaş, Y. (2014). Seasonal change in acclimatised respiration rate of *Temora longicornis*. *Marine Ecology Progress Series* **500**, 83-101.

Castellani, C., Robinson, C., Smith, T. & Lampitt, R. S. (2005). Temperature affects respiration rate of *Oithona similis*. *Marine Ecology Progress Series* **285**, 129-35.

Clarke, G. L. & Bonnet, D. D. (1939). The influence of temperature on the survival, growth and respiration of *Calanus finmarchicus*. *Biological Bulletin* **763**, 371-83.

Cruz, J., Garrido, S., Pimentel, M. S., Rosa, R., Santos, A. M. & Ré, P. (2013). Reproduction and respiration of a climate change indicator species: effect of temperature and variable food in the copepod *Centropages chierchiae*. *Journal of Plankton Research* **5**, 1046-58.

Epp, R. W. & Lewis, W. M. (1979). Metabolic responses to temperature change in a tropical freshwater copepod (*Mesocyclops brasilianus*) and their adaptive significance. *Oecologia* **2**, 123-38.

Gaudy, R., Cervetto, G. & Pagano, M. (2000). Comparison of the metabolism of *Acartia clausi* and *A. tonsa*: influence of temperature and salinity. *Journal of Experimental Marine Biology & Ecology* **1**, 5165.

Green, J. D. (1975). Feeding and respiration in the New Zealand copepod *Calamoecia lucasi* Brady. *Oecologia* **4**, 345-58.

Green, J. D. & Chapman, M. A. (1977). Temperature effects on oxygen consumption by the copepod *Boeckella dilatata*. *New Zealand Journal of Marine & Freshwater Research* **2**, 375-82.

Halcrow, K. (1963). Acclimation to temperature in the marine copepod, *Calanus finmarchicus* (Gunner). *Limnology & Oceanography* **1**, 1-8.

Hirche, H. J. (1987). Temperature and plankton. *Marine Biology* **3**, 347-56.

Ikeda, T. (1979). Respiration rates of copepod larvae and a ciliate from a tropical sea. *Journal of Oceanography* **1**, 1-8.

Isla, J. A. & Perissinotto, R. (2004). Effects of temperature, salinity and sex on the basal metabolic rate of the estuarine copepod *Pseudodiaptomus hessei*. *Journal of Plankton Research* **5**, 57983.

Isla, J. A., Lengfellner, K. & Sommer, U. (2008). Physiological response of the copepod *Pseudocalanus* sp. in the Baltic Sea at different thermal scenarios. *Global Change Biology* **4**, 895-906.

Kiko, R., Hauss, H., Buchholz, F. & Melzner, F. (2016). Ammonium excretion and oxygen respiration of tropical copepods and euphausiids exposed to oxygen minimum zone conditions. *Biogeosciences* **8**, 2241-55.

Lehette, P. (2017). Respiration rates in tropical copepods: evidence of cold developmental acclimation? *Journal of Crustacean Biology* **1**, 76-80.

Lehette, P., Ting, S. M., Chew, L. L. & Chong, V. C. (2016). Respiration rates of the copepod *Pseudodiaptomus annandalei* in tropical waters: beyond the thermal optimum. *Journal of Plankton Research* **3**, 456-67.

Li, C., Sun, S., Wang, R. & Wang, X. (2004). Feeding and respiration rates of a planktonic copepod (*Calanus sinicus*) oversummering in Yellow Sea Cold Bottom Waters. *Marine Biology* **1**, 149-57.

Li, W., Han, G., Dong, Y., Ishimatsu, A., Russell, B. D. & Gao, K. (2015). Combined effects of short-term ocean acidification and heat shock in a benthic copepod *Tigriopus japonicus* Mori. *Marine Biology* **9**, 1901-12.

Liu, X. & Ban, S. (2017). Effects of acclimatization on metabolic plasticity of *Eodiaptomus japonicus* (Copepoda: Calanoida) determined using an optical oxygen meter. *Journal of Plankton Research* **1**, 111-21.

McAllen, R., Taylor, A. C. & Davenport, J. (1999). The effects of temperature and oxygen partial pressure on the rate of oxygen consumption of the high-shore rock

pool copepod *Tigriopus brevicornis*. *Comparative Biochemistry & Physiology Part A: Molecular & Integrative Physiology* **2**, 195202.

Paffenhöfer, G. A. (2006). Oxygen consumption in relation to motion of marine planktonic copepods. *Marine Ecology Progress Series* **317**, 187-92.

Pascal, L. & Chong, V. C. (2016). Does developmental temperature modulate copepods respiratory activity through adult life? *Journal of Plankton Research* **5**, 1215-24.

Raymont, J. E. (1959). The respiration of some planktonic copepods. *Limnology & Oceanography* **4**, 479-91.

Svetlichny, L., Hubareva, E. & Isinibilir, M. (2017). Comparative trends in respiration rates, sinking and swimming speeds of copepods *Pseudocalanus elongatus* and *Acartia clausi* with comments on the cost of brooding strategy. *Journal of Experimental Marine Biology & Ecology* **488**, 2431.

Teare, M. & Price, R. (1979). Respiration of the meiobenthic harpacticoid copepod, *Tachidius discipes* Giesbrecht, from an estuarine mudflat. *Journal of Experimental Marine Biology & Ecology* **1**, 1-8.

Teuber, L., Kiko, R., Séguin, F. & Auel, H. (2013). Respiration rates of tropical Atlantic copepods in relation to the oxygen minimum zone. *Journal of Experimental Marine Biology & Ecology* **448**, 28-36.

Thuesen, E. V., Miller, C. B. & Childress, J. J. (1998). Ecophysiological interpretation of oxygen consumption rates and enzymatic activities of deep-sea copepods. *Marine Ecology Progress Series* 95-107.

Zervoudaki, S., Frangoulis, C., Giannoudi, L. & Krasakopoulou, E. (2013). Effects of low pH and raised temperature on egg production, hatching and metabolic rates of a Mediterranean copepod species (*Acartia clausi*) under oligotrophic conditions. *Mediterranean Marine Science* **1**, 74-83.